Title
The Effects of Chronic Arsenic Exposure on Thermogenesis and Type 2 Diabetes

Author
Castriota, Felicia

Publication Date
2019

Peer reviewed|Thesis/dissertation

The Effects of Chronic Arsenic Exposure on Thermogenesis and Type 2 Diabetes

by

Felicia Castriota

A dissertation submitted in partial satisfaction of the

requirements for the degree of

Doctor in Philosophy

in

Environmental Health Sciences

in the

Graduation Division

of the

University of California, Berkeley

Committee in Charge:

Professor Martyn T. Smith, Chair
Professor Ellen Eisen
Professor Michele A. La Merrill
Professor Jen-Chywan Wang

Spring 2019

ABSTRACT

The Effects of Chronic Arsenic Exposure on Thermogenesis and Type 2 Diabetes

by

Felicia Castriota

Doctor of Philosophy in Environmental Health Sciences

University of California, Berkeley

Professor Martyn T. Smith, Chair

The prevalence of type 2 diabetes (T2D) has nearly doubled since 1980. T2D is characterized by hyperglycemia, insulin resistance, and long-term complications. Poor nutrition, sedentary lifestyle, and obesity, are among the strongest risk factors for the development of this metabolic disease. Environmental pollutants however, also have the potential to alter glucose homeostasis and lead to the development of T2D. Arsenic is one of these chemicals, with epidemiologic studies worldwide supporting this association. The precise mechanism of action by which arsenic exhibits its diabetogenic effects however, remains unclear. Since the late 2000s, select heat-producing adipose depots have been identified and shown to be intricately involved in glucose metabolism. Brown and beige adipocytes are important regulators of energy expenditure and both lipid and glucose homeostasis. This dissertation aims to identify whether arsenic increases the risk of T2D development among obese individuals, and identify its effects on thermogenic adipocytes involved in glucose metabolism and energy expenditure. **Chapter 1** is a state-of-the-science review of the disruptive effects of arsenic exposure on glucose homeostasis, with an emphasis on findings from experimental studies. **Chapter 2** is a cross-sectional analysis of a unique arsenic exposed population in Northern Chile. This chapter examines the effects of arsenic exposure on T2D development, and evaluates whether arsenic and obesity may act synergistically to increase T2D risk. While proposed pathways for arsenic's role in T2D include alterations in pancreatic β-cell function and insulin secretion, these findings are reported only at high arsenic exposure concentrations. Therefore, further investigation to elucidate arsenic's diabetogenic molecular targets in mammalian models is required at relevant public health concentrations. **Chapter 3** examines the effects of chronic low-dose arsenic exposure on thermogenesis and recruitable beige adipocytes involved in key metabolic pathways *in vivo*. **Chapter 4** informs current statistical methodologies for indirect calorimetry analysis by implementing longitudinal data analysis techniques and randomization-based inference to better capture how environmental chemical exposures alter energy expenditure over time. Lastly, **Chapter 5** summarizes the current state of arsenic research within the context of metabolic biology, and highlights how interdisciplinary research has the potential to inform current environmental standards and public health interventions.

DEDICATION

I dedicate this dissertation to my mother, who raised me to have bold ambitions.
Thank you for teaching me to value education as an instrument of growth,
and for being my staunchest supporter through it all.

TABLE OF CONTENTS

ACKNOWLEDGMENTS

I am grateful for the mentorship received at all stages of my scientific training, and to all those who provided me with direction and comfort during times of trial and tribulation.

My undergraduate studies at Georgetown University sparked my intellectual curiosity in science and public health. I am particularly thankful for the extensive guidance of Dr. Amy Walsh, who first taught me how to critically read scientific papers and inspired me to venture out into the community to co-teach 9th grade biology at Duke Ellington School of the Arts. Thank you for instilling in me a greater sense of purpose, and for opening my eyes to how we can apply our academic training to educating the next generation to be informed, analytical thinkers.

My passion for environmental health sciences first blossomed from the invigorating lectures of Dr. Joseph Graziano and Dr. Greg Frier in their course on *Biological and Environmental Determinants of Health.* Thank you to Dr. Graziano and the Columbia Superfund Program for welcoming a masters student to attend your weekly meetings and advancing my knowledge on the effects of arsenic exposure. Your encouragement to pursue a doctoral degree was critical in believing in myself and in my abilities to succeed in an advanced scientific setting.

Thank you to Dr. Craig Steinmaus, who guided me during my summer practicum and supported the continuation of my training in epidemiology during my transition from Columbia to UC Berkeley. I consider myself particularly fortunate to have had his expertise and guidance in the drafting of multiple grants and manuscripts.

While at UC Berkeley, I have been extremely fortunate to have benefitted from the mentorship of experts in the fields of toxicology, metabolic biology, and epidemiology. To my advisor Dr. Martyn Smith, thank you for nurturing my inquisitive nature and fostering critical collaborations. To Dr. Luoping Zhang, for providing me with the opportunity to undertake a leadership role with the Superfund trainees, and advising me on how to become a more effective communicator. To Dr. Wally Wang, thank you for the countless hours of mentorship, and for reviewing all of my raw data. Thank you also, for fostering the opportunity to learn from leading experts in metabolic biology at UCSF. To Dr. Ellen Eisen, thank you for embracing my interdisciplinary training and continuously pushing me to expand my knowledge in the field of epidemiology. I am grateful to both you and Dr. Sadie Costello for all of your support. I am grateful to Dr. Fenna Sillé, for patiently training me in the basics: from sterile technique to animal handling, and general laboratory skills. Your work ethic and dedication to research continues to inspire me.
A special thank you to Dr. Cliona McHale, for her constant encouragement and tremendous assistance in F31 submission.

I am indebted to Dr. Michele La Merrill at UC Davis, who effortlessly succeeds at wearing multiple hats in both toxicology and epidemiology. I am grateful for how she welcomed me into her lab and advised me from afar as one of her own. Thank you for setting high standards, and ensuring I always include directional verbs in my writing. She has made me a more diligent scientist and critical thinker.

Thank you to my invaluable lab mates and peers from the Wang, Stahl, and La Merrill labs, who have become life-long friends. I am fortunate to have been surrounded by talented scientists who have provided a collaborative environment in which to thrive. Most notably, to Sylvia Sanchez, for her unwavering support and encouragement. Thank you for your patience and assistance during BSL3 training, overnights in the animal facility's cold room, and much more.

To my dearest friends, thank you for nurturing our bond with domestic travel, postcards, and weekly phone calls. I am deeply fortunate for your friendship.

I am most grateful to my family for providing me with infinite opportunities for growth and success. To my mother Barbara, for perpetually encouraging my intellectual curiosities since a young age. This is for you. To my step-father Peter, for always reminding me of my worth, and instilling in me a deep respect for our natural environment. To my father Lorenzo, for imparting a strong work ethic, and for teaching me to show up and be my best self each and every day. To my brother Sam, for providing comfort and comedic relief in times of high stress. To Nonno and Nonna, for your constant support and beaming pride in all of my academic achievements. To the rest of my extended family, thank you for your positivity and for making the trek to multiple graduations both near and far.

Lastly, to my fiancé Ryan, for supporting my journey without expectations. Your optimism and never-ending confidence in my ability to succeed has made me shine that much brighter. Throughout this journey, you have reminded me to extend the same consideration and compassion to myself, as I extend to my academic success. I am endlessly grateful for you.

Chapter 1. A State-of-the-Science Review of Arsenic's Effects on Glucose Homeostasis in Experimental Models

Felicia Castriota[1], Linda Rieswijk[1], Michele A. La Merrill[2], Craig Steinmaus[1], Martyn T. Smith[1], Jen-Chywan Wang[1,3]

[1] Superfund Research Program, University of California, Berkeley, CA, USA
[2] Department of Environmental Toxicology, University of California, Davis, CA USA
[3] Department of Nutritional Sciences & Toxicology, University of California, Berkeley, CA, USA

*A version of this manuscript is under review: Castriota F, Rieswijk L, La Merrill MA, Steinmaus C, Smith MT, Wang JC. A State-of-the-Science Review of Arsenic's Effects on Glucose Homeostasis in Experimental Models.
This chapter is printed with the explicit consent of all co-authors.

Abstract

BACKGROUND: The prevalence of type 2 diabetes (T2D) has more than doubled since 1980. Poor nutrition, sedentary lifestyle, and obesity are among the primary risk factors. While an estimated 70 percent of cases are attributed to excess adiposity, there is an increased interest in understanding the contribution of environmental agents to diabetes causation and severity. Arsenic is one of these environmental chemicals, with multiple epidemiology studies supporting its association with T2D. Despite extensive research, the molecular mechanism by which arsenic exerts its diabetogenic effects remains unclear.

OBJECTIVES: We conducted a literature search focused on arsenite exposure *in vivo* and *in vitro*, using relevant endpoints to elucidate potential mechanisms of oral arsenic exposure and diabetes development.

METHODS: We explored experimental results for potential mechanisms and elucidated the distinct effects that occur at high versus low exposure. We also performed network analyses relying on publicly available data, which supported our key findings.

RESULTS: While several mechanisms may be involved, our findings support that arsenite has effects on whole body glucose homeostasis, insulin-stimulated glucose uptake, glucose-stimulated insulin secretion, hepatic glucose metabolism, and both adipose and pancreatic β-cell dysfunction.

DISCUSSION: This review applies state-of-the-science approaches to identify the current knowledge gaps in our understanding of arsenite on diabetes development.

KEY WORDS: Arsenic; Type 2 diabetes (T2D); Insulin resistance; Insulin-stimulated glucose uptake (ISGU); Glucose-stimulated insulin secretion (GSIS)

Introduction

Arsenic is a naturally occurring metalloid in the Earth's crust, found in water, air, food, and soil (Hughes et al. 2011). More than 200 million individuals are exposed to arsenic in drinking water, with high prevalence in Taiwan, Bangladesh, India, South America, and the United States (Hughes et al. 2011). The principal route of arsenic exposure occurs via the ingestion of contaminated drinking water and food, which continues to be a widespread public health concern (ATSDR 2007). Foods that have been reported to have high levels of inorganic arsenic include rice and rice-based products, poultry, apple juice, wine, and beer (Castriota et al, 2018). Runoff and leaching from rocks, sediment, and anthropogenic sources, are significant processes of drinking water contamination (ATSDR 2007). Oral inorganic arsenic exposure is associated with a wide range of diseases, including cancers of the skin, bladder, lung, kidney, and liver, in addition to developmental, dermatological, neurological, respiratory, immune, cardiovascular, endocrine, and metabolic disorders such as type 2 diabetes (T2D) (Hughes et al. 2011; Naujokas et al. 2013).

Elemental arsenic is present in both inorganic and organic forms, and in various oxidative states (Hughes et al. 2011). Both the pentavalent form, arsenate (iAs^{V}) and the trivalent form, arsenite (iAs^{III}) are detected in drinking water (Hughes et al. 2011). Arsenite metabolism via oral exposure occurs primarily in the liver via arsenic (+3 oxidation state) methyltransferase (As3MT),

and involves sequential reduction and methylation reactions that lead to the formation of both trivalent and pentavalent monomethylated (MMA) and dimethylated (DMA) metabolites (Agusa et al. 2011). A reductive methylation model has been proposed where trivalent metabolites are conjugated to glutathione (GSH) and ultimately oxidized to pentavalent arsenical metabolites (MMA^{5+} and DMA^{5+}) as the final products (Hayakawa et al 2005; Agusa et al, 2011). In recent years, the production of trivalent methylated species has been evaluated and deemed a bioactivation process that increases an individual's susceptibility to arsenic toxicity (Agusa et al. 2011; ATSDR 2007). In fact, methylarsonous (MMA^{3+}) and dimethylarsinous acids (DMA^{3+}) have been found to be more cytotoxic (Hou et al. 2013) and genotoxic (Petrick et al. 2000; Styblo et al. 2000) than their pentavalent counterparts, in murine and human cell lines, respectively.

Differences in Existing Research

Studies have attempted to distinguish the risk of arsenic-induced T2D based on exposure level with inconsistent results across experimental models. In 2012, an expert panel assembled by the National Toxicology Program (NTP) concluded that the existing epidemiologic findings provided *limited to sufficient support* for the link between arsenic and diabetes in populations exposed to concentrations greater than 150 ppb (Maull et al. 2012). Since this evaluation, additional studies have published increasing evidence in support of the association between arsenic-induced T2D (Castriota et al. 2018; Farzan et al. 2017; Grau-Perez et al. 2017; Pan et al. 2013; Peng et al. 2015). Animal models have also been established in attempt to mimic population exposures and identify the chemical's diabetogenic effects. The concentration of arsenite in drinking water used in published *in vivo* metabolic studies have however, ranged from 100 ppb up to 50 ppm (Ditzel et al. 2015; Garciafigueroa et al. 2013; Adebayo et al. 2015; Druwe et al. 2012; Paul et al. 2011; Song et al. 2017; Maull et al. 2012). In *vivo* studies have large discrepancies in both exposure duration, concentration, and administration, many of which do not mimic those observed in human populations worldwide (Huang et al. 2011; Maull et al. 2012; Navas-Acien et al. 2005; Thayer et al. 2012). In 2012, an expert panel assembled by NTP deemed evidence for animal research on the topic of arsenic and diabetes *inconclusive* due to the dissimilarity of animal exposures across studies, and to those reported in human exposure studies (Maull et al. 2012).Treatment with arsenite *in vitro* is also highly variable in regards to both dose and duration (Maull et al. 2012). In light of these concerns, NTP recommended that future arsenic research focus on animal studies designed to mimic internal doses observed in humans, accompanied by low-dose *in vitro* studies on cell lines involved in glucose metabolism (Maull et al. 2012; Thayer et al. 2012).

There also remains a need for more uniform model selection for *in vitro* and *in vivo* study designs that are relevant to human exposures. The expression of As3MT in different cell lines may vary substantially, impacting the kinetics of arsenite metabolism and its effects in targets involved in glucose homeostasis. The assessment of sodium arsenite metabolism in four animal species, including rat, hamster, guinea pig, and mouse, found mice to be the most appropriate model to evaluate arsenic toxicity (Mitchell et al. 2000). While mice metabolize arsenic more quickly than humans, they have similar distribution parameters (Mitchell et al. 2000). The limitation of using mouse models is mostly due to low biological sample availability (e.g. plasma, urine, tissue) due to the animal's small mass (Mitchell et al. 2000). Rats are considered a less appropriate animal model for arsenic metabolism as a proxy for human exposures as compared to other mammalian models (ATSDR 2007; Lu et al. 2004; Mitchell et al. 2000). While circulating DMA^{3+} inorganic

arsenic metabolite is accumulated in erythrocytes in rats, humans experience arsenic retention in epithelial tissues, such as the skin and lung (Lu et al. 2004).

Historically, higher arsenic doses have been administered in animal studies due to the decreased susceptibility of laboratory animals to inorganic arsenic toxicity as compared to humans (ATSDR 2007). Rodents either metabolize arsenic quicker or sequester it in blood cells and thus require concentrations of arsenic above those found in exposed populations in order to achieve similar internal doses (Maull et al. 2012). However, few studies report internal dose calculations, which require comprehensive water consumption estimates (States et al. 2011). The current literature also includes broad duration exposure periods, ranging from a few days to years (Maull et al. 2012). Routes of arsenic administration also vary, and include oral exposure via drinking water, oral gavage, and intraperitoneal injection (Maull et al. 2012). Since arsenic metabolism kinetics differ between animal models and humans, calculations based solely on allometric scaling may not be valid, and therefore are usually not reported (States et al. 2011). The use of genetic biomarkers and histopathology of select tissues have instead been more widely employed to convey equivalence to arsenic toxicity in humans (States et al. 2011).

This review highlights key *in vivo* studies with supporting associations observed *in vitro* (Figures 2 and 3). This targeted approach relies on quantitative methodologies to qualitatively synthesize the most relevant studies and address inconsistencies in arsenical species, route of administration, and duration of exposure, reported in the literature. We provide mechanistic evidence to support epidemiologic findings and advance our understanding of arsenic and T2D development.

Methods

Literature Search and Study Selection

We performed a literature review search using the Health Assessment Workspace Collaborative (HAWC) Literature Search tool (https://hawcproject.org/) starting on June 2018, to locate studies focusing specifically on arsenite exposure and T2D. We used key terms and medical subject headings (MeSH) as follows: ("Arsenite" AND "Type 2 Diabetes") OR ("Arsenite" AND "Insulin Resistance") OR ("Arsenite" AND "Chronic") OR ("Arsenic" AND "In Vitro") OR ("Arsenite" AND "Epidemiology") OR ("Arsenite" AND "Mus Musculus"). A total of 500 studies were obtained, with 99 additional relevant studies uploaded manually into the HAWC database. HAWC allows researchers to perform a PubMed database (https://www.ncbi.nlm.nih.gov/pubmed/) literature search where studies from the results of the query are imported and tagged for either inclusion or exclusion. All studies, whether searched directly in HAWC or uploaded manually, underwent an identical tagging process. A total of 599 references underwent tagging based on established exclusion and inclusion criteria. The inclusion criteria for experimental studies and literature reviews were based on exposure to arsenite and T2D as the primary outcome of interest. The exclusion criteria for experimental studies and literature reviews were *a)* no data on arsenic *b)* included arsenicals as a mixture or those other than those in the trivalent form of arsenite *c)* included routes of exposure other than via drinking water (oral) for *in vivo* studies *d) in utero* exposure only *e)* relied on animal models other than mice *f)* the assessment of the target organ or cell line was not relevant to T2D development *g)* duplicate study. These criteria were established based on the research question of interest, which focused on the effect of oral arsenite exposure either in mice, or in rodent or human cell lines relevant to T2D, to assess the effect of the chemical on mechanisms involved in dysregulation of glucose homeostasis.

The study tagging was conducted by two researchers (F.C., L.R.) and any inconsistencies were resolved by consensus. HAWC visualization tools were used to create a literature tag-tree to illustrate study identification and classification (Figure 1). A total of 85 studies were selected for inclusion using the HAWC search database. We referred to the NTP Office of Health Assessment and Translation (OHAT)'s risk of bias rating tool to assess the quality of the animal studies included in this review (OHAT 2015). A total of 14 animal studies were rated for each of the 9 risk-of-bias questions outlined for animal studies by OHAT' guidelines (OHAT 2015). The risk-of-bias rating was based on a 4-point scale, which included: *definitively low* risk of bias (++), *probably low* risk of bias (+), *probably high* risk of bias (-/NR), and *definitely high* risk of bias (--). Based on our assessment, there is a low probability of risk-of-bias (Figure SF1). The most important considerations for potential bias include the presence of an unintended co-exposure, such as high levels of arsenic in standard rodent chow, lack of research blinding, and lack of randomization in the allocation of treatment versus vehicle control.

Network Analyses

In addition to literature review, we also relied on chemical- and disease-related gene association data using the publicly available Comparative Toxicogenomics Database (CTD) (http://ctdbase.org), to identify genes that are associated with arsenic and T2D (Davis et al. 2017). Within CTD, chemicals and diseases are annotated with MeSH identifiers (https://www.nlm.nih.gov/mesh/) that facilitate searching within the database. After individual gene lists were obtained, we identified 16 genes commonly affected by sodium arsenite, insulin resistance, and T2D (Figure 4). The Venn diagram was created using Venny 2.1 (http://bioinfogp.cnb.csic.es/tools/venny/) (Figure 4). A potential limitation of using specific key terms is the potential of missing relevant genes, exemplified by the hypermethylation of KCNQ1, a gene involved in insulin secretion that did not appear in our original search. Despite this limitation, MeSH identifiers continue to be widely used based on narrow research criteria.

To further investigate the biological processes enriched for the obtained list of genes, we used the ClueGO app (Bindea et al. 2009) within Cytoscape (Lotia et al. 2013) together with the WikiPathways repository (Slenter et al. 2018). Cytoscape (http://www.cytoscape.org/) is able to visualize molecular interaction networks and integrate these with gene expression profiles and other data. Additional features are available as applications. For gene set enrichment analysis (GSEA) we used the WikiPathways repository (accessed on February 14, 2018) containing 418 curated human pathways and 5866 human genes. The advantage of using the ClueGO app within Cytoscape together with GSEA is that it enables the visualization of non-redundant and highly connected pathways in one functionally grouped network. Pathway selection criteria included a minimum number or percentage of genes (at least 3 genes or 4 percent of the total). The selection of highly connected pathways was based on Kappa statistics (Kappa Score > 0.4). In this way, functionally related biological pathways (containing the same genes) are clustered together.

Results

Based on our review of the current literature we propose biological mechanisms to explain the association between arsenic exposure and dysregulation of glucose homeostasis. We further explore and validate published *in vivo* and *in vitro* targets via the use of network analyses from publicly available data.

Whole Body Glucose Homeostasis

In vivo studies found impaired glucose tolerance in mice treated at high levels (ppm range) of arsenite. Persistent impaired glucose tolerance was observed in 8-week old C57BL/6J male mice based on glucose tolerance tests (GTT) performed (Kirkley et al. 2017). A study comparing 1, 10, 20, or 50 ppm 8-week arsenite found that 4-week old C57BL/6J male mice developed impaired glucose tolerance only at the highest exposure dose (Paul et al. 2007; 2008). While relatively lower dose (3 ppm) of arsenite treatment for 16 weeks did not affect glucose tolerance in 7-week old non-diabetic C57BLKS/$J^{db/m}$ male mice, such treatment increased susceptibility to impaired glucose tolerance in 7-week old diabetic C57BKS/$Lepr^{db/db}$ male mice (Liu et al. 2014).

Studies in genetic obese C57BKS/$Lepr^{db/db}$ male mice suggest the potential for a synergistic interaction between arsenic exposure and nutritional overload on the development of metabolic disorders. We identified five rodent studies that assessed the effects of arsenic co-exposures with high fat diet (Ditzel et al. 2015; Shi et al. 2014; Paul et al, 2011; Wu et al. 2008; Tan et al. 2011). Swiss Webster mice were treated with arsenic (100 ppb) after weaning for 10 weeks (to 13-weeks of age) (Ditzel et al. 2015). During the course of treatment, high fat diet was administered to assess the effects on fatty liver disease. Increased ectopic fatty lipid deposition and liver damage were observed in these mice (Ditzel et al. 2015). However, despite the induction of hepatic fibrosis, no significant increase in HOMA-IR, a measure of insulin resistance, was observed (Figure 2) (Ditzel et al. 2015). However, when mice were exposed to arsenic from embryonic day 5 to 13 weeks of age, and also fed a high fat diet after weaning, the effects on hepatic lipid accumulation and fibrosis were even more pronounced, and HOMA-IR was significantly elevated (Ditzel et al. 2015). These findings elucidate important differences for *in utero* versus *postnatal* arsenic dosing.

4-week old C57BL/6J male mice were exposed to both arsenite (50 ppm) and high fat diet for 20 weeks. While these mice exhibited impaired insulin secretion, no changes were observed in fasting blood glucose (FBG), which suggests pancreatic β-cell dysfunction (Paul et al. 2011). Oral GTT showed impaired glucose tolerance was more pronounced in arsenite and high fat diet-treated mice compared to mice administered high fat diet alone (Paul et al. 2011).

Overall, *in vivo* studies show that impaired glucose tolerance is observed only under exposure to high doses of arsenic, such as 50 ppm (Figure 2). Figure 2 provides a graphical representation of whole body glucose homeostasis and insulin resistance observed in the *in vivo* studies reviewed on arsenite exposure. Figure 2 reveals that exposure to lower doses of arsenic, such as 4.9 ppm and below, does not seem to alter glucose homeostasis, unless combined with genetic-induced diabetic models.

Insulin Stimulated Glucose Uptake (ISGU)

Insulin is an anabolic hormone secreted by pancreatic β-cells in response to high blood glucose levels (Figure 6). One of the major functions of insulin is to promote glucose uptake and utilization in peripheral tissues, such as skeletal muscle and white adipose tissue (Figure 6). During insulin resistance, the ability of insulin to promote glucose utilization in skeletal muscle and white adipose tissue is impaired (Saltiel and Kahn 2001).

Using 3T3-L1 adipocytes as a model, 4h sodium arsenite treatment at 100 μM (13 ppm) reduced both basal and ISGU (Walton et al. 2004). Treatment at 20 μM (2.6 ppm) also decreased both insulin-stimulated and basal glucose uptake (Walton et al. 2004). At 50 μM (6.5 ppm) arsenite, 4h of exposure significantly reduced both insulin-stimulated phosphorylated AKT levels, and the expression of AKT protein (Walton et al. 2004). Similar concentration-dependent effects on ISGU were observed with metabolites methylarsine oxide and iododimethylarsine (Walton et

al. 2004). Notably, the authors did not examine whether 20 μM of arsenite treatment for 4h was sufficient to alter AKT expression. Xue et al treated 3T3-L1 adipocytes with 0.25-2 μM (32-260 ppb) of arsenite for 7 days (Xue et al. 2011). The authors observed decreased insulin-stimulated AKT phosphorylation on serine residue 473, a hallmark of AKT activation. A significant reduction in ISGU was noted at 2 μM arsenite treatment, although a decreasing trend in glucose uptake was observed starting at lower concentrations (0.25-1 μM) (Hamann et al. 2014). These responses were correlated to a dose-dependent increase of intracellular GSH, and the expression of nuclear factor erythroid 2-related factor 2 (NRF2), which is a central transcription factor regulating cellular adaptive response to oxidative stress (Xue et al. 2011). Enhanced NRF2 activity has been shown to reduce insulin stimulated AKT phosphorylation and GLUT4 translocation in white adipose tissue (Xu et al. 2012). Arsenite treatment at 1 and 2 μM for 7 days also attenuated insulin-induced peroxide production, which is required for the induction of GLUT4 translocation (Mahadev et al. 2001; Xue et al. 2011). This study however, did not directly examine the induction of NRF2 activity and the reduced peroxide production to the suppressive effect of arsenite on insulin response in 3T3-L1 adipocytes (Mahadev et al. 2001).

Divya et al treated 3T3-L1 pre-adipocytes and C2C12 myoblasts with 0.5, 1 and 2 μM arsenite for 8 weeks. At the end of treatment, cells were differentiated to either adipocytes or myotubes (Padmaja Divya et al. 2015). All three concentrations decreased ISGU (Padmaja Divya et al. 2015) While 0.5 μM of arsenite showed no significant reduction in the expression of GLUT4 in 3T3-L1 adipocytes or C2C12 myotubes, both 1 and 2 μM arsenite decreased GLUT4 expression in these cell lines (Padmaja Divya et al. 2015). Notably, mitochondrial membrane potential was also reduced in 2 μM arsenite treatment in both 3T3-L1 adipocytes and C2C12 myotubes (Padmaja Divya et al. 2015). This observation coincided with the decreased expression of protein deacetylase SIRT3 and the recruitment of FOXO3A, a transcription factor that regulates reactive oxygen species (ROS) metabolism, to its binding sites in the manganese superoxide dismutase (MnSOD) and PGC1α gene (Sundaresan et al. 2009). Overexpression of SIRT3 and MnSOD in C2C12 myotubes enhanced mitochondrial membrane potential and restored ISGU that was shown to be suppressed by arsenite (Padmaja Divya et al. 2015). Interestingly, SIRT3 appeared to deacetylate FOXO3A, MnSOD and PGC1α (Padmaja Divya et al. 2015). The deacetylation of FOXO3A at the lysine 100 residue was upregulated with arsenic exposure in C2C12 myoblasts, which promoted FOXO3A's nuclear localization and subsequent inactivation (Padmaja Divya et al. 2015). *In vitro*, arsenite has been shown to inhibit SIRT3-FOXO3A signaling to reduce mitochondria activity and impair ISGU (Padmaja Divya et al. 2015).

Arsenite exposure has widespread metabolic effects, also influencing peripheral glucose uptake in the central nervous system (Rodríguez et al. 2016). The brain has an obligate glucose requirement and therefore is especially vulnerable to impairments to glucose transporters (GLUT1 and GLUT3) required for glucose to cross the blood brain barrier and be delivered to neurons (Rodríguez et al. 2016). Recent findings reported male C57BL/6J mice exposed to 50 ppm for 1-month experienced a decrease in GLUT1 and GLUT3 mRNA levels in the brain, despite a lack of significant change of serum glucose concentrations (Rodríguez et al. 2016). Interestingly, arsenite administration significantly increased insulin receptor expression in the hippocampus (Rodríguez et al. 2016). However, it is unclear whether the change in glucose tolerance was due to the reduction of GLUT1 and GLUT3 expression in hippocampus (Rodríguez et al. 2016).

A recent study showed impaired brown adipose tissue activity (BAT) in female C57BL/6J exposed to 5 or 20 ppm arsenic for 17 weeks (Zuo et al. 2019). While these mice experienced no changes in body weight, BAT mass was significantly elevated in the 5 ppm exposure group, with

significantly increased adipocyte droplets based on histopathological analysis (Zuo et al. 2019). Moreover, insulin levels were significantly elevated at both concentrations of exposure, with a significant decrease in genes involved in thermogenesis (UCP1 and PGC1α) and mitochondrial respiratory chain activity (COX IV and NDUFS4) (Zuo et al. 2019).

Studies focused on arsenic's effects on ISGU have most frequently relied on 3T3-L1 adipocytes to demonstrate impaired effects at both high and low exposures (Figure 3). Skeletal muscle, however, is primarily responsible for the majority of insulin-dependent glucose utilization in the body (DeFronzo 2009). The only cell culture model used to study the effects of arsenic on myotubes is C2C12 myotubes, and arsenite exposure has also been shown to impair C2C12 differentiation *in vitro* (Hong and Bain 2012). Future studies should focus on the effects of arsenic on primary myotubes isolated from both rodents and humans. A recent study reported impaired skeletal muscle function, myofiber hypertrophy, mitochondrial myopathy, and altered oxygen consumption after 5-week arsenite exposure (100 ppb) in 5-6 week old C57BL/6NTac male mice (Ambrosio et al. 2014). While these *in vivo* findings support the evidence found in cultured myotubes (C2C12), additional studies will provide valuable insight regarding arsenic toxicity.

The network analyses performed in this review support experimental findings, and highlight genes involved in insulin resistance and metabolic disorders. These include insulin, insulin receptor substrate 1 and 2, and heme oxygenase 1 (Figure 4). Arsenic's effects on alterations in gene expression associated with these pathways can have deleterious effects on ISGU and whole body glucose homeostasis, as demonstrated in Figures 2 and 3.

Hepatic Glucose Metabolism and Insulin Signaling

The liver is a key target tissue for arsenic-induced insulin resistance due to its role in both arsenic metabolism and glucose production. Insulin suppresses hepatic gluconeogenesis and glycogenolysis, which are impaired in T2D (Basu et al. 2004). Gluconeogenesis is mainly regulated by the modulation of the transcription of rate-controlling enzymes in the pathway, such as phosphoenolpyruvate carboxykinase (PCK1) and the catalytic subunit of glucose 6 phosphatase (G6PC) (Pilkis and Granner 1992). Insulin inhibits the transcription of both PCK1 and G6PC. To inhibit glycogenolysis, insulin activates protein phosphatase 1 (PP1) that inhibits glycogen phosphorylase, which catalyzes the rate-limiting step of glycogenolysis (Petersen et al. 2017).

Identified studies showed that treating C57BLKS/$J^{db/m}$ and C57BLKS/$J^{db/db}$ male mice with 3 ppm arsenite for 16 weeks increased PCK1 overexpression (Liu et al. 2014). Protein levels of Na^+K^+-ATPase in the liver were increased in arsenite treated mice (Liu et al. 2014). Arsenite treatment did not affect FBG levels in C57BLKS/$J^{db/m}$ mice. However, arsenite treatment elevated fasting glucose levels in C57BLKS/$J^{db/db}$ mice (Liu et al. 2014). The rate of gluconeogenesis and glycogenolysis was not measured in this study (Liu et al. 2014). Thus, the exact mechanism governing the elevation of FBG is unclear in C57BLKS/$J^{db/db}$ mice.

A recent study reported a dose-dependent decrease in glycogen content in mouse primary hepatocytes treated with low-dose (0.5-2 μM) arsenite for 4 hrs (Zhang et al. 2017). Exposure to arsenite resulted in a dose-dependent reduction in insulin-dependent activation of glycogen synthase (GS), the rate-controlling enzyme in glycogenesis, and activation of glycogen phosphorylase (GP), the rate-controlling enzyme in glycogenolysis (Zhang et al. 2017). Notably, arsenite treatment for 4 hrs also inhibited insulin stimulated AKT phosphorylation at serine 308 and 473, characteristic of AKT activity (Zhang et al. 2017). In contrast, the activity of GSK3, a downstream effector of AKT, was not affected by exposure to arsenite (Zhang et al. 2017). Inhibition of insulin-dependent AKT phosphorylation has also been reported *in vivo,* corroborating

in vitro findings in both hepatocytes and adipocytes (Chakraborty et al, 2012).

The dose and duration of arsenic treatment *in vitro* can be a critical factor in identifying targets of arsenic toxicity relevant to human exposures. A study found that chronic treatment in mice (8 weeks) with high arsenite exposure (150 ppm) resulted in hepatic damage, with observed tissue necrosis and significantly elevated serum glutamate-pyruvate transaminase (SGPT) (Noman et al. 2015). HepG2 human hepatoma cells have been used as a model to study both the long- and short-term effects of arsenite on insulin signaling. While a 1h exposure to arsenite at concentrations up to 1 mM did not alter cell viability, the authors observed a decrease in GSH (Hamann et al. 2014). Conversely, cell viability was greatly reduced after 24 hrs of arsenite treatment (Hamann et al. 2014). Notably, HepG2 cells treated with 3 or 10 μM of arsenite for 24 hrs attenuated insulin's ability to activate AKT (Hamann et al. 2014). The phosphorylation of IR by insulin was reduced with exposure to 10 μM, but not 3 μM of arsenite (Hamann et al. 2014). Similar to findings from murine primary hepatocytes, arsenite treatment did not induce changes in GSK3 activity (Hamann et al. 2014). The phosphorylation of another insulin-induced downstream effector of AKT, FOXO1, was also not affected by arsenite treatment (Hamann et al. 2014). Surprisingly, while insulin inhibits the expression of G6PC in healthy individuals (Hutton and O'Brien 2009), 24 hrs of arsenite treatment (1, 3 and 10 μM) also significantly suppressed G6PC expression (Hamann et al. 2014). The combinatorial effect of insulin and arsenite on G6PC expression, however, was not examined. For short-term exposures, HepG2 cells treated with 100 and 300 μM of arsenite for 1h induced both AKT and FOXO1 phosphorylation (Hamann et al. 2014). Thus, in contrast to the inhibitory effect on insulin action observed after 24 hr arsenite treatment, 1h arsenite treatment mimicked insulin-like signaling (Hamann et al. 2014). These findings highlight how the duration of arsenite exposure *in vitro* may have significant implications on our interpretation of epidemiologic findings.

Additional studies assessing arsenic's effects on hepatic glucose regulation are needed. While the current literature is sparse, studies suggest that low dose arsenite treatment of more than 4 hrs may alter insulin's anabolic activity in hepatocytes *in vitro*. The network analyses highlight genes involved in hepatic lipid metabolism and inflammation, such as SIRT1 and SREBP (Figure 5). This however, contrasts findings that report arsenic to have insulin-mimetic properties at high doses during acute exposures. The chemical's pronounced effects on liver function, hepatic steatosis, and injury, have also been widely reported in murine models (Ditzel et al. 2015; Shi et al. 2014; Noman et al. 2015). However, whether arsenic exposure modulates gluconeogenesis and glycogenolysis *in vivo* remains unexplored.

Glucose Stimulated Insulin Secretion (GSIS) and β-cell Function

Pancreatic β-cells respond to elevated plasma glucose levels to secrete insulin, which in turn stimulates glucose utilization in skeletal muscle and white adipose tissue (Figure 7). This process allows mammals to maintain plasma glucose levels in a narrow range of homeostasis. Identified studies showed that treating 8-week old C57BL/6J male mice with 50 ppm arsenite for 8-weeks resulted in impaired glucose tolerance (Kirkley et al. 2017). Whereas no differences in peripheral insulin sensitivity were observed between groups, arsenic-treated mice experienced a reduction in GSIS compared to controls (Kirkley et al. 2017). High dose exposure did not affect pancreatic β-cell mass or structure, suggesting that arsenite affects β-cell function (Kirkley et al. 2018). The ability of arsenic to induce reactive oxygen species (ROS) and free radicals has been previously reported in human fibroblast cells (Hu et al. 2002). The pancreas has low antioxidant capabilities, and therefore may be especially vulnerable to arsenic-induced oxidative stress (Keane

et al. 2015). INS-1 832/13 cells treated with low-dose arsenite for 24 hrs decreased both GSIS and mitochondrial respiration in a dose-dependent manner (Dover et al. 2018). Low levels (0.25 and 0.5 μM) of arsenite treatment for 96 hrs dampened glucose-induced insulin secretion in INS-1 832/13 rat pancreatic β-cells by activating NRF2 activity, which activates the transcription of genes involved in antioxidant defenses. Once activated, these genes decreased endogenous peroxide production necessary for adequate glucose induced insulin secretion (Fu et al. 2010). Arsenite treatment did not affect insulin gene expression in this report, which suggests that the secretion of insulin, but not its synthesis, is the target of arsenic toxicity (Fu et al. 2010). Additional studies report similar findings, as arsenic attenuates glucose stimulated insulin secretion without affecting insulin synthesis (Figure 3) (Douillet et al. 2013; Díaz-Villaseñor et al. 2008). Another report, however, shows that high levels of sodium arsenite treatment (5 μM) for 72 and 144 hrs in pancreatic β-cells isolated from male Wistar rats resulted in significantly lower insulin gene expression (54 and 72 percent, respectively) (Díaz-Villaseñor et al. 2006). These dose of treatment also requires careful consideration, as 5 μM significantly decreased pancreatic β-cell viability after 144 hrs, but not 72 hrs (Díaz-Villaseñor et al. 2006).

Arsenite may reduce GSIS by interfering with calcium-mediated signaling required for insulin secretory granule exocytosis (Figure 7). Calpains are calcium-sensing proteases that activate proteins such as SNAP25, involved in insulin secretory vesicle exocytosis (Marshall et al. 2005). SNAP25 and CALPAIN10 both mediate the fusion of insulin granules with the plasma membrane (Marshall et al. 2005). While low-dose (0.5-1 μM) arsenite treatment of RINm5F rat pancreatic β-cells for 72 hrs did not decrease CAPLAIN10 activity with either 5.6 or 15.6 mM stimulation, CALPAIN10 activity was significantly increased only at 2 μM (Díaz-Villaseñor et al. 2008). Treatment with 1 μM arsenite during insulin-stimulated glucose secretion *in vitro* decreased calpain activity, measured as SNAP-25 proteolysis (Díaz-Villaseñor et al. 2008). Oddly, 2 μM arsenite treatment did not affect calpain activity. While CALPAIN10 activity was significantly increased only after 2 μM arsenite treatment, its activity was trending upward starting at 0.5 μM (Díaz-Villaseñor et al. 2008). Arsenite concentrations at 1, 2, and 5 μM significantly reduced cell viability (Díaz-Villaseñor et al. 2008).

Endoplasmic reticulum (ER) stress is an additional mechanism involved in impaired GSIS (Hasnain et al. 2016). Sodium arsenite (4 μM) treatment in INS-1 cells for 3, 6, 12, and 24 hrs activated ER stress, as measured by PERK activity (Wu et al. 2018). Treating arsenite-treated pancreatic islets with PERK inhibitor restored the capacity of glucose stimulated insulin secretion (Wu et al. 2018). This finding suggests arsenite-induced ER stress can suppress glucose stimulated insulin secretion (Figure 3). The induction of ER stress and autophagy is likely to be cell autonomous, as treating INS-1 rat insulinoma cells with arsenite (4 μM) for 6 hrs potentiated PERK activity and altered the expression of autophagy makers (Wu et al. 2018).

Oxidative stress induced by arsenite treatment in β-cells has been shown to induce apoptosis. INS-1 832/13 pancreatic β-cells treated with sodium arsenite (2.5-10 μM) exhibited increased intracellular ROS levels and apoptosis (Pan et al. 2014). Arsenite exposure also significantly reduced mitochondrial membrane potential and lysosomal membrane composition (Pan et al. 2014). Low-dose arsenite (0.25-1 μM) exposure in INS-1 832/13 pancreatic β-cells for 96 hrs decreased cell viability and thioredoxin reductase (TRX) activity in a dose-dependent manner (Yao et al. 2015). TRX is an enzyme that protects cells from oxidative damage and also associates and suppresses the activity of ASK1, a protein kinase involved in apoptosis (Soga et al. 2012). Indeed, the levels of ASK1 protein were increased in cell culture media upon arsenite

treatment (Yao et al. 2015). Moreover, reducing ASK1 expression by RNA interference attenuated arsenite-induced cytotoxicity (Yao et al. 2015). Thus, arsenic reduced TRX activity, which in turn activated ASK1 to induce apoptosis in INS-1 cells. Notably, although NRF2 activation reduced GSIS as previously described, NRF2-induced antioxidant response has been shown to be involved in protecting pancreatic β-cells from arsenic-induced cellular damage. Both NRF2-knockdown MIN6 pancreatic β-cells and pancreatic islets isolated from NRF2-knockout mice experienced increased cytotoxicity upon 2-6 hrs of arsenite (2-10 μM) treatment (Yang et al. 2012). MIN6 NRF1-knockdown cells also had decreased antioxidant capabilities (Cui et al. 2017). *In vitro* findings showed arsenite treatment decreased cell viability (1-20 μM for 24 hrs) and enhanced expression of genes involved in arsenic metabolism (Cui et al. 2017). These results further corroborate the role of arsenite-induced oxidative stress in pancreatic β-cell apoptosis. HepG2 cells treated with low-dose arsenite (0.13-2 μM) for 24 hrs experienced a significant rise in C-reactive protein (CRP), which is secreted in response to increased inflammation (Druwe et al. 2012). These experimental findings are consistent with the increased levels of CRP observed in FVB female mice treated with 100 ppb via drinking water for 22 weeks (Druwe et al. 2012). Another study found 16-week arsenite (3 ppm) exposure increased inflammation, ROS, and vacuole formation in pancreatic islet of db/m mice, and further exacerbated these conditions in db/db mice (Liu et al. 2014).

In vivo studies that assess the effect of arsenic on the pancreas are conducted by exposing rodents at ppm levels for a duration of at least 8 weeks. Several of these studies showed that arsenic treatment increased pancreatic damage, which is in agreement with *in vitro* studies that report exposures starting at 1 μM to induce apoptosis. Most studies (Díaz-Villaseñor et al. 2008; Douillet et al. 2013; Díaz-Villaseñor et al. 2006; Hamann et al. 2014) that treat with arsenic levels > 1 μM report a reduction in GSIS, which supports dose-specific effects on glucose homeostasis (Figure 3). Studies suggest that lower dose and/or shorter exposure duration (Fu et al. 2010; Yao et al. 2015; Wu et al. 2018; Pan et al. 2014) affect the ability of pancreatic β-cells inflammation, with decreased pancreas weight (Liu et al. 2014; Kirkley et al. 2017). Discrepancies in experimental findings reported across animal studies may also be due to different susceptibilities across animal strains and species (Gentry et al. 2004). Several mechanisms were identified as mediating arsenic-induced β-cell apoptosis, including upregulated oxidative and ER stress (Figure 3). Interestingly, arsenic activation of NRF2 may inhibit endogenous ROS necessary for glucose uptake and insulin secretion (Xu et al. 2012). However, the activation of NRF2 also protects β-cells from apoptosis (Masuda et al. 2015), and therefore has multiple implications in maintaining glucose homeostasis at various arsenic exposure concentrations. The network analyses performed reveal 5 genes associated with oxidative stress and inflammatory responses, including C3, TNF, NOS3, HMOX1 and SOD2 (Figure 5). Further investigation of these mechanisms at chronic low doses relevant to human exposures are necessary going forward (Hectors et al. 2011).

Adipose Tissue Function

White adipose tissue is the primary organ responsible for the storage of lipids in the form of triglycerides. Increased lipolysis contributes to ectopic lipid deposition in target tissues involved in glucose metabolism, such as the liver and skeletal muscle (Rosen and Spiegelman 2006), Ectopic lipid deposition is one of the major mechanisms of insulin resistance. Thus, both excess storage of lipids in white adipose tissue, such as obesity, and lipodystrophy, have significant effects on insulin sensitivity and glucose homeostasis (Rosen and MacDougald 2006; Rosen and Spiegelman 2006). Adipose tissue is also an endocrine organ that secretes various adipokines to

modulate metabolic functions (Coelho et al. 2013; Kershaw and Flier 2004). Both *in vivo* and *in vitro* studies have found arsenic treatment to modulate adipocyte function and differentiation (Figures 2 and 3, respectively). Exposure to arsenite (5 or 50 ppm) in 4-week old C57BL/6J male mice for 18 weeks significantly decreased serum adiponectin levels (Song et al. 2017), a key adipokine in insulin sensitivity (Rosen and Spiegelman 2006; Ye and Scherer 2013). However, it remains unclear whether the reduction of plasma adiponectin levels contributes to arsenic's effects.

Most of the *in vivo* studies of chronic arsenite exposure found in our search showed no significant differences in weight gain or overall body mass (Figure 2) (Adebayo et al. 2015; Ambrosio et al. 2014; Kirkley et al. 2017; Song et al. 2017). Treating 5-6 week old C57BL/6J male mice with (100 ppb) arsenite for 5 weeks induced lipid mobilization that resulted in elevated ectopic accumulation of lipids in skeletal muscle (Garciafigueroa et al. 2013). Treating adipocytes differentiated from human mesenchymal stem cells with 1 μM arsenite for 72 hrs increased glycerol release, an indicator of the lipolytic activity in adipocytes (Garciafigueroa et al. 2013). Interestingly, arsenite treatment also results in lower expression of PERILIPIN1, a lipid droplet protein found in adipocytes (Garciafigueroa et al. 2013). These responses were reduced by pertussis toxin, an inhibitor of Gi-α subunit of heterotrimeric G protein. Indeed, antagonizing Gi-coupled endothelin-1 type A receptor attenuated arsenite's lipolytic response, whereas antagonizing endothelin-1 type B receptor reduced the ability of arsenite to suppress PERILIPIN1 expression (Garciafigueroa et al. 2013). These results suggest that arsenic modulates PERILIPIN1 expression and lipolysis through different mechanisms (Figure 3). PERILIPIN1 does, however, play an important role in the regulation of lipolysis in adipocytes (Sztalryd and Brasaemle 2017). PERILIPIN1 associates with and inhibits adipocyte triglyceride lipase (ATGL), an enzyme that hydrolyzes triacylglycerol to diacylglycerol. Upon the induction of protein kinase A (PKA) signaling by norepinephrine, PERILIPIN1 is phosphorylated by PKA, which prompts its dissociation from ATGL. Phosphorylated PERILIPIN1 subsequently recruits phosphorylated hormone sensitive lipase, which hydrolyzes diacylglycerol to monoacylglycerol. This process enhances lipolysis in adipocytes. Thus, reducing the expression of PERILIPIN1 will result in the augmentation of basal lipolysis, yet also attenuate norepinephrine-cAMP induced lipolysis.

Adipocyte number (hyperplasia) and size (hypertrophy) are important features of white adipose tissue. 5-week arsenite exposure (100 ppb) *in vivo* was shown to reduce adipocyte numbers in white adipose tissue (Garciafigueroa et al. 2013). These results suggest arsenite treatment impairs adipogenesis (Figure 3). Pertussis toxin and antagonists of endothelin-1 type A and B receptors reduced arsenite's ability to inhibit human mesenchymal stem cells (hMSCs) differentiation into adipocytes (Klei et al. 2012). Moreover, reduced expression of endothelin-1 type A and B receptors in pre-adipocytes attenuated arsenite-inhibited adipogenesis (Klei et al. 2012). These results suggest that the ability of arsenite to inhibit adipogenesis, like its effect on lipolysis, requires, or at least in part, endothelin-1 type A and B receptors.

A multitude of studies observe the suppressive effect of arsenite on adipogenesis (Figure 3) (Ceja-Galicia et al. 2017; Hou 2012; Trouba et al. 2000; Wauson et al. 2002). Arsenite (0.2-4 μM) treatment of hMSCs impaired differentiation to adipocytes (Yadav et al. 2012). Perhaps unsurprisingly, the expression of transcription factors involved in adipogenesis, such as peroxisome proliferator-activated receptor γ (PPARγ) and CCAAT-enhancer binding protein α and β (C/EBPα and C/EBPβ), were also reduced, whereas the expression of adipogenic inhibitor Wnt3a was increased (Yadav et al. 2012). Arsenite treatment in 3T3-L1 pre-adipocytes also suppressed differentiation to adipocytes (Hou et al. 2013). Arsenite treatment resulted in higher levels of CCAAT-enhancer-binding protein homologous protein-10, CHOP10, an endoplasmic

reticulum (ER)-stress response protein involved in the unfolded protein response (UPR) (Hou et al. 2013). CHOP10 is a negative regulator of C/EBPβ, which acts upstream of PPAR actors involved in adipogenesis, such as PPARγ and C/EBPα in the transcriptional cascade regulating adipogenesis (Hou et al. 2013). C3H 10T1/2 pre-adipocytes exposed to sodium arsenite (6 mM) for 8 weeks also experienced altered morphology and impaired differentiation (Trouba et al. 2000). Arsenite-treated human hMSCs (1 μM for 24 and 48 hrs) exhibited significantly altered function of non-coding microRNA involved in adipogenesis (Beezhold et al. 2017; Renu et al. 2018). Both culture adipocytes and primary hMSCs isolated from mice treated with arsenite *in vivo* (100-250 ppb) increased miR-29 and CYCLIND expression, furthering cell growth rather than adipogenic differentiation (Beezhold et al. 2017).

Recent findings suggest low and moderate dose arsenite exposure induces lipolysis and impairs adipogenesis (Renu et al. 2018). Mechanistic studies indicate a dose-dependent inhibition of adipocyte differentiation, altering critical pro-adipogenic programming (Figure 3). Arsenic's effects in adipose tissue also manifest in increased ectopic lipid deposition in both the liver and skeletal muscle, which could contribute to the development of insulin resistance (Renu et al. 2018). Gene lists obtained from our network analyses complement findings in both *in vivo* and *in vitro* studies, and support adipose tissue as a target of arsenic toxicity. Many of the genes highlighted in the network analyses (Figure 5) are directly involved in adipogenesis, altered energy storage, adipokine secretion, and ectopic lipid deposition, further supporting the experimental evidence reported. Figure 5 lists the pathways related with arsenic-induced insulin resistance and also depicts the interaction network of both these pathways and select genes identified.

Trivalent Arsenical Metabolites – DMA^{3+} and MMA^{3+}

Since epidemiologic studies have reported the association of arsenic and T2D, the primary focus of laboratory research in the context of diabetes has relied on the parent compound as the chemical of exposure (Castriota et al. 2018; Farzan et al. 2017; Grau-Perez et al. 2017; Pan et al. 2013; Peng et al. 2015). Recent evidence however, has shown trivalent arsenical species to interfere with metabolic pathways responsible for glucose homeostasis. A dose-dependent decrease in mitochondrial respiration associated with GSIS in INS-1 832/13 pancreatic β-cells was observed for both arsenite and MMA^{3+}, but not for DMA^{3+} (Dover et al. 217). MMA^{3+} decreased GSIS in INS-1 cells after 24-hr exposure at both 0.375 and 0.5 μM (Dover et al. 2017). There was however, no significant decrease observed upon 24 hr DMA exposure, even at the highest dose (Dover et al. 2017). This research highlights key differences in the effects of arsenical species on GSIS, warranting increased laboratory research on this pathway.

4 hr exposure to arsenite and MMA^{3+} concentrations as low as 0.5-2 μM decreased glycogen levels in insulin-stimulated in primary murine hepatocytes by interfering with rate-limiting glycogenesis genes GS and GP, and increasing glucose output (Zhang et al. 2017). Both arsenite and MMA^{3+} downregulated GS and upregulated GP, in addition to inhibiting AKT phosphorylation, insulin's regulatory step for glycogen synthesis (Zhang et al. 2017). This finding parallels results of arsenic-treated adipocytes, with impaired AKT-dependent GLUT4 mobilization in trivalent arsenical-treated 3T3-L1 pre-adipocytes (Walton et al. 2004).

3T3-L1 pre-adipocytes, SVCs, and human adipose tissue-derived stem cells (hADSCs), treated with low concentrations of DMA^{3+} (≤ 2 μM) or MMA^{3+} (≤ 1 μM) all experienced impaired adipogenesis mediated by UPR and ER stress (Hou et al. 2013). While arsenite and MMA^{3+} interfered with adipogenesis via CHOP10 in the early stages of differentiation, DMA^{3+}

did not, suggesting its anti-adipogenic effects are mediated via a different target (Hou et al. 2013). In addition, greater cytotoxicity was observed for both MMA^{3+} and DMA^{3+} in 3T3-L1 pre-adipocytes, SVCs, and hADSCs, compared to arsenite (Hou et al. 2013). Future research should focus on the specific effects of trivalent arsenical metabolites on metabolic pathways to increase our understanding of the diabetogenic potential of arsenic metabolism, and its intermediates.

Discussion

Our review of the literature on the laboratory research of arsenite exposure and its effects on glucose homeostasis suggests that several mechanisms may be involved, including insulin-stimulated glucose uptake, glucose-stimulated insulin secretion, hepatic glucose metabolism, and adipose and pancreatic β-cell dysfunction. Arsenite has wide physiological effects, affecting multiple metabolic organs involved in glucose homeostasis. Although the effects of arsenic exposure on the integrity and the physiology of various tissues are reported (Figure 2), the molecular mechanisms underlying these findings are mostly unknown. The *in vitro* studies and targets identified via *–omic* databases of publicly available data have the potential to unravel these mechanisms. Different strains of rodents that respond to arsenic differently could also be utilized. The expert panel assembled by the NTP has therefore, encouraged researchers to assess arsenic's metabolic effects in strain susceptible to these metabolic endpoints (Maull et al. 2012).

Current advances in *omics* technologies have been paralleled with the use of publicly available databases. Together, these tools have the ability to expand our understanding of chemically-induced diseases. A recent study on the use of CTD for the creation of adverse outcome pathways assessed arsenical exposures and dysregulation of glucose homeostasis as one of its primary case studies (Davis et al. 2018). This further emphasizes the relevance of elucidating potential mechanisms of action for a relevant topic in the fields of comparative toxicogenomics and environmental epidemiology (Davis et al. 2018). We were able to identify 16 genes commonly affected by sodium arsenite, insulin resistance, and T2D.

Evidence from *in vitro* and *in vivo* studies suggest that arsenite interferes with signaling involved in glucose uptake and insulin secretion, downregulating molecular targets such as AKT and glucose transporters (GLUT 1, 3, 4), and calcium signaling pathways involved in insulin exocytosis and secretion from pancreatic β-cells, respectively. Arsenite has been shown to interfere with adipogenesis, which has implications for altered energy storage and ectopic lipid deposition. Hepatic manifestations are also present upon exposure, with the upregulation of PCK1 and other rate-limiting enzymes of gluconeogenesis (Liu et al. 2014). Trivalent methylated arsenical metabolites MMA and DMA share similar effects to their parent compound, interfering with metabolic pathways involved in glucose homeostasis (Zhang et al. 2017; Hou et al. 2013; Douillet et al. 2013).

The 16 genes identified in our CTD analysis encode proteins that are involved in glucose homeostasis, oxidative stress, inflammation, lipid metabolism, energy balance, lipid metabolism, and adipogenesis, among other processes. Midst these targets, insulin, insulin receptor, insulin receptor substrate 1 and 2 (IRS1 and IRS2, respectively) and SLC2A4 (also known as GLUT4) are components of the insulin signaling pathway that regulate glucose utilization in peripheral tissues. Leptin and leptin receptor are components of leptin signaling, which increases satiety and controls energy balance. PPARγ encodes a nuclear receptor that positively regulates insulin sensitivity (Rosen and Spiegelman 2006). Thiazolidinediones (TZD), a class of anti-diabetic drugs, act as agonists of PPARγ (Tontonoz and Spiegelman 2008). SIRT1 encodes a protein deacetylase,

which positively regulates insulin sensitivity. As discussed above, adiponectin (ADIPOQ) encodes a hormone secreted from white adipose tissue that improves insulin sensitivity (Rosen and Spiegelman 2006). An additional 5 genes (C3, TNF, NOS3, HMOX1 and SOD2) encode proteins involved in the inflammatory response. SOD2 (MnSOD) protein also clears mitochondrial ROS to reduce oxidative stress (Padmaja Divya et al. 2015). Interestingly, this analysis indicates that advanced glycosylated end products (AGEs) bind to their receptors (RAGEs), which can activate inflammatory pathways.

Conclusions and Future Directions

While epidemiology studies have linked arsenic exposure to the development of T2D in populations worldwide, the current mechanism by which arsenic contributes to dysregulation of glucose homeostasis remains elusive in humans despite well-established laboratory models. In the last two decades, efforts have focused on assessing arsenic's effects on metabolic target tissues, including the pancreas, adipose, liver, and skeletal muscle. Most *in vivo* studies have relied on rodents, administering higher arsenite concentrations at ppm levels due to the species' accelerated arsenic metabolism compared to humans. Nonetheless, it is critical to model our experimental designs to internal doses that are relevant to human health and exposures. Human exposure assessment is also limited by the measurement of total arsenic concentration, which also include organic arsenicals that are not considered hazardous to human health and irrelevant to toxicity associated with inorganic arsenic exposures.

Inconsistencies in the literature highlight the need for additional research characterizing the metabolic effects at chronic, low-dose exposures. High exposure *in vivo* studies have shown that arsenic treatment alone can reduce GSIS (Liu et al. 2014; Kirkley et al. 2017). High exposure *in vivo* studies report arsenic treatment alone to affect glucose homeostasis by damaging the integrity of the pancreas, and reducing GSIS (Liu et al. 2014). However, lower dose arsenite treatment alone has been found to exacerbate genetic and diet-induced insulin resistance and impaired glucose tolerance (Liu et al. 2014; Ditzel et al. 2015; Paul et al. 2011). *In vitro* studies on pancreatic β-cells mostly confirm that high dose arsenic exposure increases apoptosis, whereas low dose arsenic inhibits GSIS (Pan et al. 2014; Lu et al. 2011; Díaz-Villaseñor et al. 2008). Many other *in vitro* results, however, require the corroboration of *in vivo* studies. For example, arsenic has been shown to affect ISGU in adipocytes and myotubes, increasing the breakdown of glycogen in hepatocytes, and reducing insulin signaling in these cell types (Padmaja Divya et al. 2015). However, the effects of arsenic on peripheral glucose utilization and hepatic glucose production and insulin signaling *in vivo*, have not been extensively explored. Another area of increasing interest is the interaction between arsenic and obesity, as an excess body mass index is a causal factor for T2D development. Recent suggest a synergistic relationship with chronic arsenic exposure and obesity on T2D, with obese individuals being the most susceptible to T2D development (Castriota et al, 2018).

We used publicly available *omics* data and performed pathway identification using online tools to validate the relationship between arsenic and T2D, complementing experimental findings. This analysis resulted in the identification of key genes and pathways involved in arsenite-induced insulin. These data-driven approaches can assist researchers to harmonize, summarize, and structure existing mechanistic knowledge underlying arsenite-induced dysregulation of glucose homeostasis. These techniques can identify knowledge gaps and aid in the development of more focused study designs.

Insulin resistance is a chronic condition with epidemic proportions. The increasing prevalence of T2D both domestically and worldwide, in addition to arsenic's widespread exposure, motivates our efforts to determine arsenic's contribution to the etiology of this metabolic disorder (Zimmet et al. 2016). We hope this review will help to inform public health interventions due to the growing burden of T2D and ongoing arsenic exposure in vulnerable communities worldwide.

Glossary

ADIPOQ	Adiponectin
ASK1	Apoptosis signal-regulating kinase 1
ATGL	Adipocyte triglyceride lipase
C/EBP	CCAAT-enhancer-binding protein alpha and beta
CHOP10	CCAAT-enhancer-binding protein homologous protein-10
DMA^{3+}	Dimethylarsinous acid
EPA	Environmental Protection Agency
ER	Endoplasmic reticulum
FBG	Fasting Blood Glucose
FOXO	Forkhead box transcription factor
G6Pase	Glucose-6-phosphatase
GLUT	Glucose transporter type
GSH	Glutathione
GSIS	Glucose stimulated insulin secretion
GSK3	Glycogen synthase kinase 3
GTP	Guanosine triphosphate
hADSCs	Human adipose tissue-derived stem cells
hMSCs	Human Mesenchymal Stem Cells
HOMA-IR	Homeostatic model assessment of insulin resistance
IR	Insulin receptor
IRS1	Insulin receptor substrate 1
ISGU	Insulin Stimulated Glucose Uptake
MAPK	Mitogen-activated protein kinase
MMA^{3+}	Methylaronous acid
NRC	National Resource Council
NRF1/2	Nuclear factor-erythroid related factor 1/2
NTP	National Toxicology Program
PEPCK	Phosphoenolpyruvate carboxykinase
PERK	Eukaryotic translation initiation factor 2 alpha kinase 3
PGC1α	Peroxisome proliferator activated receptor gamma coactivator 1 alpha
PI3K	Phosphoinositide 3-kinase
PIP3	Phosphatidylinositol 3,4,5-triphosphate
PKB/AKT	Protein kinase B
PPARγ	Peroxisome proliferator activated receptor gamma
PPB	Parts per billion (μg/L)
PPM	Parts per million (mg/L)
ROS	Reactive oxygen species
SIRT3	Sirtuin 3
SLC2A4	Glucose transporter type-4
SNAP25	Synaptosome associated protein 25
SOD2	Manganese-dependent superoxide dismutase 2
SREBP	Sterol regulatory element-binding protein
SVCs	Stromal vascular cells
T2D	Type 2 diabetes

TRX	Thioredoxin reductase
UPR	Unfolded protein response
WHO	World Health Organization

References

Adebayo AO, Zandbergen F, Kozul-Horvath CD, Gruppuso PA, Hamilton JW. 2015. Chronic Exposure to Low-Dose Arsenic Modulates Lipogenic Gene Expression in Mice: Arsenic Effect on Lipid-Regulating Genes. J Biochem Mol Toxicol 29:1–9; doi:10.1002/jbt.21600.

Agusa T, Fujihara J, Takeshita H, Iwata H. 2011. Individual Variations in Inorganic Arsenic Metabolism Associated with AS3MT Genetic Polymorphisms. Int J Mol Sci 12:2351–2382; doi:10.3390/ijms12042351.

Ambrosio F, Brown E, Stolz D, Ferrari R, Goodpaster B, Deasy B, et al. 2014. Arsenic induces sustained impairment of skeletal muscle and muscle progenitor cell ultrastructure and bioenergetics. Free Radic Biol Med 74:64–73; doi:10.1016/j.freeradbiomed.2014.06.012.

ATSDR (U.S. Department of Health and Human Services, Public health Service, Agency for Toxic Substances and Disease Reigstry, Atlanta, GA). 2007. Toxicological Profile for Arsenic. (Available): <https: https://www.atsdr.cdc.gov/toxprofiles/tp2.pdf>

Basu R, Basu A, Johnson CM, Schwenk WF, Rizza RA. 2004. Insulin Dose-Response Curves for Stimulation of Splanchnic Glucose Uptake and Suppression of Endogenous Glucose Production Differ in Nondiabetic Humans and Are Abnormal in People With Type 2 Diabetes. Diabetes 53:2042–2050; doi:10.2337/diabetes.53.8.2042.

Bazuine M, Ouwens DM, Gomes de Mesquita DS, Maassen JA. 2003. Arsenite stimulated glucose transport in 3T3-L1 adipocytes involves both Glut4 translocation and p38 MAPK activity. Eur J Biochem 270(19):3891-3903; doi: 10.1046/j.1432-1033.2003.03771.x

Beezhold K, Klei LR, Barchowsky A. 2017. Regulation of cyclin D1 by arsenic and microRNA inhibits adipogenesis. Toxicol Lett 265:147–155; doi:10.1016/j.toxlet.2016.12.002.

Bindea G, Mlecnik B, Hackl H, Charoentong P, Tosolini M, Kirilovsky A, et al. 2009. ClueGO: a Cytoscape plug-in to decipher functionally grouped gene ontology and pathway annotation networks. Bioinformatics 25:1091–1093; doi:10.1093/bioinformatics/btp101.

Castriota F, Acevedo J, Ferreccio C, Smith AH, Liaw J, Smith MT, et al. 2018. Obesity and increased susceptibility to arsenic-related type 2 diabetes in Northern Chile. Environ Res 167:248–254; doi:10.1016/j.envres.2018.07.022.

Ceja-Galicia ZA, Daniel A, Salazar AM, Pánico P, Ostrosky-Wegman P, Díaz-Villaseñor A. 2017. Effects of arsenic on adipocyte metabolism: Is arsenic an obesogen? Mol Cell Endocrinol 452:25–32; doi:10.1016/j.mce.2017.05.008.

Chakraborty D, Mukherjee A, Sikdar S, Paul A, Ghosh S, Khuda-Bukhsh AR. [6]-Gingerol isolated from ginger attenuates sodium arsenite induced oxidative stress and plays a corrective role in improving insulin signaling in mice. Toxicol Lett 210(1): 34-43. doi: 10.1016/j.toxlet.2012.01.002

Coelho M, Oliveira T, Fernandes R. 2013. State of the art paper Biochemistry of adipose tissue: an endocrine organ. Arch Med Sci 2:191–200; doi:10.5114/aoms.2013.33181.

Cui Q, Fu J, Hu Y, Li Y, Yang B, Li L, et al. 2017. Deficiency of long isoforms of Nfe2l1 sensitizes MIN6 pancreatic β cells to arsenite-induced cytotoxicity. Toxicol Appl Pharmacol 329:67–74; doi:10.1016/j.taap.2017.05.013.

Davis AP, Grondin CJ, Johnson RJ, Sciaky D, King BL, McMorran R, et al. 2017. The Comparative Toxicogenomics Database: update 2017. Nucleic Acids Res 45:D972–D978; doi:10.1093/nar/gkw838.

Davis AP, Wiegers TC, Wiegers J, Johnson RJ, Sciaky D, Grondin CJ, et al. 2018. Chemical-induced phenotypes at CTD help inform the pre-disease state and construct adverse outcome pathways. Toxicol Sci 165(1):145-156; doi: 10.1093/toxsci/kfy131.

DeFronzo RA. 2009. From the Triumvirate to the Ominous Octet: A New Paradigm for the Treatment of Type 2 Diabetes Mellitus. Diabetes 58:773–795; doi:10.2337/db09-9028.

Díaz-Villaseñor A, Burns AL, Salazar AM, Sordo M, Hiriart M, Cebrián ME, et al. 2008. Arsenite reduces insulin secretion in rat pancreatic β-cells by decreasing the calcium-dependent calpain-10 proteolysis of SNAP-25. Toxicol Appl Pharmacol 231(3):291–299; doi: 10.1016/j.taap.2008.05.018

Díaz-Villaseñor A, Burns A, Salazar A, Sordo M, Hiriart M, Cebrian M, et al. 2008. Arsenite reduces insulin secretion in rat pancreatic β-cells by decreasing the calcium-dependent calpain-10 proteolysis of SNAP-25. Toxicol Appl Pharmacol 231:291–299; doi:10.1016/j.taap.2008.05.018.

Díaz-Villaseñor A, Sánchez-Soto MC, Cebrián ME, Ostrosky-Wegman P, Hiriart M. 2006. Sodium arsenite impairs insulin secretion and transcription in pancreatic β-cells. Toxicol Appl Pharmacol 214:30–34; doi:10.1016/j.taap.2005.11.015.

Ditzel EJ, Nguyen T, Parker P, Camenisch TD. 2015. Effects of Arsenite Exposure during Fetal Development on Energy Metabolism and Susceptibility to Diet-Induced Fatty Liver Disease in Male Mice. Environ Health Perspect 124; doi:10.1289/ehp.1409501.

Douillet C, Currier J, Saunders J, Bodnar WM, Matoušek T, Stýblo M. 2013. Methylated trivalent arsenicals are potent inhibitors of glucose stimulated insulin secretion by murine pancreatic islets. Toxicol Appl Pharmacol 267:11–15; doi:10.1016/j.taap.2012.12.007.

Dover EN, Beck R, Huang MC, Douillet C, Wang Z, Klett EL, et al. 2018. Arsenite and methylarsonite inhibit mitochondrial metabolism and glucose-stimulated insulin secretion in INS-1 832/13 β cells. Arch Toxicol 92:693–704; doi:10.1007/s00204-017-2074-y.

Druwe IL, Sollome JJ, Sanchez-Soria P, Hardwick RN, Camenisch TD, Vaillancourt RR. 2012. Arsenite activates NFκB through induction of C-reactive protein. Toxicol Appl Pharmacol 261:263–270; doi:10.1016/j.taap.2012.04.005.

Farzan SF, Howe CG, Zens MS, Palys T, Channon JY, Li Z, et al. 2017. Urine Arsenic and Arsenic Metabolites in U.S. Adults and Biomarkers of Inflammation, Oxidative Stress, and Endothelial Dysfunction: A Cross-Sectional Study. Environ Health Perspect 125; doi:10.1289/EHP2062.

Fu J, Woods CG, Yehuda-Shnaidman E, Zhang Q, Wong V, Collins S, et al. 2010. Low-Level Arsenic Impairs Glucose-Stimulated Insulin Secretion in Pancreatic Beta Cells: Involvement of Cellular Adaptive Response to Oxidative Stress. Environ Health Perspect 118:864–870; doi:10.1289/ehp.0901608.

Garciafigueroa DY, Klei LR, Ambrosio F, Barchowsky A. 2013. Arsenic-Stimulated Lipolysis and Adipose Remodeling Is Mediated by G-Protein-Coupled Receptors. Toxicol Sci 134:335–344; doi:10.1093/toxsci/kft108.

Gentry PR, Covington TR, Mann S, Shipp AM, Yager JW, Clewell III HJ. 2004. Physiologically Based Pharmacokinetic Modeling of Arsenic in the Mouse. J Toxicol Environ Health A 67:43–71; doi:10.1080/15287390490253660.

Grau-Perez M, Kuo C-C, Gribble MO, Balakrishnan P, Jones Spratlen M, Vaidya D, et al. 2017. Association of Low-Moderate Arsenic Exposure and Arsenic Metabolism with Incident Diabetes and Insulin Resistance in the Strong Heart Family Study. Environ Health Perspect 125; doi:10.1289/EHP2566.

Hamann I, Petroll K, Hou X, Anwar-Mohamed A, El-Kadi AOS, Klotz L-O. 2014. Acute and long-term effects of arsenite in HepG2 cells: modulation of insulin signaling. BioMetals 27:317–332; doi:10.1007/s10534-014-9714-y.

Hasnain SZ, Prins SZ, McGukin MA. 2016. Oxidative and endoplasmic reticulum stress in β-cell dysfunction in diabetes. J Mol Endocrinol 56(2):R33-54; doi: 10.1530/JME-15-0232.

Hayakawa T, Kobayashi Y, Cui X, Hirano S. 2005. A new metabolic pathway of arsenite: Arsenic-glutathione complexes are substrates for human arsenic methyltransferase Cyt19. Arch Toxicol 79(4):183-191; doi: 10.1007/s00204-004-0620-x.

Hectors TLM, Vanparys C, van der Ven K, Martens GA, Jorens PG, Van Gaal LF, et al. 2011. Environmental pollutants and type 2 diabetes: a review of mechanisms that can disrupt beta cell function. Diabetologia 54:1273–1290; doi:10.1007/s00125-011-2109-5.

Hong G-M, Bain LJ. 2012. Sodium arsenite represses the expression of myogenin in C2C12 mouse myoblast cells through histone modifications and altered expression of Ezh2, Glp, and Igf-1. Toxicol Appl Pharmacol 260:250–259; doi:10.1016/j.taap.2012.03.002.

Hou Y, Xue P, Woods CG, Wang X, Fu J, Yarborough K, et al. 2013. Association between Arsenic Suppression of Adipogenesis and Induction of CHOP10 via the Endoplasmic Reticulum Stress Response. Environ Health Perspect 121:237–243; doi:10.1289/ehp.1205731.

Hu Y, Jin X, Snow ET. 2002. Effect of arsenic on transcription factor AP-1 and NF-κB DNA binding activity and related gene expression. Toxicol Lett 133: 33–45.

Huang CF, Chen YW, Yang CY, Tsai KS, Yang RS, Liu SH. 2011. Arsenic and diabetes: Current perspectives. Kaohsiung J Med Sci 27:402–410; doi:10.1016/j.kjms.2011.05.008.

Hughes MF, Beck BD, Chen Y, Lewis AS, Thomas DJ. 2011. Arsenic Exposure and Toxicology: A Historical Perspective. Toxicol Sci 123:305–332; doi:10.1093/toxsci/kfr184.

Hutton JC, O'Brien RM. 2009. Glucose-6-phosphatase Catalytic Subunit Gene Family. J Biol Chem 284(43):29241-29245; doi: 10.1074/jbc.R109.025544.

Keane KN, Cruzat VF, Carlessi R, de Bittencourt PIH, Newsholme P. 2015. Molecular Events Linking Oxidative Stress and Inflammation to Insulin Resistance and β -Cell Dysfunction. Oxid Med Cell Longev 2015:1–15; doi:10.1155/2015/181643.

Kershaw EE, Flier JS. 2004. Adipose Tissue as an Endocrine Organ. J Clin Endocrinol Metab 89:2548–2556; doi:10.1210/jc.2004-0395.

Kirkley AG, Carmean CM, Ruiz D, Ye H, Regnier SM, Poudel A, et al. 2017. Arsenic exposure induces glucose intolerance and alters global energy metabolism. Am J Physiol-Regul Integr Comp Physiol 314:R294–R303; doi:10.1152/ajpregu.00522.2016.

Klei LR, Garciafigueroa DY, Barchowsky A. 2012. Arsenic Activates Endothelin-1 Gi Protein–Coupled Receptor Signaling to Inhibit Stem Cell Differentiation in Adipogenesis. Toxicol Sci 131:512–520; doi:10.1093/toxsci/kfs323.

Liu S, Guo X, Wu B, Yu H, Zhang X, Li M. 2014. Arsenic induces diabetic effects through beta-cell dysfunction and increased gluconeogenesis in mice. Sci Rep 4; doi:10.1038/srep06894.

Lotia S, Montojo J, Dong Y, Bader GD, Pico AR. 2013. Cytoscape App Store. Bioinformatics 29:1350–1351; doi:10.1093/bioinformatics/btt138.

Lu M, Wang H, Li X-F, Lu X, Cullen WR, Arnold LL, et al. 2004. Evidence of Hemoglobin Binding to Arsenic as a Basis for the Accumulation of Arsenic in Rat Blood. Chem Res Toxicol 17:1733–1742; doi:10.1021/tx049756s.

Mahadev K, Wu X, Zilbering A, Zhu L, Lawrence JTR, Goldstein BJ. 2001. Hydrogen Peroxide Generated during Cellular Insulin Stimulation Is Integral to Activation of the Distal Insulin Signaling Cascade in 3T3-L1 Adipocytes. J Biol Chem 276:48662–48669; doi:10.1074/jbc.M105061200.

Marshall C, Hitman GA, Partridge CJ, Clark A, Ma H, Shearer TR, et al. 2005. Evidence that an isoform of calpain-10 is a regulator of exocytosis in pancreatic beta-cells. Mol Endocrinol 19(1):213-224; doi: 10.1210/me.2004-0064.

Masuda Y, Vaziri ND, Li S, Le A, Hajighasemi-Ossareh M , Robles L, et al. 2015. The effect of Nrf2 pathway activation on human pancreatic islet cells. PLoS One 10(6):e0131012; doi: 10.1371/journal.pone.0131012.

Maull EA, Ahsan H, Edwards J, Longnecker MP, Navas-Acien A, Pi J, et al. 2012. Evaluation of the association between arsenic and diabetes: a National Toxicology Program workshop review. Environ Health Perspect 120: 1658-1670; doi: 10.1289/ehp.1104579.

Mitchell RD, Ayala-Fierro F, Carter DE. 2000. Systemic Indicators of Inorganic Arsenic Toxicity in Four Animal Species. J Toxicol Environ Health A 59:119–134; doi:10.1080/009841000157014.

Naujokas MF, Anderson B, Ahsan H, Aposhian HV, Graziano JH, Thompson C, et al. 2013. The broad scope of health effects from chronic arsenic exposure: update on a worldwide public health problem. Environ Health Perspect 121: 295-302; doi: 10.1289/ehp.1205875.

Navas-Acien A, Silbergeld EK, Streeter RA, Clark JM, Burke TA, Guallar E. 2005. Arsenic Exposure and Type 2 Diabetes: A Systematic Review of the Experimental and Epidemiologic Evidence. Environ Health Perspect 114:641–648; doi:10.1289/ehp.8551.

Noman ASM, Dilruba S, Mohanto NC, Rahman L, Khatun Z, Riad W, et al. 2015. Arsenic-induced Histological Alterations in Various Organs of Mice. J Cytol Histol 06(3):pii323 ; doi: 10.4172/2157-7099.1000323.

OHAT (National Toxicology Program Office of Health Assessment and Translation, Reseach Triangle Park, NC). 2015. OHAT Risk of Bias Tool. (Available): <https://ntp.niehs.nih.gov/pubhealth/hat/review/index-2.html>

Padmaja Divya S, Pratheeshkumar P, Son Y-O, Vinod Roy R, Andrew Hitron J, Kim D, et al. 2015. Arsenic Induces Insulin Resistance in Mouse Adipocytes and Myotubes Via Oxidative Stress-Regulated Mitochondrial Sirt3-FOXO3a Signaling Pathway. Toxicol Sci 146:290–300; doi:10.1093/toxsci/kfv089.

Pan W-C, Seow WJ, Kile ML, Hoffman EB, Quamruzzaman Q, Rahman M, et al. 2013. Association of Low to Moderate Levels of Arsenic Exposure With Risk of Type 2 Diabetes in Bangladesh. Am J Epidemiol 178:1563–1570; doi:10.1093/aje/kwt195.

Pan X, Jiang L, Zhong L, Geng C, Jia L, Liu S, et al. 2014. Arsenic induces apoptosis by the lysosomal-mitochondrial pathway in INS-1 cells: Arsenic Induces Apoptosis by the Lysosomal-Mitochondrial Pathway in Ins-1 Cells. Environ Toxicol 31:133–141; doi:10.1002/tox.22027.

Paul DS, Hernández-Zavala A, Walton FS, Adair BM, Dědina J, Matoušek T, et al. 2007. Examination of the effects of arsenic on glucose homeostasis in cell culture and animal studies: Development of a mouse model for arsenic-induced diabetes. Toxicol Appl Pharmacol 222:305–314; doi:10.1016/j.taap.2007.01.010.

Paul DS, Devesa V, Hernandez-Zavala A, Adair BM, Walton FS, Drobna Z, et al. 2008. Environmental arsenic as a disruptor of insulin signaling. Met Ions Biol Med 10:1-7.

Paul DS, Walton FS, Saunders RJ, Styblo M. 2011. Characterization of the Impaired Glucose Homeostasis Produced in C57BL/6 Mice by Chronic Exposure to Arsenic and High-Fat Diet. Environ Health Perspect 119: 1104-1109; doi: 10.1289/ehp.1003324.

Peng Q, Harlow SD, Park SK. 2015. Urinary arsenic and insulin resistance in US adolescents. Int J Hyg Environ Health 218:407–413; doi:10.1016/j.ijheh.2015.03.006.

Petersen MC, Vatner DF, Shulman GI. 2017. Regulation of hepatic glucose metabolism in health and disease. Nat Rev Endocrinol 13:572–587; doi:10.1038/nrendo.2017.80.

Petrick JS, Ayala-Fierro F, Cullen WR, Carter DE, Vasken Aposhian H. 2000. Monomethylarsonous acid (MMA(III)) is more toxic than arsenite in Chang human hepatocytes. Toxicol Appl Pharmacol 163(2):203-207; doi: 10.1006/taap.1999.8872.

Pilkis SJ, and Granner DK. 1992. Molecular Physiology of the Regulation of Hepatic Gluconeogenesis and Glycolysis. Annu Rev Physiol 54:885-909;
doi: 10.1146/annurev.ph.54.030192.004321

Renu K, Madhyastha H, Madhyastha R, Maruyama M, Arunachlam S, V.G. A. 2018. Role of arsenic exposure in adipose tissue dysfunction and its possible implication in diabetes pathophysiology. Toxicol Lett 284:86–95; doi:10.1016/j.toxlet.2017.11.032.

Rodríguez VM, Limón-Pacheco JH, Del Razo LM, Giordano M. 2016. Effects of inorganic arsenic exposure on glucose transporters and insulin receptor in the hippocampus of C57BL/6 male mice. Neurotoxicol Teratol 54:68–77; doi:10.1016/j.ntt.2016.02.001.

Rosen ED, MacDougald OA. 2006. Adipocyte differentiation from the inside out. Nat Rev Mol Cell Biol 7:885–896; doi:10.1038/nrm2066.

Rosen ED, Spiegelman BM. 2006. Adipocytes as regulators of energy balance and glucose homeostasis. Nature 444:847–853; doi:10.1038/nature05483.

Saltiel AR, Kahn CR. 2001. Insulin signalling and the regulation of glucose and lipid metabolism. Nature 414: 799; doi: 10.1038/414799a.

Shi X, Wei X, Koo I, Schmidt RH, Yin X, Kim SH, et al. 2014. Metabolomic Analysis of the Effects of Chronic Arsenic Exposure in a Mouse Model of Diet-Induced Fatty Liver Disease. J Proteome Res 13:547–554; doi:10.1021/pr400719u.

Slenter DN, Kutmon M, Hanspers K, Riutta A, Windsor J, Nunes N, et al. 2018. WikiPathways: a multifaceted pathway database bridging metabolomics to other omics research. Nucleic Acids Res 46:D661–D667; doi:10.1093/nar/gkx1064.

Soga M, Matsuzawa A, Ichijo H. 2012. Oxidative Stress-Induced Diseases via the ASK1 Signaling Pathway. Int J Cell Biol; doi: 10.1155/2012/439587.

Song X, Li Y, Liu J, Ji X, Zhao L, Wei Y. 2017. Changes in Serum Adiponectin in Mice Chronically Exposed to Inorganic Arsenic in Drinking Water. Biol Trace Elem Res 179:140–147; doi:10.1007/s12011-017-0950-1.

States JC, Barchowsky A, Cartwright IL, Reichard JF, Futscher BW, Lantz RC. 2011. Arsenic Toxicology: Translating between Experimental Models and Human Pathology. Environ Health Perspect 119:1356–1363; doi:10.1289/ehp.1103441.

Styblo M, Del Razo LM, Vega L, Germolec DR, LeCluyse, Hamilton GA, et al. 2000. Comparative toxicity of trivalent and pentavalent inorganic and methylated arsenicals in rat and human cells. Arch Toxicol 74(6):289-299.

Sundaresan NR, Gupta M, Kim G, Rajamohan SB, Isbatan A, Gupta MP. 2009. Sirt3 blocks the cardiac hypertrophic response by augmenting Foxo3a-dependent antioxidant defense mechanisms in mice. J Clin Invest 119(9): 2758-2771; doi: 10.1172/JCI39162

Sztalryd C, Brasaemle DL. 2017. The perilipin family of lipid droplet proteins: Gatekeepers of intracellular lipolysis. Biochim Biophys Acta BBA - Mol Cell Biol Lipids 1862:1221–1232; doi:10.1016/j.bbalip.2017.07.009.

Tan M, Schmidt RH, Beier JI, Watson WH, Zhong H, States CJ, et al. 2011. Chronic subhepatoxic exposure to arsenic enhances hepatic injury caused by high fat diet in mice. Toxicol Appl Pharmacol 257(3): 356-364; doi: 10.1016/j.taap.2011.09.019.

Thayer KA, Heindel JJ, Bucher JR, Gallo MA. 2012. Role of environmental chemicals in diabetes and obesity: a National Toxicology Program workshop review. Environ Health Perspect 120: 779-789; doi: 10.1289/ehp.1104597.

Tontonoz P, Spiegelman BM. 2008. Fat and Beyond: The Diverse Biology of PPARg. Annu Rev Biochem 77:289-312. doi: 10.1146/annurev.biochem.77.061307.091829.

Trouba KJ, Wauson EM, Vorce RL. 2000. Sodium Arsenite Inhibits Terminal Differentiation of Murine C3H 10T1/2 Preadipocytes. Toxicol Appl Pharmacol 168:25–35; doi:10.1006/taap.2000.9012.

Walton F. 2004. Inhibition of insulin-dependent glucose uptake by trivalent arsenicals: possible mechanism of arsenic-induced diabetes. Toxicol Appl Pharmacol 198:424–433; doi:10.1016/j.taap.2003.10.026.

Wauson EM, Langan AS, Vorce RL. 2002. Sodium arsenite inhibits and reverses expression of adipogenic and fat cell-specific genes during in vitro adipogenesis. Toxicol Sci 65: 211–219.

Wu J, Liu J, Waalkes MP, Cheng M-L, Li L, Li C-X, et al. 2008. High Dietary Fat Exacerbates Arsenic-Induced Liver Fibrosis in Mice. Exp Biol Med 233:377–384; doi:10.3181/0710-RM-269.

Wu W, Yao X, Jiang L, Zhang Q, Bai J, Qiu T, et al. 2018. Pancreatic islet-autonomous effect of arsenic on insulin secretion through endoplasmic reticulum stress-autophagy pathway. Food Chem Toxicol 111:19–26; doi:10.1016/j.fct.2017.10.043.

Xu J, Kulkarni SR, Donepudi AC, More VR, Slitt AL. 2012. Enhanced Nrf2 Activity Worsens Insulin Resistance, Impairs Lipid Accumulation in Adipose Tissue, and Increases Hepatic Steatosis in Leptin-Deficient Mice. Diabetes 61:3208–3218; doi:10.2337/db11-1716.

Xue P, Hou Y, Zhang Q, Woods CG, Yarborough K, Liu H, et al. 2011. Prolonged inorganic arsenite exposure suppresses insulin-stimulated AKT S473 phosphorylation and glucose uptake in 3T3-L1 adipocytes: Involvement of the adaptive antioxidant response. Biochem Biophys Res Commun 407:360–365; doi:10.1016/j.bbrc.2011.03.024.

Yadav S, Anbalagan M, Shi Y, Wang F, Wang H. 2012. Arsenic inhibits the adipogenic differentiation of mesenchymal stem cells by down-regulating peroxisome proliferator-activated receptor gamma and CCAAT enhancer-binding proteins. Toxicol In Vitro 27:211–219; doi:10.1016/j.tiv.2012.10.012.

Yang B, Fu J, Zheng H, Xue P, Yarborough K, Woods CG, et al. 2012. Deficiency in the nuclear factor E2-related factor 2 renders pancreatic β-cells vulnerable to arsenic-induced cell damage. Toxicol Appl Pharmacol 264:315–323; doi:10.1016/j.taap.2012.09.012.

Yao X-F, Zheng B-L, Bai J, Jiang L-P, Zheng Y, Qi B-X, et al. 2015. Low-level sodium arsenite induces apoptosis through inhibiting TrxR activity in pancreatic β-cells. Environ Toxicol Pharmacol 40:486–491; doi:10.1016/j.etap.2015.08.003.

Ye R, Scherer PE. 2013. Adiponectin, driver or passenger on the road to insulin sensitivity? Mol Metab 2:133–141; doi:10.1016/j.molmet.2013.04.001.

Zhang C, Fennel EMJ, Douillet C, Stýblo M. 2017. Exposures to arsenite and methylarsonite produce insulin resistance and impair insulin-dependent glycogen metabolism in hepatocytes. Arch Toxicol 91:3811–3821; doi:10.1007/s00204-017-2076-9.

Zimmet PK, Alberti G, Magliano DJ, Bennett PH. 2016. Diabetes mellitus statistics on prevalence and mortality: facts and fallacies. Nat Rev Endocrinol 12(10):616-622; doi: 10.1038/nrendo.2016.105.

Zuo Z, Liu Z, Gao T, Yin Y, Wang Z, Hou Y, et al. 2019. Prolonged inorganic arsenic exposure via drinking water impairs brown adipose tissue function in mice. Sci. Total Environ 668:310-317. doi: 10.1016/j.scitotenv.2019.03.008.

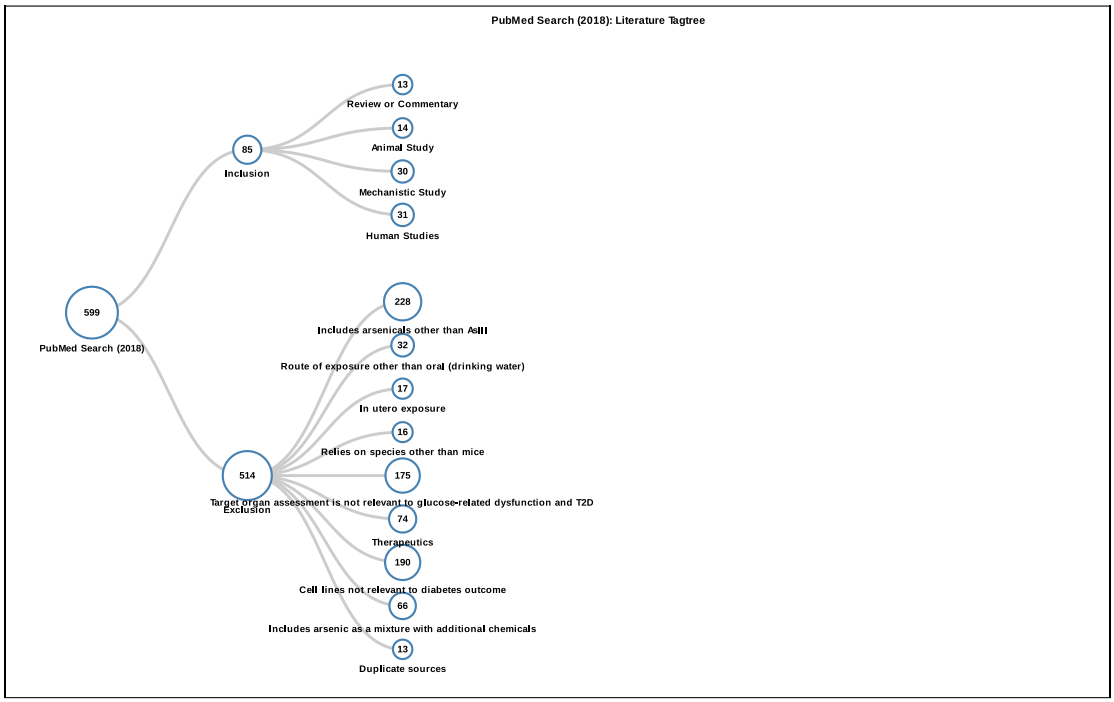

Figure 1. Literature Tag-tree, illustrating the inclusion and exclusion criteria for arsenic and T2D studies selected. We used relevant MeSH terms and targeted searches using PubMed (https://www.ncbi.nlm.nih.gov/pubmed) and literature tagging and visualization tools from the HAWC Project (https://hawcproject.org/).

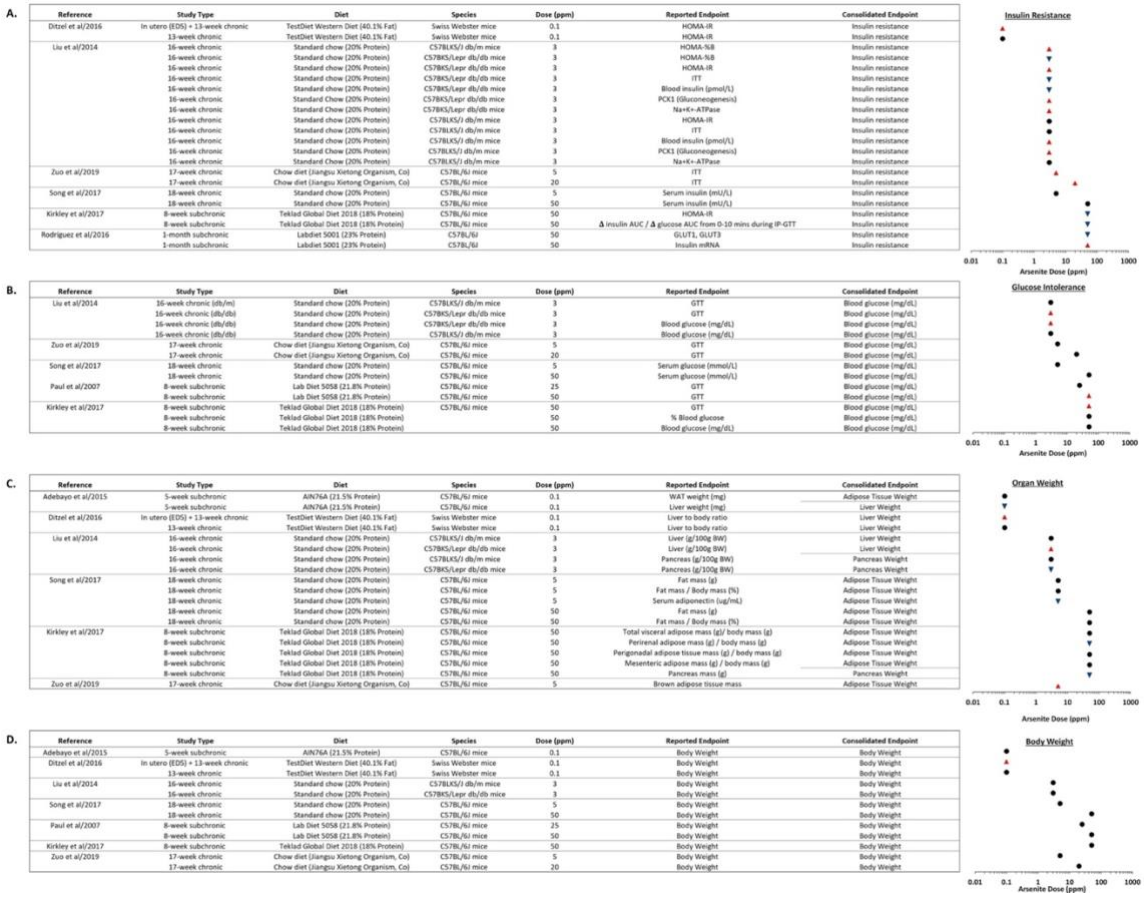

Figure 2. Graphical representation of the direction of the associations between oral exposure to arsenite and (A) Insulin resistance, (B) Impaired glucose tolerance, (C) Organ weight, and (D) Body weight, from in vivo studies. Symbols: upward-pointing red triangle, significantly higher outcome; downward-pointing blue triangle, significantly lower outcome; black circle, no statistical effect. Abbreviations: Glucose tolerance test (GTT); Body weight (BW); Homeostatic model assessment for insulin resistance (HOMA-IR); Insulin tolerance test (ITT); White adipose tissue (WAT).

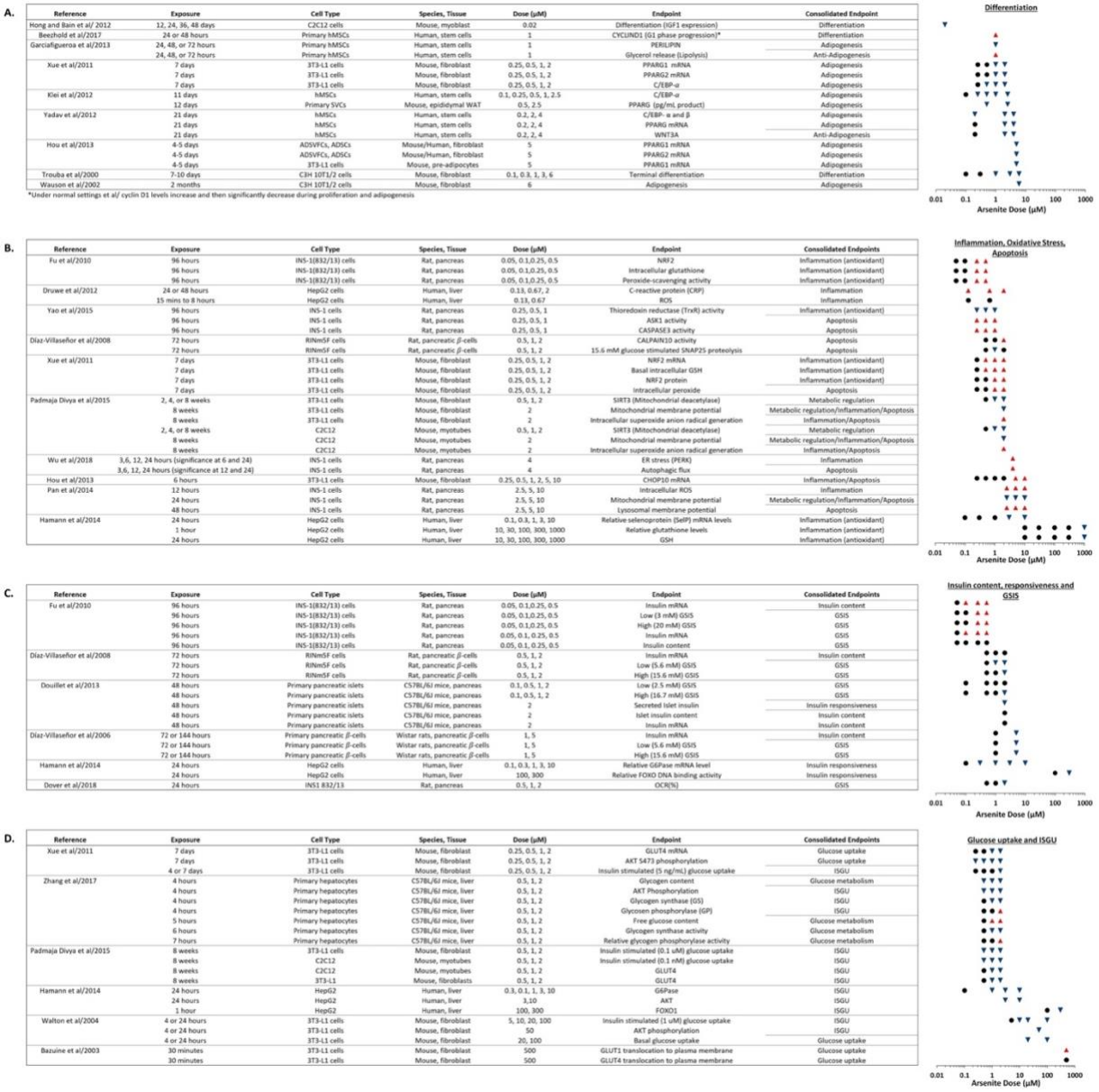

Figure 3. Graphical representation of the direction of the associations between arsenite treatment and (A) Differentiation, (B) Oxidative Stress and Inflammation, (C) Glucose-Stimulated Insulin Secretion (GSIS), and (D) Insulin-Stimulated Glucose Uptake (ISGU), from in vitro studies. Symbols: upward-pointing red triangle, significantly higher outcome; downward-pointing blue triangle, significantly lower outcome; black circle, no statistical effect. Abbreviations: Peroxisome proliferator activated receptor (PPAR); CCAAT-enhancer-binding protein α and β (C/EBP); Nuclear factor-erythroid related factor 2 (NRF2); Apoptosis signal-regulating kinase 1(ASK1); Sirtuin 3 (SIRT3); Eukaryotic translation initiation factor 2 alpha kinase 3 (PERK); CCAAT-enhancer-binding protein homologous protein-10 (CHOP10); Reactive oxygen species (ROS); Glucose-6-phosphatase (G6Pase); Forkhead box transcription factor (FOXO); Oxygen consumption rate (OCR); Protein kinase B (AKT); Glucose transporter type (GLUT).

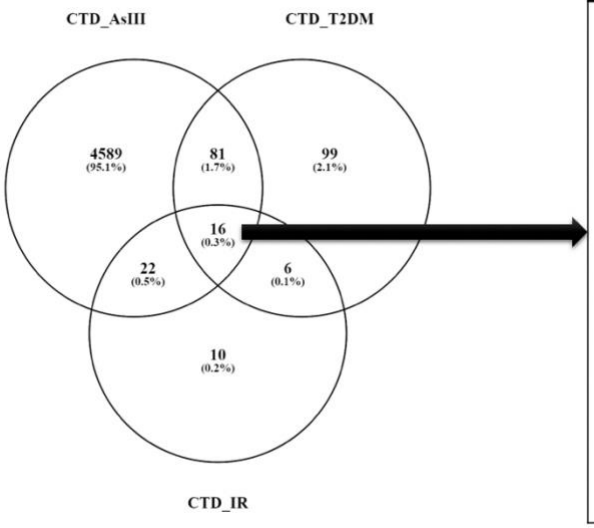

Gene Symbol	Gene description
ADIPOQ	Adiponectin, C1Q and collagen domain containing
C3	Complement C3
EGFR	Epidermal growth factor receptor
HMOX1	Heme oxygenase 1
INS	Insulin
INS1	Insulin I
IRS1	Insulin receptor substrate 1
IRS2	Insulin receptor substrate 2
LEP	Leptin
LEPR	Leptin receptor
NOS3	Nitric oxide synthase 3
PPARG	Peroxisome proliferator activated receptor gamma
SIRT1	Sirtuin 1
SLC2A4	Solute carrier family 2 member 4
SOD2	Superoxide dismutase 2
TNF	Tumor necrosis factor

Figure 4. Chemical- and disease-related gene association data. Findings were obtained by searching the publicly available Comparative Toxicogenomics Database (CTD) (http://ctdbase.org) using MeSH identifiers (https://www.nlm.nih.gov/mesh/) for sodium arsenite (iAs3+) (MeSH:C017947), insulin resistance (MeSH: D007333), and Type 2 Diabetes (T2D) (MESH: D003924). On the left, a Venn diagram is shown depicting the overlapping genes between the different gene sets. On the right, 16 genes are presented. Venn diagrams were created using Venny 2.1 (http://bioinfogp.cnb.csic.es/tools/venny/). Abbreviations: CTD_AsIII = sodium arsenite associated genes obtained from the Comparative Toxicogenomics Database, CTD_T2DM = Type 2 Diabetes Mellitus associated genes obtained from the Comparative Toxicogenomics Database, and CTD_IR = insulin resistance associated genes obtained from Comparative Toxicogenomics Database).

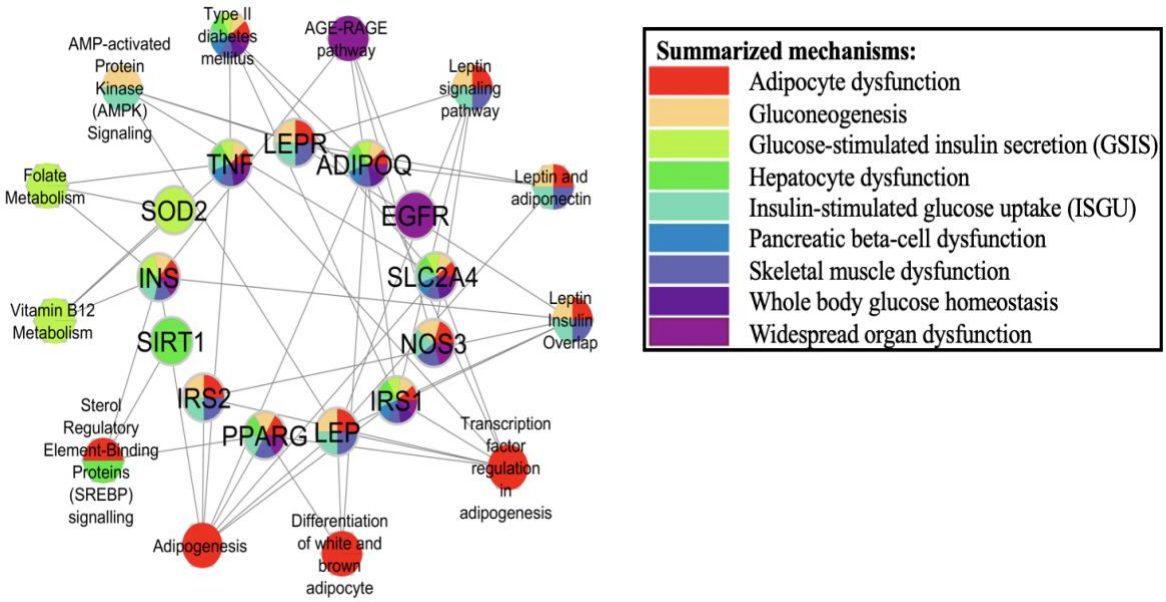

Figure 5. A network of biological pathways and connected genes that were in common between arsenic (iAs3+), insulin resistance, and Type 2 Diabetes (T2D) as found using publicly available gene association data from the Comparative Toxicogenomics Database. A network of 12 biological pathways and 13 connected genes that were in common between arsenic (iAs3+) exposure, insulin resistance (IR) and Type 2 Diabetes (T2D) as found using publicly available gene association data from the Comparative Toxicogenomics Database. Gene set enrichment analysis (GSEA) was performed with the Cytoscape app ClueGO using the WikiPathways repository (https://www.wikipathways.org/index.php/WikiPathways) (version February 2, 2018 containing 418 human pathways and 5866 human genes). Only pathways containing, more than 3 genes or comprising 4% of the total number of genes in a pathway, are depicted in the network. Following GSEA, pathways and genes were assigned to either of the 9 summarized phenotypes as described in the paper. The colored pie charts, depicted in the network nodes, represent the different phenotypes associated with that specific pathway or gene. For the label of the gene node the official HGNC-approved human gene name is used. The label of the pathway node contains the WikiPathway name of the pathway.

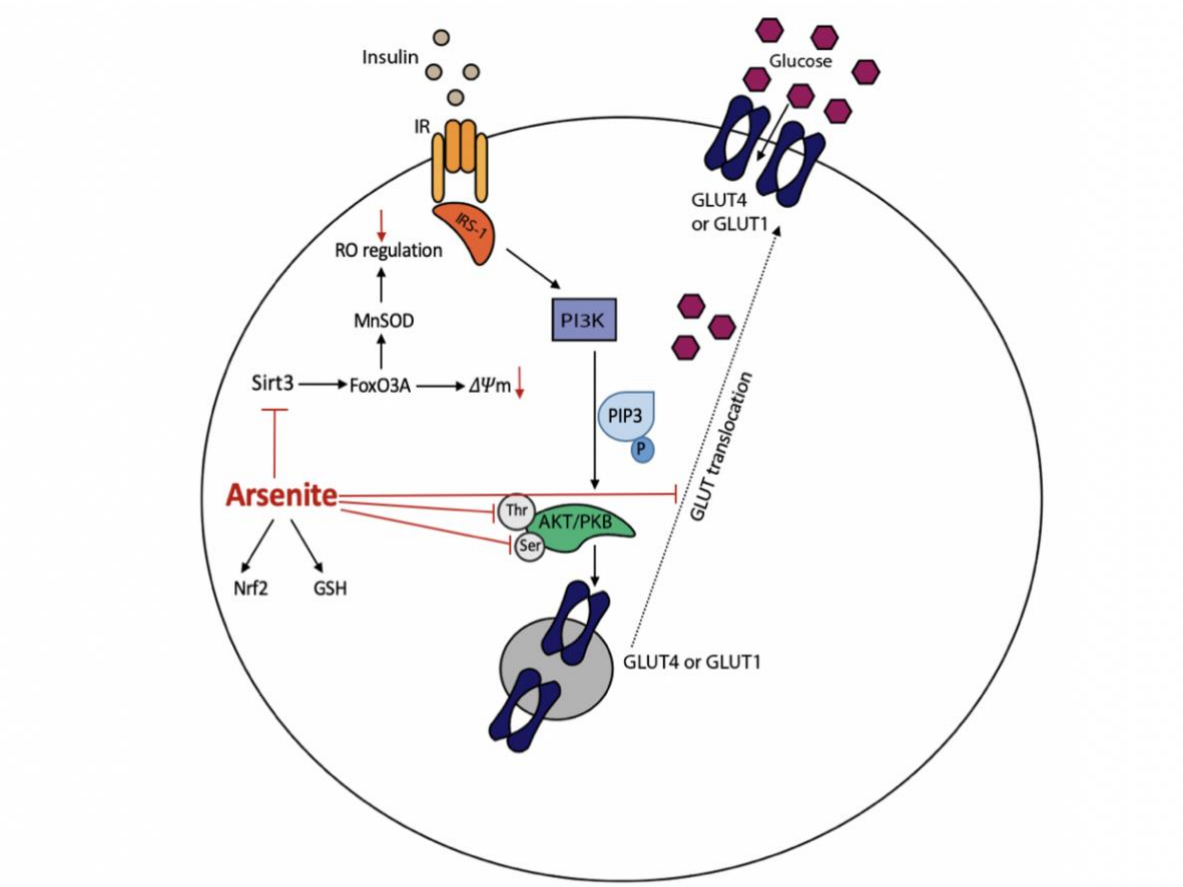

Figure 6. Arsenite impairs insulin stimulated glucose uptake (ISGU) in adipocytes and myotubes. Arsenite has been shown to downregulate AKT and glucose transporter translocation to the plasma membrane in both adipocytes and myotubes (Walton et al. 2004; Xue et al. 2011). Arsenite also upregulates antioxidant defenses such as NRF2 and GSH, inhibiting endogenous ROS involved in ISGU (Xue et al. 2011; Xu et al. 2012). *In vitro*, arsenite has been shown to inhibit SIRT3-FOXO3A signaling to reduce mitochondrial activity and impair ISGU (Padmaja Divya et al. 2015). Abbreviations: Protein kinase B (AKT/PKB); Nuclear factor-erythroid related factor 2 (NRF2); Glutathione (GSH); Reactive oxygen species (ROS); Sirtuin 3 (SIRT3); Forkhead box O3 (FOXO3A); Insulin receptor (IR); Insulin receptor substrate-1 (IRS1); Phosphoinositide 3-kinase (PI3K); Phosphatidylinositol 3,4,5-triphosphate (PIP3); Glucose transporter type (GLUT).

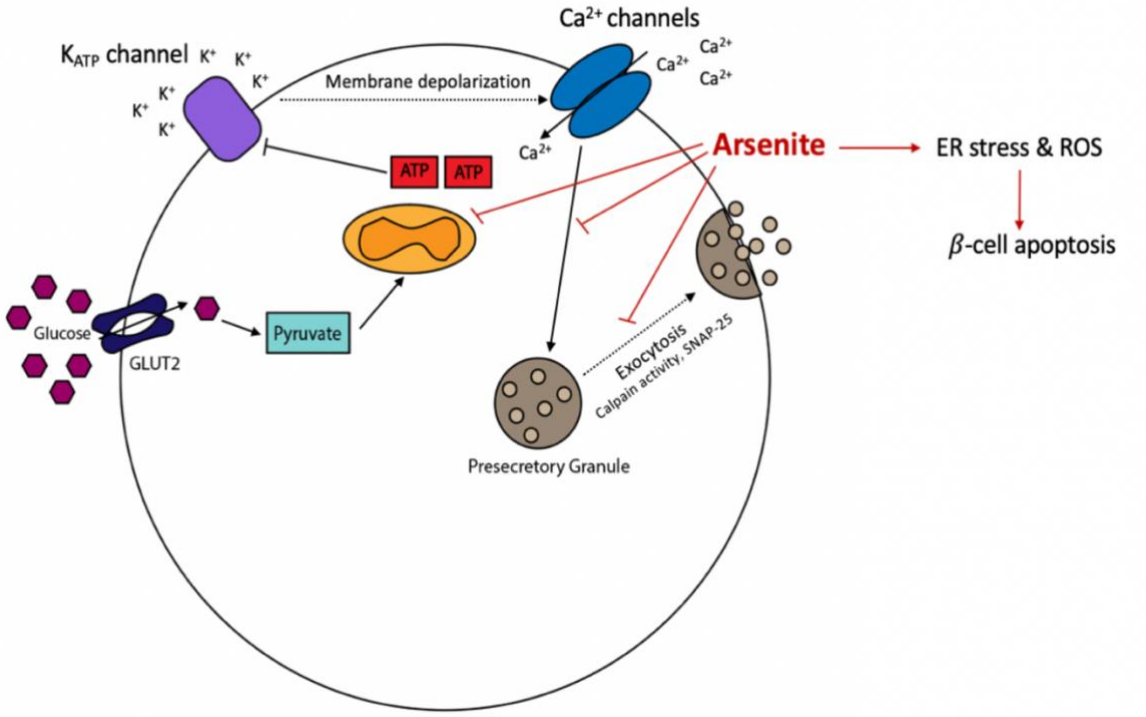

Figure 7. Arsenite disrupts glucose stimulated insulin secretion (GSIS) in pancreatic -cells. Arsenite treatment *in vitro* has been reported to decrease calpain activity, measured as SNAP25 proteolysis. SNAP25 and CALPAIN10 are both needed to fuse insulin pre-secretory granules with the plasma membrane for insulin secretion. At higher doses, arenite has also been shown to increase ER oxidative stress, which can lead to apoptosis of pancreatic -cells due to the tissue's low abundance of antioxidants (Wu et al. 2018; Pan et al. 2016; Yao et al. 2015). Abbreviations: Synaptosome associated protein 25 (SNAP25); Endoplasmic reticulum (ER); Reactive oxygen species (ROS); Glucose transporters (GLUT); Potassium (K); Calcium (Ca^{2+}).

Supplementary Material

Supplementary Figure 1 (SF1) – Office of Health Assessment and Translation (OHAT) Risk of Bias Rating Framework.

Figure SF1.Office of Health Assessment and Translation (OHAT) Risk of Bias Rating Framework. OHAT's guidelines include 11 total risk-of-bias questions, with 9 applicable to experimental animal studies (OHAT 2015). A total of 14 *in vivo* studies were summarized in the manuscript, and therefore included in the risk-of-bias rating tool. Questions are rated based on 4 possible answers: ++ ***Definitely low*** risk of bias, + ***Probability of low*** risk of bias, -NR ***Probability high*** risk of bias (or not reported due to insufficient information), -- ***Definitely high*** risk of bias. *None of these studies reported loss of animals; **Studies that included blinding in some of the outcomes assessment received ++. †Examples include issues with statistical methods, failure to adjust for litter, and unintended co-exposures

	Risk of Bias Questions								
Study	1. Administered dose or exposure level adequately randomized?	2. Allocation to study groups adequately concealed?	5. Experimental conditions identical across study groups?	6. Research personnel blinded to the study group during the study?	7. Outcome data complete without attrition or exclusion from analysis?*	8. Confident in the exposure characterization?	9. Confident in the outcome assessment?**	10. All measured outcomes reported?	11. No other potential threats to internal validity?†
Ditzel et al/2016	NR	+	+	+	NR	+	++	++	+
Liu et al/2014	+	+	++	+	NR	+	+	++	-
Zuo et al/2019	+	+	+	+	NR	+	+	++	-
Song et al/2017	+	+	++	+	NR	+	+	++	+
Kirkley et al/2017	NR	+	++	+	NR	+	+	++	+
Rodriguez et al/2016	+	+	++	+	NR	+	+	++	+
Paul et al/2007	NR	+	++	+	NR	++	+	++	-
Adebayo et al/2015	NR	+	+	+	NR	NR	+	++	-
Wu et al/2008	NR	+	+	+	NR	+	+	++	-
Shi et al/2014	NR	+	++	+	NR	NR	+	++	+
Paul et al/2011	NR	+	++	+	NR	++	+	++	+
Ambrosio et al/2014	NR	+	+	+	NR	NR	+	++	+
Noman et al/2015	+	+	++	+	NR	+	+	++	-
Garciafigueroa et al/2013	NR	+	+	+	NR	+	+	++	-

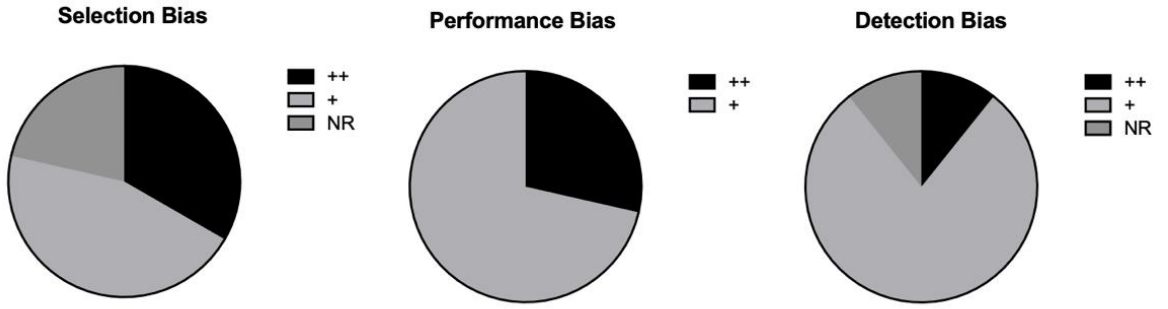

Chapter 2. Obesity and Increased Susceptibility to Arsenic-Related Type 2 Diabetes in Northern Chile

Felicia Castriota[1], Johanna Acevedo[2], Catterina Ferreccio[2], Allan H. Smith[3], Jane Liaw[3], Martyn T. Smith[1], Craig Steinmaus[3,4]

[1] Environmental Health Sciences Division, School of Public Health, University of California, Berkeley, CA
[2] Pontificia Universidad Católica de Chile, Santiago, Chile, Advanced Center for Chronic Diseases, ACCDiS
[3] Arsenic Health Effects Research Program, School of Public Health, University of California, Berkeley, CA
[4] Office of Environmental Health Hazard Assessment, California Environmental Protection Agency, Oakland, CA

*A version of this manuscript has been published: Castriota F, Acevedo J, Ferreccio C, Smith AH, Liaw J, Smith MT, Steinmaus C. Obesity and increased susceptibility to arsenic-related type 2 diabetes. *Environmental Res* 2018. 167:248-254. doi: 10.1016/j.envres.2018.07.022.
This chapter is printed with the explicit consent of all co-authors.

Abstract

BACKGROUND: The prevalence of type 2 diabetes (T2D) has nearly doubled since 1980. Elevated body mass index (BMI) is the leading risk factor for T2D, mediated by inflammation and oxidative stress. Arsenic shares similar pathogenic processes, and may contribute to hyperglycemia and β-cell dysfunction.

OBJECTIVES: We assessed a unique situation of individuals living in Northern Chile with comprehensive data on lifetime drinking water arsenic exposure to evaluate the relationship between arsenic and T2D, and investigate possible interactions between arsenic and BMI.

METHODS: We analyzed data collected from October 2007-December 2010 from an arsenic-cancer case-control study. Information on self-reported weight and height, smoking, diet, and other factors were obtained. Diabetes was defined by self-reported physician-diagnoses or use of hypoglycemic medication. A total of 1053 individuals, 234 diabetics and 819 without known diabetes were included.

RESULTS: The T2D odds ratio (OR) for cumulative arsenic exposures of 610-5279 and ≥5280 μg/L-years >40 years in the past were 0.97 (95% CI: 0.66-1.43) and 1.53 (95% CI: 1.05-2.23), respectively. Arsenic-associated T2D ORs were greater in subjects with increased BMIs. For example, the ORs for past cumulative exposures ≥5280 μg/L-years was 1.45 (95% CI: 0.74-2.84) in participants with BMIs <25 kg/m^2 but 2.64 (95% CI: 1.14-6.11) in those with BMIs ≥30 kg/m^2 (synergy index = 2.49, 95% CI: 0.87-7.09). Results were similar when cancer cases were excluded.

CONCLUSIONS: These findings identify increased odds of T2D with arsenic exposure, which are significantly increased in individuals with excess BMI.

KEYWORDS: Arsenic; Type 2 diabetes (T2D); Obesity; Body Mass Index (BMI); Synergy

Introduction

More than 200 million individuals worldwide are exposed to arsenic-contaminated drinking water above the World Health Organization (WHO)'s permissible limit of 10 μg/L (Naujokas et al. 2013). Ingested arsenic is an established carcinogen and prevalent at high concentrations in drinking water sources in Taiwan, Bangladesh, India, Chile, Argentina, the US, and elsewhere (ATSDR 2007; IARC 2004, 2012). In the US, an estimated 12% of all public water systems have arsenic concentrations near 10 μg/L (U.S. EPA 2000), the current US regulatory standard. Millions more people are likely exposed to even higher arsenic water concentrations from private wells, which are not regulated (Steinmaus 2005). Arsenic also occurs in apple juice, chicken, wine, and beer (Marshall 2012; Nachman et al. 2013; Schute 2013; Wilson et al. 2012), and the US Food and Drug Administration (FDA) found arsenic in almost all 193 brands of rice, rice baby foods, and rice cereals tested (U.S. FDA 2012). Arsenic is also common at industrial waste sites and is currently ranked first on the Superfund hazardous waste site priority list in terms of toxicity and prevalence of exposure (ATSDR 2013).

Type 2 diabetes (T2D) is a chronic condition of increasing prevalence, affecting an estimated 415 million individuals worldwide, projected to increase to 642 million by the year 2040 (Zimmet et al. 2016). In Chile, the prevalence of diabetes mellitus has increased from 4.2% in 2003 to 12.3% in 2016 (Ministerio de Salud, 2017). Although obesity is the primary risk factor for T2D, other factors may also play a role in either directly causing T2D or in enhancing the role of excess BMI on T2D risks (Thayer et al. 2012). Arsenic has been linked to T2D in areas with high exposures (Huang et al. 2011; Maull et al. 2012), but studies of lower exposures (e.g., <100 μg/L) have produced very mixed and unclear or unusual results (Smith, 2013). Although the primary mechanism of arsenic toxicity is unknown, it has been shown to affect several mechanistic pathways that are linked to both obesity and T2D. For example, both arsenic and obesity have been associated with mitochondrial dysfunction and with increases in reactive oxygen species (ROS), two processes that are thought to play an important role in T2D development (Pan et al. 2016; Tseng et al. 2004; Bournat and Brown 2010). Given these and other shared pathologic processes, we hypothesized that arsenic and obesity might interact to increase T2D risk.

Many of the water sources in Northern Chile are contaminated with naturally-occurring arsenic, with concentrations ranging from <10 to >800 μg/L. This geographical area contains the Atacama Desert, which is the driest inhabited place on earth. Because it is so dry, almost everyone in the area lives in one of the cities or towns in the area, and each city and town has its own single water supply. Extensive historical records of arsenic concentrations in all this area's major water sources are available, and because of this, comprehensive estimates of people's lifetime arsenic exposure, from birth through adulthood, can be made simply by knowing the cities or towns in which they have lived (Ferreccio et al. 2000). These types of lifetime exposure data are not available anywhere else in the world. The largest city in the area, Antofagasta, experienced a period of very high arsenic exposure (average of 860 μg/L) starting in 1958, when two rivers with high arsenic concentrations were diverted to the city for drinking. The high exposures ended in the 1970s, when arsenic treatment plants were installed. Except for the installation of arsenic treatment plants in Antofagasta and several other cities, arsenic concentrations in drinking water have been very stable over time (Ferreccio et al. 2000).

For this paper, we used this unique exposure scenario to assess the effects of arsenic exposure on T2D development, and to evaluate whether arsenic and obesity may act

synergistically to increase T2D risk. To our knowledge, the present study is the first to examine the possible interaction between arsenic and obesity on the development of T2D.

Materials and Methods

Study area and subject ascertainment

Study design details are published elsewhere (Steinmaus et al. 2013). Briefly, all subjects were participants in an arsenic-cancer case-control study which involved two contiguous regions (Regions I and II) in Northern Chile. Institutional review board approval was obtained in both the US and Chile. Participation was voluntary, and written informed consent was obtained from all subjects or next of kin. Cancer cases in the underlying study included all people who: (i) had newly diagnosed primary lung, bladder, or kidney cancer between October 2007 and December 2010; (ii) lived in Regions I or II at the time of diagnosis; (iii) were >25 years old when diagnosed; and (iv) were able to provide interview data or had a close relative who could. Cases were ascertained using a rapid case ascertainment system established for the study which involved all pathologists, hospitals, and radiologists in the study area, and most cases were interviewed within three months of diagnosis. Hospital cancer committees and death records were used to identify missing cases. Cancer-free controls, frequency matched to cancer cases by sex and five-year age groups, were randomly selected from the Chile Electoral Registry. This Registry contains >95% of people over age 50 years based on population numbers for Regions I and II recorded in the Chilean Census.

Participant interviews

Participants were interviewed in person using a standardized study questionnaire. For deceased participants, we interviewed the next of kin (proxy). Participants were asked to provide all lifetime residences, water sources (e.g. public water, bottled) and water filter use at each residence, and all jobs held for at least six months. Participants were also asked about specific occupational exposures including asbestos, arsenic, silica, and solvents. Questions regarding tobacco smoke included age of smoking began, periods of no smoking, years smoked, number of cigarettes smoked per day, and childhood or adult secondhand smoke exposure. Participants were also asked about typical water intake, both currently and 20 years ago. Typical dietary intakes in the year preceding interview and 20 years earlier were assessed using a modified version of the National Cancer Institute's Diet History Questionnaire. A 14-point socioeconomic status (SES) scoring system was developed by asking subjects about household items (e.g. computer), cars, and use of domestic help. Information on all medical conditions (e.g. hypertension) and medications were collected. For the analyses presented here, diabetics were defined as people who self-reported physician-diagnosed diabetes or who used a hypoglycemic medication.

Body mass index (BMI)

Subjects and proxy respondents were asked to provide the subjects' adult height, typical weight at ages 20 and 40, and typical weight in the ten years preceding the interview or cancer diagnosis. BMI at each period in time was calculated as weight (kg)/height (m^2). Category cut-off points were based on the WHO definition for overweight and obesity in adults of 25 mg/kg^2 and 30 mg/kg^2, respectively, for both men and women.

Exposure indices

For each subject, each residence in Chile was linked to a water arsenic measurement for that location and the years the subject lived there. Using this process, we could assign an arsenic concentration to each year of each subject's life. Arsenic water records for all cities and towns in Regions I and II, and for all large cities in Chile outside these regions, were collected from governmental agencies, research studies, and water suppliers (Ferreccio et al. 2000). Overall, arsenic water concentrations could be linked to >95% of all subject residences. Use of bottled water or sources with reverse osmosis filtering were assigned arsenic concentrations of zero. The yearly arsenic exposure estimates for each subject were then used to calculate several metrics of arsenic exposure. These included lifetime cumulative exposure (the sum of each subjects' yearly water concentrations), average exposure (the mean of all of each subject's yearly water concentrations), and lifetime highest (the single highest arsenic water concentration at any year in a subject's life). Results are given for each of these metrics since it is unknown which might be most strongly associated with arsenic-related diabetes. Forty-year lag periods, which ignored all arsenic exposure in the 40 years preceding cancer diagnosis (cases) or interviews (cancer-free controls), were applied in some analyses. This was done because exposures in the area were highest >40 years ago (before arsenic treatment plants were installed in several cities). Category cut-off points are tertiles unless otherwise stated.

Statistical analysis

Odds ratios (OR) for T2D were calculated using unconditional logistic regression for various categories and metrics of arsenic exposure. No heterogeneity in results was observed by sex in analyses of arsenic and T2D, thus males and females were combined. Our inclusion of our lung, bladder and kidney cancer cases could potentially introduce bias if these types of cancers were associated with T2D. In unadjusted analyses we found that T2D was more common among the bladder cancer cases than among cancer-free controls (OR=1.34, 95% CI: 0.95-1.88). Although not statistically significant, the fact that this OR was moderately above 1.0 suggests including these bladder cancer cases could introduce some bias. For this reason, these subjects were excluded here. Neither lung nor kidney cancers were associated with T2D in our study (see Results section and Table 1). As such, all kidney and lung cancer cases were included in most of the analyses. The advantage of including these cases is that it leads to a greater sample size and thus more precise estimates of odds ratios. Possible bias from including these cases was assessed by performing separate analyses with these subjects excluded.

Potential biological interactions between arsenic and increased BMI were assessed by calculating T2D odds ratios for various levels of arsenic exposure in analyses stratified by healthy (<25 kg/m^2), overweight (≥ 25 to <30 kg/m^2), and obese (≥ 30 kg/m^2) BMI. BMI based on subjects typical height and weight in the ten years preceding cancer diagnosis (cancer cases) or interview (cancer-free controls) was used in our main analyses, although BMIs at other periods (ages 20 or 40 years) were also assessed. Greater than additive interaction was assessed using the Rothman synergy index (Rothman 1976). Here, T2D ORs were calculated separately for people with elevated BMI (≥ 30 kg/m^2) and low arsenic, people with elevated arsenic and low BMI (<30 kg/m^2), and people with both elevated arsenic and elevated BMI, using people with low BMI and low arsenic as the reference group. For these analyses, high and low arsenic was defined as exposures above or below the upper tertile cut-off point for cumulative exposure lagged 40 years. The impact of BMI on arsenic-related T2D risk was displayed visually by calculating T2D ORs for a 10,000 μg/L-year increase in cumulative arsenic exposure (lagged 40 years) in analyses of subjects below

each integral of BMI, beginning at 20 and ending at 34 kg/m^2 (Figure 1). Here, 10,000 μg/L-year was selected because this was the approximate difference in the means of the upper and lower tertiles. Potential confounding variables entered into the final logistic regression models included sex, age (age <60, 60-70, >70 years), BMI (in analyses not stratified by BMI; <25, 25-<30, ≥30 kg/m^2), and smoking (average cigarettes per day of 0, >0-<10, ≥10 when smoking). These were entered *a priori* since each is a known risk factor for T2D, as shown in the directed acyclic causal graph in Supplementary Figure 1. Age can potentially confound analyses of cumulative exposure so additional analyses were done entering age in 5-year categories, as a continuous variable (each 1 year), and by restricting subjects to narrower age groups (e.g. ages 60-70). Sixteen subjects with no BMI information were excluded. The impact on results of adjustments for other factors potentially related to arsenic exposure or diabetes risk was also assessed. These factors included mining work (ever vs. never), occupational arsenic exposure (ever vs. never), typical fruit and vegetable consumption (above or below one serving per day), water intake (typical intake in L/day), education (high school diploma), adult and child second hand smoke, SES scores (above or below the lower tertile), hypertension, and race (European vs. other descent). The impact of including proxy respondents was evaluated by performing analyses after excluding these subjects. Analyses were conducted using STATA version 13.1 (StataCorp, College Station, TX) and SAS version 9.2 (SAS Institute Inc., Cary NC).

Results

A total of 1053 subjects were included in the main analyses, 634 cancer-free participants and 419 cancer cases, and 234 and 819 people with and without known diabetes. The mean age, BMI, and unlagged cumulative arsenic exposure in these participants were 65.7 years (standard deviation (SD)=11.2), 26.4 kg/m^2 (SD=4.6), and 6527.3 μg/L-years (SD=5646.8), respectively. Clear evidence of an association between T2D and either kidney or lung cancer was not seen, with unadjusted T2D odds ratios for both cancers below 1.0 (Table 1). Adjustment for age, sex, and smoking gave similar results. Subjects with T2D were more likely to be females, above the age of 70, not currently smoking, hypertensive, and have elevated BMIs (≥30 mg/kg^2) (Table 1).

Compared with subjects in the lowest tertile of cumulative arsenic exposure lagged 40 years (0-609 μg/L-years), adjusted T2D ORs were 0.97 (95% CI: 0.66-1.43) and 1.53 (95% CI: 1.05-2.23) for those in the middle (610-5279 μg/L-years) and highest (≥5280 μg/L-years) exposure categories, respectively (Table 2). Similar ORs were seen for unlagged cumulative and average lifetime exposure metrics (Table 2), and in analyses using other arsenic category cut-offs (Table S1). Additional adjustments for daily fruit and vegetable consumption, typical water intake, SES scores, occupation, hypertension, and race had little impact on results. For example, the T2D ORs for cumulative exposures lagged 40 years ≥5280 μg/L were 1.53 (95% CI: 1.05-2.23) and 1.61 (95% CI: 1.04-2.50), respectively, before and after adjustment for these additional factors. Entering age in 5-year categories, as a continuous variable, and restricting subjects to narrower age groups (e.g. ages 60-75) gave similar results. In addition, arsenic-T2D ORs were similar after excluding cancer cases (Table S2). For example, the T2D OR for lagged cumulative arsenic exposures ≥5280 vs. <610 μg/L-years was 1.53 (95% CI:1.05-2.23) in the analyses that included these cases and 1.56 (95% CI: 0.97-2.51, p-trend=0.03) in analyses where they were excluded. Similar findings were also observed when bladder cancer cases were included; the T2D OR for lagged cumulative arsenic exposures ≥5280 vs. <610 μg/L-years was 1.59 (95% CI: 1.13-2.23).
In analyses excluding proxy subjects, arsenic-related T2D ORs were mostly higher. For example, the T2D OR for the highest vs. lowest tertile of cumulative arsenic exposure (lagged 40 years) was

1.67 (95% CI: 1.10-2.54) after excluding proxy subjects.

When analyses were stratified by BMI, ORs for T2D associated with arsenic were markedly higher in subjects who were obese (BMI ≥30 mg/kg^2) (Table 3). For example, adjusted T2D ORs for cumulative arsenic exposures lagged 40 years of >5280 vs. <610 μg/L-years were 1.45 (95% CI: 0.74-2.84) in those with healthy BMIs, but 2.64 (95% CI: 1.14-6.11) in obese subjects. When cancer cases were excluded, the corresponding ORs were 1.41 (95% CI: 0.58-3.38) and 2.23 (95% CI: 0.74-6.70), respectively (Table S3). A similar pattern was seen for other arsenic exposure metrics although with somewhat lower ORs (data not shown). Figure 1 shows the T2D ORs for each 10,000 μg/L increase in cumulative arsenic exposure (lagged 40 years) by increasing levels of BMI. As shown, arsenic-related T2D ORs increase as BMI increases beginning at BMIs of about 24-25 kg/m^2. Similar patterns were seen for unlagged cumulative exposure and average lifetime arsenic exposure although with slightly lower ORs.

The ORs used in the calculations of the Rothman synergy index are shown in Table 4. The T2D adjusted ORs for people with elevated BMI and low arsenic, people with elevated arsenic and low BMI, and people with both elevated arsenic and BMI were 1.99 (95% CI: 1.30-3.05), 1.41 (95% CI: 0.99-2.00), and 4.48 (95% CI: 2.25-8.92), respectively, with a Rothman synergy index of 2.49 (95% CI: 0.87-7.09) (Table 4). When cancer cases were excluded, the corresponding ORs were 2.29 (95% CI: 1.36-3.87), 1.43 (95% CI: 0.90-2.28), and 6.39 (95% CI: 2.63-15.55), with a Rothman synergy index of 3.12 (95% CI: 0.91-10.70) (Table S4). Clear evidence of synergy was not seen for BMI at ages 20 or 40 (data not shown).

Discussion

Overall, we found evidence of an association between high exposures to arsenic in drinking water and increased risks of T2D. These results are consistent with several other studies which have found associations at high exposure levels (e.g. arsenic water concentrations >200 μg/L) (Huang et al. 2011; Maull et al. 2012). We did not find evidence of strong associations at more moderate exposure levels (e.g. <200 μg/L). However, our study did not have sufficient statistical power to detect ORs much below 1.5 in each tertile, which may have limited our ability to detect associations at these more moderate exposure levels. A unique aspect of our study is that we identified higher arsenic-associated T2D ORs in subjects with higher BMIs, results that provide evidence that arsenic and excess BMI interact in a greater than additive manner to increase the risk of T2D. The consistency of findings across several arsenic exposure metrics and cut-off points further support these conclusions (Table S1).

Findings from other investigations support the biological plausibility of our results. For example, a number of studies have shown that arsenic can play a role in glucose dysfunction and insulin resistance (Tseng 2004). Arsenic increases the production of ROS and free radicals, which have been implicated in chronic inflammation and apoptosis of pancreatic β-cells (Martin et al. 2017). Arsenic also upregulates the expression of inflammatory genes such as NFκB, tumor necrosis factor-α(TNF-α), and interleukin (IL)-6 (Tseng 2004). These inflammatory factors can injure the pancreas and interfere with glucose-mediated insulin secretion (Martin et al. 2017; Walton et al. 2004). Several environmental pollutants have been shown to impair thermogenic adipose tissue involved in glucose and lipid metabolism (Zhang et al. 2016), and arsenic's effect on adiposity, specifically on brown and beige adipocytes, may also be a mechanism by which it affects diabetes risk (Maull et al. 2012).

The results from previous studies also support our findings that arsenic and obesity may act synergistically. In Taiwan, although T2D was not specifically assessed, chronic arsenic

exposure and obesity were reported to synergistically contribute to insulin resistance in children (Lin et al. 2014). In Bangladesh, some evidence of synergy for T2D was seen between arsenic in water and BMIs >25 kg/m^2, although <10% of subjects had diabetes and <1% were obese (Pan et al., 2013). In mice, chronic arsenic exposure was shown to act synergistically with high fat diet-induced obesity to produce glucose intolerance (Paul et al. 2007; 2011).

Although the mechanism by which arsenic and excess BMI may act synergistically is unknown, several possibilities exist. Obesity is associated with chronic inflammation and pro-inflammatory markers like C-reactive protein (CRP), TNF-α, interleukins (IL)-6, -8, -12, plasminogen activator inhibitor (PAI)-1, vascular endothelial growth factor (VEGF), and monocyte chemoattractant protein (MCP)-1 (Dutta et al. 2015; Ramos et al. 2003; van Kruijsdijk et al. 2009; Weisberg et al. 2003). These same markers are also increased by arsenic. For example, in two studies from arsenic-exposed regions in West Bengal, increased IL-6, IL-8, IL-12 and MCP-1, CRP, TNF-αwere observed in subjects chronically exposed to arsenic via drinking water (Das et al. 2012; Sinha et al. 2014). Another mechanism may involve mitochondrial dysfunction (Divya et al. 2015; Pan et al. 2016; Bournat and Brown 2010; Jelenik and Roden 2013). Obesity is associated with a decreased number and function of mitochondria. This decline in density and function impairs fatty acid oxidation, contributing to lipid accumulation, increases in ROS and stress kinases, and decreased glucose uptake (Koves et al. 2008; Bournat and Brown 2010). A number of studies have also linked arsenic to increases in ROS (Tseng et al. 2004; Maull et al. 2012), and mitochondrial dysfunction has been shown to be a significant contributor to arsenic-induced ROS (Divya et al. 2015; Pan et al. 2016). For example, arsenic has been shown to downregulate the expression of key proteins involved in mitochondrial respiration and biogenesis in both adipose tissue and skeletal muscle (Divya et al. 2015). Chronic arsenic exposure increases oxidative stress, which may induce changes in the mitochondrial membrane potential that decrease the expression of important ROS scavengers, affecting glucose transporters and insulin-stimulated glucose uptake (Divya et al. 2015; Pan et al. 2016). Overall, arsenic and obesity have been shown to impact a variety of the same processes thought to be involved in T2D development. Importantly though, the actual mechanism by which arsenic impacts T2D and the mechanism by which it may interact with obesity are unknown, and further research is needed to explore these issues.

Misclassification of BMI could have resulted from our use of self-reported height and weight. The literature suggests that women and men tend to under- and over-estimate their weights, respectively (Perry et al. 1995). Importantly though, despite these individual-level errors, self-reports seem to be fairly accurate for classifying subjects relative to one another. For example, in a study of 6,101 subjects in the US National Health and Nutrition Examination Survey (NHANES), measured weights from 10-20 years prior were recalled incorrectly by an average of 3.9 lbs. (Kovalchik 2009). However, the correlation coefficient between measured and recalled weights was 0.96. This high correlation suggests that despite widespread under- or over-estimation, recalled weight can be used to fairly accurately place subjects into low and high categories, like those used in our study. In addition, despite the presence of inherent biases in the self-reporting of anthropometric data, research suggests self-reported weight, height, and BMI to be adequate estimates in population studies (Fonseca et al. 2004). Data from the NHANES show that shifting social attitudes since the 1990s regarding obesity have increased the accuracy of self-reported weight and height metrics, leading to more accurate BMI categorizations from questionnaires (Stommel and Osier 2013).

Another potential issue is confounding. Obesity and increasing age are by far the greatest risk factors for T2D but our results were either adjusted for or stratified on both of these factors.

Other factors including diet, smoking, race and SES can be related to both obesity and T2D but these were either not associated with or were only weakly associated with arsenic exposure in our study, or adjusting for them had little impact on results. Other factors like rare genetic or medical conditions are likely not prevalent enough to cause major confounding in this study (Axelson, 1978). Overall, while residual confounding by the factors we evaluated or confounding by some unknown variable is possible, this seems an unlikely cause for the associations observed in this study.

It has been estimated that 22.5% of diabetics in Chile are not diagnosed (Ministerio de Salud, 2009). Chile has a public health care system with wide access. As such, the bias from under-diagnosis of diabetes would most likely be non-differential and towards the null, not towards the positive results we identified. Correcting the OR of 1.53 we identified for cumulative arsenic exposure >5280 μg/L-year for a non-differential under-diagnosis rate of 22.5% would give an OR of 1.57, a relatively small increase. Misclassification of arsenic exposure may have occurred from missing exposure data, inexact residential history, or arsenic exposure from non-water sources (Steinmaus et al. 2015). Since arsenic exposure was assessed similarly in diabetics and non-diabetics, any bias would likely be non-differential, and most likely bias ORs towards the null. Furthermore, arsenic exposure assessment was primarily based on the cities and towns where the subjects lived, and errors in the subjects' recall of their residential history is most likely minimal. Non-water sources of arsenic exposure are probably negligible compared to historical exposures from water, as most of the food in this region is imported due to the arid climate and limited land use for agriculture. Air and food samples tested for arsenic revealed relatively low arsenic concentrations, with similar levels in the parts of our study area with and without high arsenic water concentrations, and generally accounted for inorganic arsenic intakes of roughly <1-13 μg/day (Ferreccio and Sancha 2006). In contrast, intakes from water would be about 1720 μg/day in those drinking 2 L/day of water with arsenic concentrations of 860 μg/L, the level in the large city of Antofagasta during the high exposure period.

We evaluated whether the cancer case-control study design we used here could have introduced major bias, and found fairly strong evidence that it did not. Cancer cases were ascertained identically throughout the study region, regardless of arsenic exposure levels (Steinmaus et al. 2014). Most importantly, bias might have occurred if the cancer cases in our study had higher rates of T2D than the cancer-free controls. Importantly, we did not find any evidence of an association between T2D and lung and kidney cancer, the two cancer types we included here. We did find evidence that bladder cancer might be related to T2D in our study population, but these subjects were excluded from all analyses. In addition, we repeated all analyses after excluding all cancer cases, and found that these exclusions had little impact on the odds ratio estimates, although precision was reduced by having smaller numbers.

The non-cancer control participants in our study were randomly selected from the Chilean voter registration list, matched to cases by age and sex. At the time of selection, the cities of residence of the participating controls were similar to the population distribution of the 2002 Chilean census, providing evidence that the selected controls were a good representation of the study area given the matching criteria (Steinmaus et al. 2014). Matching of controls to cancer cases was done in our original study to help limit the impact of these variables on our arsenic-cancer analyses. Importantly though, this matching was done independently of either arsenic exposure or of T2D status. As such, it is unlikely to have introduced selection bias or to have caused the elevated ORs for T2D we identified. Overall, we found little evidence that the underlying case-control study design used here caused major bias.

Conclusions

Overall, our study is the first human epidemiologic investigation of T2D to identify a synergistic relationship between arsenic and obesity. Clearly, obesity is the primary risk factor for T2D and most efforts aimed at preventing and treating T2D should focus on preventing or reducing obesity. However, the synergistic relationship we identified between arsenic and BMI suggests that arsenic might worsen or increase the risk of obesity-related T2D. Given the current obesity epidemic and the widespread occurrence of arsenic exposure worldwide, this synergistic relationship could have significant public health implications. Because our findings are novel, future research in arsenic exposed areas like Northern Chile, which have a wide range of arsenic exposure, good data on lifetime exposure, and adequate information on potential confounding variables, should seek to replicate these findings. The mechanism of the synergistic relationship we identified is unknown although several possibilities exist. New information on this mechanism could help further support the biologic plausibility for our findings and might provide insights into new ways to diagnose, prevent, or treat T2D.

References

ATSDR. 2013. Priority List of Hazardous Substances. Agency for Toxic Substances and Disease Registry, Atlanta GA. Available: http://www.atsdr.cdc.gov/spl/ [accessed 05/18/2015].

ATSDR. 2007. Toxicological Profile for Arsenic. U.S., Department of Health and Human Services, Public Health Service, Agency for Toxic Substances and Disease Registry, Atlanta, GA. Available: https://www.atsdr.cdc.gov/toxprofiles/tp2.pdf [accessed 05/18/2015].

Axelson O. 1978. Aspects on confounding in occupational health epidemiology. Scand J Work Environ Health 4: 85-89.

Bournat JC, Brown CW. 2010. Mitochondrial dysfunction in obesity. Curr Opin Endocrinol Diabetes Obes. 17(5):446-52. PMID: 20585248 PMCID: PMC5001554 DOI: 10.1097/MED.0b013e32833c3026.

Das N, Paul S, Chatterjee D, Banerjee N, Majumder NS, Sarma N, et al. 2012. Arsenic exposure through drinking water increases the risk of liver and cardiovascular diseases in the population of West Bengal, India. BMC Public Health 10(12):639. PMID: 22883023 PMCID: PMC3441389 DOI: 10.1186/1471-2458-12-639.

Divya PS, Pratheeshkumar P, Son YO, Vinod RR, Hitron AJ, Kim D, Dai J, et al. 2015. Arsenic induces insulin resistance in mouse adipocytes and myotubes via oxidative stress-regulated mitochondrial sirt3-FOXO3a signaling pathway. Toxicol Sci 146(2):290-300. PMID: 25979314 DOI: 10.1093/toxsci/kfv089.

Dutta K, Prasad P, Sinha D. 2015. Chronic low level arsenic exposure evokes inflammatory responses and DNA damage. Int J Hyg Environ Health 218(6):564-74. PMID: 26118750 DOI: 10.1016/j.ijheh.2015.06.003.

Ferreccio C, González C, Milosavjlevic V, Marshall G, Sancha AM, Smith AH. 2000. Lung cancer and arsenic concentrations in drinking water in Chile. Epidemiology 11:673-79.
PMID: 11055628.

Ferreccio C, Sancha AM. 2006. Arsenic exposure and its impact on health in Chile. J Health Popul Nutr 24:164-75. PMID: 17195557.

Fonseca MeJ, Faerstein E, Chor D, Lopes CS. 2004. Validity of self-reported weight and height and the body mass index within the "Pró-saúde" Study. Rev Saude Publica 38:392-398. PMID: 15243669 DOI: /S0034-89102004000300009.

Huang CF, Chen YW, Yang CY, Tsai KS, Yang RS, Liu SH. 2011. Arsenic and diabetes: Current perspectives. Kaohsiung Journal of Medical Sciences 27(9):402-10. DOI: 10.1016/j.kjms.2011.05.008.

IARC. 2004. Arsenic and arsenic compounds. International Agency for Research on Cancer Monographs 100C. Available: http://monographs.iarc.fr/ENG/Monographs/vol100C/mono100C-6.pdf [accessed 05/15/2017].

IARC. 2012. A review of human carcinogens: Arsenic, metals, fibres, and dusts. International Agency for Research on Cancer 100C. Available: http://monographs.iarc.fr/ENG/Monographs/vol100C/mono100C.pdf [accessed 05/15/2017].

Jelenik T and Roden M. 2013. Mitochondrial Plasticity in Obesity and Diabetes Mellitus. Antioxid Redox Signal 19(3):258-68. DOI: 10.1089/ars.2012.4910.

Kovalchik S. 2009. Validity of adult lifetime self-reported body weight. Public Health Nutr 12(8):1072-7. PMID: 18789171 DOI: 10.1017/S1368980008003728

Koves TR, Ussher JR, Noland RC, Slentz D, Mosedale M, Ilkayeva O, et al. Mitochondrial overload and incomplete fatty acid oxidation contribute to skeletal muscle insulin resistance. Cell Metab 7(1):45-56. PMID: 18177724 DOI: 10.1016/j.cmet.2007.10.013.

Lin HC, Huang YK, Shiue HS, Chen LS, Choy CS, Huang SR, Han BC, et al. 2014. Arsenic methylation capacity and obesity are associated with insulin resistance in obese children and adolescents. Food Chem Toxicol 74:60-7. DOI: 10.1016/j.fct.2014.08.018.

Marshall T. 2012. Arsenic in apple juice: How much is too much? Tampa Bay Times. Available: http://www.tampabay.com/news/health/arsenic-in-apple-juice-how-much-is-too-much/1079395. [accessed 09/08/2017].

Martin EM, Styblo M, Fry RC. 2017. Genetic and epigenetic mechanisms underlying arsenic-associated diabetes mellitus: a perspetive of the current evidence. Epigenomics 9(5):701-10. PMID: 28470093 PMCID: PMC5480787 [Available on 2018-05-01] DOI: 10.2217/epi-2016-0097.

Maull EA, Ahsan H, Edwards J, Longnecker MP, Navas-Acien A, Pi J, Sc. 2012. Evaluation of the association between arsenic and diabetes: A National Toxicology Program workshop review. Environ Health Perspect 120:1658-1670. PMID: 22889723 PMCID: PMC3548281 DOI: 10.1289/ehp.1104579.

Ministerio de Salud. Gobierno de Chile. Departmento de Epidemiologia (2017). "Encuesta Nacional de Salud 2016-2017: Primaeros resultatdos." Retrieved 4/5/2018, from www.minsal.cl/wp.../ENS-2016-17_PRIMEROS-RESULTADOS.pdf.

Ministerio de Salud. 2009. Implementación del enfoque de riesgo en el Programa de Salud Cardiovascular. Retrieved 4/5/2018, from http://buenaspracticasaps.cl/wp-content/uploads/2014/07/MINSAL-2009-enfoque-riesgo-CV.pdf2009.

Nachman KE, Baron PA, Raber G, Francesconi KA, Navas-Acien A, Love DC. 2013. Roxarsone, inorganic arsenic, and other arsenic species in chicken: A U.S.-based market basket sample. Environ Health Perspect 121:818-24. PMID: 23694900 PMCID: PMC3701911. DOI: 10.1289/ehp.1206245.

Naujokas MF, Anderson B, Ahsan H, Aposhian HV, Graziano JH, Thompson C, et al. 2013. The broad scope of health effects from chronic arsenic exposure: update on a worldwide public health problem. Environmental Health Perspect 121:295-302. PMID: 23458756 PMCID: PMC3621177 DOI: 10.1289/ehp.1205875.

Pan WC, Seow WJ, Kile ML, Hoffman EB, Quamruzzaman Q, Rahman M, Mahiuddin G, Mostofa G, Lu Q, Christiani DC. 2013. Association of low to moderate levels of arsenic exposure with risk of type 2 diabetes in Bangladesh. Am J Epidemiol. 15;178:1563-70. DOI: 10.1093/aje/kwt195.

Pan X, Jiang L, Zhong L, Geng C, Jia L, Liu S, et al. 2016. Arsenic induces apoptosis by the lyosomal-mitochondrial pathway in INS-1 cells. Environ Toxicol 31(2):133-41. PMID: 25077447 DOI: 10.1002/tox.22027.

Paul DS, Hernández-Zavala A, Walton FS, Adair BM, Dedina J, Matousek et al. 2007. Examination of the effects of arsenic on glucose homeostasis in cell culture and animal studies: development of a mouse model for arsenic-induced diabetes. Toxicol Appl Pharmacol 222(3):305-14. PMID: 17336358 PMCID: PMC2680915 DOI: 10.1016/j.taap.2007.01.010.

Paul DS, Walton FS, Saunders RJ, Styblo M. Characterization of the impaired glucose homeostasis produced in C57BL/6 mice by chronic exposure to arsenic and high-fat diet. 2011. Environ Health Perspect 119(8):1104-9. PMID: 21592922 PMCID: PMC3237360 DOI: 10.1289/ehp.1003324.

Perry G.S. et al. 1995. The validity of self-reports of past body weights by U.S. adults. Vol. Epidemiology 6(1): 61-66. PMID: 7888448.

Ramos EJ, Xu Y, Romanova I, Middleton F, Chen C, Quinn R, et al. 2003. Is obesity an inflammatory disease? Surgery 134(2):329-35. PMID: 12947337 DOI: 10.1067/msy.2003.267.

Rothman KJ. 1976. The estimation of synergy or antagonism. Am J Epidemiol 103(5):506-511. PMID: 1274952.

Schute N. 2013. Arsenic in beer may come from widely used filtering process. National Public Radio. Available: http://www.npr.org/sections/thesalt/2013/04/08/176587506/arsenic-in-beer-may-come-from-widely-used-filtering-process [accessed 07/15/2017].

Sinha D, Mukherjee B, Bindhani B, Dutta K, Saha H, Prasad P, et al. 2014. Chronic low level arsenic exposure inflicts pulmonary and systemic inflammation. J Cancer Sci 6:62-9. DOI:10.4172/1948-5956.1000250.

Smith AH. 2013. Arsenic and diabetes. Environ Health Perspect 121(3):A70-1. DOI: 10.1289/ehp.1206100.

Steinmaus C. 2005. Arsenic in drinking water: Health effects and current issues. Available: https://www.cdc.gov/NCEH/tracking/webinars/sep05/steinmaus.pdf [accessed 07/11/2017].

Steinmaus C, Ferreccio C, Acevedo J, Yuan Y, Liaw J, Durán V, et al. 2014. Increased lung and bladder cancer incidence in adults after in utero and early-life arsenic exposure. Cancer Epidemiol Biomarkers Prev 23:1529-1538. PMID: 24859871 PMCID: PMC4344186 DOI: 10.1158/1055-9965.EPI-14-0059.

Steinmaus C, Castriota F, Ferreccio C, Smith AH, Yuan Y, Liaw J, et al. 2015. Obesity and excess weight in early adulthood and high risks of arsenic-related cancer in later life. Environ Res 142:594-601. PMID: 26301739 PMCID: PMC4664040 DOI: 10.1016/j.envres.2015.07.021.

Steinmaus CM, Ferreccio C, Romo JA, Yuan Y, Cortes S, Marshall G, et al. 2013. Drinking water arsenic in Northern Chile: High cancer risks 40 years after exposure cessation. Cancer Epidemiol Biomarkers Prev 22:623-630. PMID: 23355602 PMCID: PMC3848421 DOI: 10.1158/1055-9965.EPI-12-1190.

Stommel M, Osier N. 2013. Temporal changes in bias of body mass index scores based on self-reported height and weight. Int J Obes 37:461-67. PMID: 22546777 PMCID: PMC3595465 DOI: 10.1038/ijo.2012.67.

Thayer KA, Heindel JJ, Bucher JR, Gallo MA. 2012. Role of Environmental Chemicals in Diabetes and Obesity: A National Toxicology Program Workshop Review. Environ Health Perspect 120(6):779-89. PMID: 22296744 PMCID: PMC3385443 DOI: 10.1289/ehp.1104597.

Tseng CH. 2004. The potential biological mechanisms of arsenic-induced diabetes mellitus. Toxicol Appl Pharmacol 197:67-83. PMID: 15163543 DOI: 10.1016/j.taap.2004.02.009.

U.S. EPA. 2000. Arsenic occurrence in public drinking water supplies. EPA-815-R-00-23. Washington, DC: U.S. Environmental Protection Agency. EPA-815-R-00-23. Available: https://www.epa.gov/sites/production/files/2015-09/documents/2005_11_10_arsenic_occurrence-appendices.pdf [accessed 06/15/2017].

U.S. FDA. 2012. Arsenic in rice: Full analytical results from rice/rice product sampling - September 2012. U.S. Food and drug administration. Available: http://www.fda.gov/Food/FoodborneIllnessContaminants/Metals/ucm319916.htm [accessed 11/29/12].

van Kruijsdijk RC, van der Wall E, Visseren FL. 2009. Obesity and cancer: the role of dysfunctional adipose tissue. Cancer Epidemiol Biomarkers Prev 18(10):2569-78. PMID: 19755644 DOI: 10.1158/1055-9965.EPI-09-0372.

Walton FS, Harmon AW, Paul DS, Drobná Z, Patel YM, Styblo M. 2004. Inhibition of insulin-dependent glucose uptake by trivalent arsenicals: possible mechanism of arsenic-induced diabetes. Toxicol Appl Pharmacol 198(3):424-33. PMID: 15276423 DOI: 10.1016/j.taap.2003.10.026

Weisberg SP, McCann D, Desai M, Rosenbaum M, Leibel RL, Ferrante AW Jr. 2003. Obesity is associated with macrophage accumulation in adipose tissue. J Clin Invest 112(12):1796-808. PMID: 14679176 PMCID: PMC296995 DOI: 10.1172/JCI19246.

Wilson D, Hooper C, Shi X. 2012. Arsenic and lead in juice: apple, citrus, and apple-base. J Environ Health 75:14-20. PMID: 23270108.

Zhang G, Sun Q, Liu C. 2016. Influencing factors of thermogenic adipose tissue activity. Front Physiol 7(29):1-11. PMID: 26903879 PMCID: PMC4742553 DOI: 10.3389/fphys.2016.00029.

Zimmet P, Alberti KG, Magliano DJ, Bennett PH. 2016. Diabetes mellitus statistics on prevalence and mortality: facts and fallacies. Nat Rev Endocrinol 12:616-22. PMID: 27388988 DOI: 10.1038/nrendo.2016.105.

Table 1. Sociodemographic characteristics of study participants with and without diabetes

	Diabetes		
	Yes	**No**	**OR (95% CI)**
	n	**n**	
Total	234	819	
Sex			
Male	144	556	1.00 (Ref)
Female	90	263	1.32 (0.98-1.79)
Age (years old)			
<60	46	258	1.00 (Ref)
>60-70	88	285	1.73 (1.17-2.57)
>70	100	276	2.03 (1.38-3.00)
Cancer case-control status			
Control	145	489	1.00 (Ref)
Cancer cases: all	89	330	0.91 (0.67-1.23)
Lung	67	234	0.97 (0.70-1.34)
Kidney	22	96	0.77 (0.47-1.27)
Proxy			
No	187	657	1.00 (Ref)
Yes	47	162	1.02 (0.71-1.47)
Mining work			
No	186	637	1.00 (Ref)
Yes	48	182	0.90 (0.63-1.29)
Cigarette smoking			
Never	84	252	1.00 (Ref)
Former	103	322	0.96 (0.69-1.34)
Current	47	245	0.58 (0.39-0.86)
Average cigarettes (per day)*			
>0-5	15	82	1.00 (Ref)
6-15	19	61	1.70 (0.80-3.62)
>15	13	102	0.70 (0.31-1.55)
Cumulative pack years*			
Low	18	87	1.00 (Ref)
Middle	27	146	0.89 (0.47-1.72)
High	2	12	0.81 (0.17-3.91)
Adult secondhand smoke**			
No	58	188	1.00 (Ref)
Yes	26	64	1.32 (0.77-2.27)
Childhood secondhand smoke**			
No	59	181	1.00 (Ref)
Yes	25	71	1.08 (0.63-1.86)
BMI recent (kg/m^2)#			
<25	66	346	1.00 (Ref)
25-30	105	344	1.60 (1.14-2.25)
≥30	63	129	2.56 (1.72-3.82)
BMI age 40 (kg/m^2)			
<25	93	472	1.00 (Ref)
25-30	84	255	1.78 (1.28-2.46)
≥30	49	84	2.96 (1.95-4.49)
BMI age 20 (kg/m^2)			
<25	159	638	1.00 (Ref)
25-30	55	148	1.49 (1.05-2.13)
≥30	20	33	2.43 (1.36-4.35)
Hypertension			
No	149	653	1.00 (Ref)
Yes	85	166	2.24 (1.64-3.08)
Fruit and vegetable intake##			
≤1/day	14	74	1.00 (Ref)
1-2/day	50	208	1.27 (0.66-2.43)

>2/day	114	362	1.66 (0.91-3.06)
Race			
Hispanic/European descent	171	600	0.99 (0.71-1.37)
Other	63	219	1.00 (Ref)
SES scores			
Low	73	208	1.00 (Ref)
Middle	80	364	0.63 (0.44-0.90)
High	81	247	0.93 (0.65-1.35)

Abbreviations: BMI, body mass index; CI, confidence interval; OR, odds ratio; SES, socioeconomic
*Among current smokers only
**Among never smokers only
#Typical BMI in the ten years preceding cancer diagnosis (cancer cases) or interview (cancer-free controls)
##Dietary data only collected in non-proxy subjects

Table 2. Diabetes odds ratios for tertiles of various metrics of arsenic water concentrations

Arsenic metric	Arsenic level	Diabetes		Unadjusted OR (95% CI)	Adjusted* OR (95% CI)
		Yes	No		
Cumulative exposure: 0 year lag (µg/L-years)	0-2416	70	281	1.00 (Ref)	1.00 (Ref)
	2417-8664	74	276	1.08 (0.75-1.55)	1.14 (0.78-1.66)
	≥8665	90	262	1.38 (0.97-1.97)	1.50 (1.03-2.19)
	p-trend			0.06	0.03
Cumulative exposure: 40 year lag (µg/L-years)	0-609	70	276	1.00 (Ref)	1.00 (Ref)
	610-5279	68	278	0.96 (0.66-1.40)	0.97 (0.66-1.43)
	≥5280	93	254	1.44 (1.01-2.06)	1.53 (1.05-2.23)
	p-trend			0.016	0.009
Highest year exposure: 0 year lag (µg/L)	0-60	85	326	1.00 (Ref)	1.00 (Ref)
	61-635	68	222	1.17 (0.82-1.69)	1.28 (0.88-1.85)
	≥636	81	271	1.15 (0.81-1.62)	1.28 (0.89-1.84)
	p-trend			0.63	0.25
Highest year exposure: 40 year lag (µg/L)	0-60	102	364	1.00 (Ref)	1.00 (Ref)
	61-286	49	176	0.99 (0.68-1.46)	1.04 (0.70-1.55)
	≥287	80	268	1.07 (0.76-1.49)	1.16 (0.82-1.64)
	p-trend			0.69	0.39
Average lifetime exposure: 0 year lag (µg/L)	0-38	74	276	1.00 (Ref)	1.00 (Ref)
	39-129	72	279	0.96 (0.67-1.39)	1.02 (0.70-1.48)
	≥130	88	264	1.24 (0.87-1.77)	1.43 (0.98-2.07)
	p-trend			0.16	0.04
Average exposure: 40 year lag (µg/L)	0-22	73	273	1.00 (Ref)	1.00 (Ref)
	23-222	74	272	1.02 (0.71-1.46)	0.99 (0.68-1.44)
	≥223	84	263	1.19 (0.84-1.71)	1.36 (0.93-1.97)
	p-trend			0.28	0.07

Abbreviations: CI, confidence interval; OR, odds ratio; Ref, reference group

*Adjusted for age (<60, 60-70, >70 years old), sex, BMI (<25, 25-30, ≥30 kg/m^2), cancer status, smoking (never-smokers, >0 to <10, ≥10 cigarettes/day)

Table 3. Diabetes odds ratios for categories of cumulative arsenic water concentrations lagged 40 years stratified by healthy (<25 kg/m^2), overweight (≥25 to <30 kg/m^2), and obese (≥30 kg/m^2) BMI

BMI level (kg/m^2)	Arsenic level (µg/L)	Diabetes		Unadjusted OR (95% CI)	Adjusted* OR (95% CI)
		Yes	No		
Healthy (<25)	0-609	18	102	1.00 (Ref)	1.00 (Ref)
	610-5279	16	116	0.78 (0.38-1.61)	0.75 (0.36-1.56)
	≥5280	32	123	1.47 (0.78-2.78)	1.45 (0.74-2.84)
	p-trend			0.08	0.09
Overweight (≥25 to <30)	0-609	27	113	1.00 (Ref)	1.00 (Ref)
	610-5279	34	117	1.22 (0.69-2.15)	1.12 (0.62-2.00)
	≥5280	43	111	1.62 (0.94-2.80)	1.34 (0.76-2.35)
	p-trend			0.08	0.31
Obese (≥30)	0-609	25	61	1.00 (Ref)	1.00 (Ref)
	610-5279	18	45	0.98 (0.48-2.00)	1.04 (0.49-2.20)
	≥5280	18	20	2.20 (1.00-4.83)	2.64 (1.14-6.11)
	p-trend			0.04	0.02

Abbreviations: BMI, body mass index; CI, confidence interval; OR, odds ratio; Ref, reference group
*Adjusted for age (<60, 60-70, >70 years old), sex, cancer status, smoking (never-smokers, >0 to <10, ≥10 cigarettes/day)
[#]Similar findings among cancer cases vs controls

Table 4. Diabetes odds ratios and Rothman synergy indices by categories of low and high BMI and arsenic

BMI*	Arsenic*	Diabetes		Unadjusted OR (95% CI)	Adjusted[#] OR (95% CI)
		Yes	No		
Low	Low	95	448	1.00 (Ref)	1.00 (Ref)
High	Low	43	106	1.91 (1.26-2.91)	1.99 (1.30-3.05)
Low	High	75	234	1.51 (1.07-2.13)	1.41 (0.99-2.00)
High	High	18	20	4.24 (2.16-8.33)	4.48 (2.25-8.92)
Rothman synergy index				2.28 (0.82-6.36)	2.49 (0.87-7.09)

Abbreviations: BMI, body mass index; CI, confidence interval; OR, odds ratio; Ref, reference group

*Low and high BMI defined as < and ≥30 kg/m^2. Low and high arsenic defined as <5280 and ≥5280 cumulative arsenic water concentration lagged 40 years

[#]Adjusted for age (<60, 60-70, >70 years old), sex, cancer status, smoking (never-smokers, >0 to <10, ≥10 cigarettes/day)

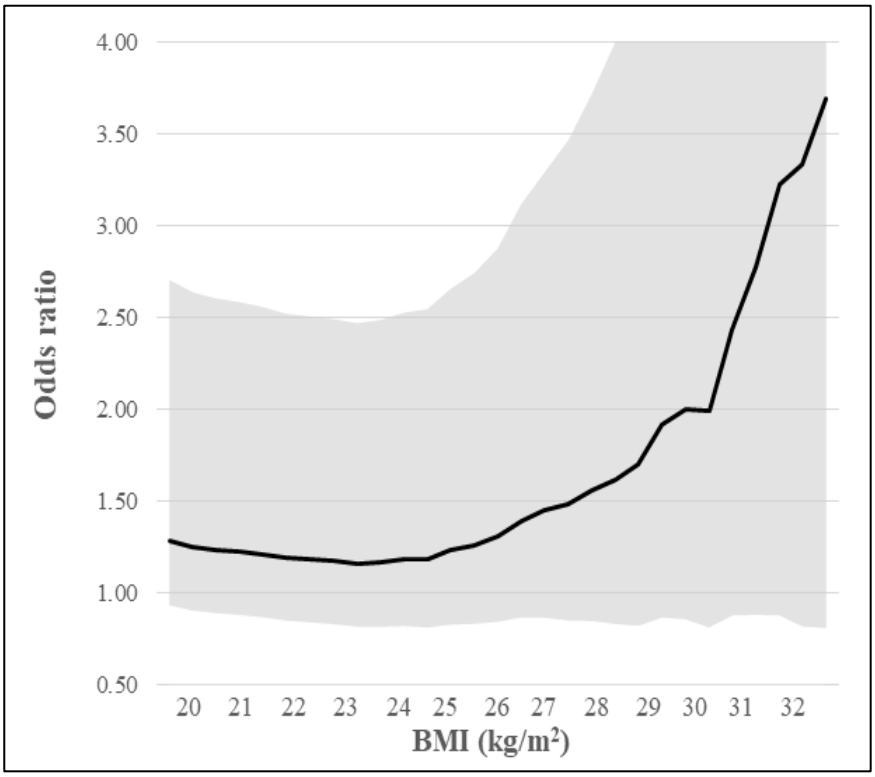

Figure 1. Odds ratios for diabetes for high arsenic exposure (each 10,000 µg/L-year increase in cumulative exposure lagged 40 years) by increasing levels of BMI. Dark line represents the odds ratios. Shaded area represents the 95% confidence intervals. 10,000 µg/L is approximately the range between lower and upper tertile groups of arsenic exposure.

Supplementary Material

Supplementary Figure 1 (SF1) – Directed acyclic graph of arsenic and T2D

Supplementary Table 1 (S1) – Diabetes odds ratios for various cut-offs of cumulative and average cumulative metrics of arsenic water concentrations

Supplementary Table 2 (S2) – Diabetes odds ratios for tertiles of various metrics of arsenic water concentrations among cancer cases or non-cancer controls

Supplementary Table 3 (S3) - Diabetes odds ratios for categories of cumulative arsenic water concentrations lagged 40 years stratified by healthy (<25 kg/m2), overweight (≤25 to <30 kg/m2), and obese (≥30 kg/m2) BMI among all subjects and in only non-cancer controls

Supplementary Table 4 (S4) - Diabetes odds ratios and Rothman synergy indices by categories of low and high BMI and arsenic among all subjects and in only non-cancer controls

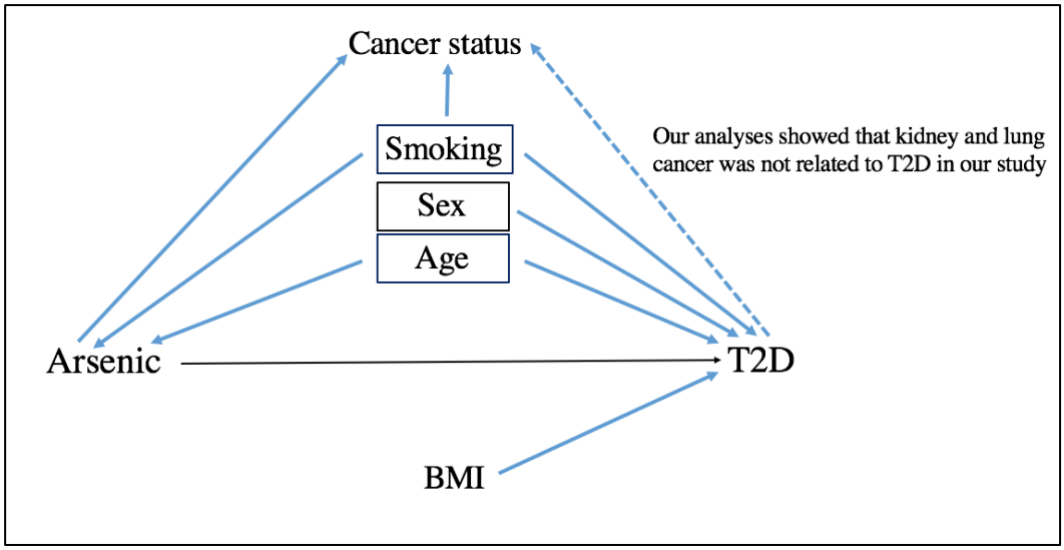

Figure SF1. Directed acyclic graph of arsenic and T2D based on covariate data collected

*Abbreviations: BMI, body mass index; T2D, type 2 diabetes

**The explanation for the edges drawn are as follows: Arsenic is a known human carcinogen, and thereby causes cancer status. Some cancer types are related to T2D, while others are not. For lung and kidney cancers, most studies show that they are not related to T2D (Giovannucci et al, 2010; Larsson and Wolk, 2011). A recent meta-analysis involving 21 cohort studies found a summary relative risk for T2D and bladder cancer of 1.21, therefore bladder cancer cases were excluded from our analyses (Xu et al, 2017). Since cigarettes contain arsenic, smoking causes arsenic exposure, and smoking is also associated with a 30 to 40 percent increased risk of T2D development (CDC 2014). Age is associated with both the exposure and the outcome; age determines whether the individuals were alive and exposed during the period of arsenic-contaminated municipal drinking water, and T2D risk also increases with age. Excess BMI contributes to 70 percent of the etiology of T2D development.

Table S1. Diabetes odds ratios for various cut-offs of cumulative and average metrics of arsenic water concentrations

Arsenic metric	Arsenic level (µg/L)	Diabetes		Unadjusted OR (95% CI)	Adjusted* OR (95% CI)
		Yes	No		
Cumulative exposure: 40 year lag (µg/L-years)	0-1000	82	317	1.00 (Ref)	1.00 (Ref)
	1001-5000	54	230	0.91 (0.62-1.33)	0.89 (0.60-1.32)
	≥5001	95	261	1.41 (1.00-1.97)	1.46 (1.02-2.10)
	p-trend			0.019	0.012
Cumulative exposure: 40 year lag (µg/L-years)	0-2000	115	430	1.00 (Ref)	1.00 (Ref)
	2001-8000	42	182	0.86 (0.58-1.28)	0.92 (0.61-1.38)
	≥8001	74	196	1.41 (1.01-1.98)	1.51 (1.05-2.16)
	p-trend			0.03	0.02
Average lifetime exposure: 40 year lag (µg/L)	0-49	99	338	1.00 (Ref)	1.00 (Ref)
	50-149	33	156	0.72 (0.47-1.12)	0.75 (0.48-1.17)
	≥150	98	309	1.08 (0.79-1.49)	1.22 (0.87-1.71)
	p-trend			0.37	0.11
Average exposure: 40 year lag (µg/L)	0-99	126	453	1.00 (Ref)	1.00 (Ref)
	100-199	17	74	0.83 (0.47-1.45)	0.85 (0.48-1.50)
	≥200	87	281	1.11 (0.82-1.52)	1.27 (0.91-1.75)
	p-trend			0.48	0.15

Abbreviations: BMI, body mass index; CI, confidence interval; OR, odds ratio; Ref, reference group

*Adjusted for age (<60, 60-70, >70 years old), sex, BMI (<25, 25-30, ≥30 kg/m^2), cancer status, smoking (never-smokers, >0 to <10 cigarettes/day)

Table S2. Diabetes odds ratios for tertiles of various metrics of arsenic water concentrations among all subjects and in only non-cancer controls

Arsenic metric	Arsenic level (µg/L)	All subjects	Non-cancer controls only
		OR (95% CI)*	OR (95% CI)*
Cumulative exposure: 0 year lag (µg/L-year)	0-2416	1.00 (Ref)	1.00 (Ref)
	2417-8664	1.14 (0.78-1.66)	1.19 (0.75-1.89)
	≥8665	1.50 (1.03-2.19)	1.53 (0.94-2.47)
	p-trend	0.03	0.09
Cumulative exposure: 40 year lag (µg/L-year)	0-609	1.00 (Ref)	1.00 (Ref)
	610-5279	0.97 (0.66-1.43)	0.93 (0.58-1.49)
	≥5280	1.53 (1.05-2.23)	1.56 (0.97-2.51)
	p-trend	0.009	0.03
Highest year exposure: 0 year lag (µg/L)	0-60	1.00 (Ref)	1.00 (Ref)
	61-635	1.28 (0.88-1.85)	1.33 (0.83-2.10)
	≥636	1.28 (0.89-1.84)	1.34 (0.84-2.13)
	p-trend	0.25	0.27
Highest year exposure: 40 year lag (µg/L)	0-60	1.00 (Ref)	1.00 (Ref)
	61-286	1.04 (0.70-1.55)	1.04 (0.63-1.72)
	≥287	1.16 (0.82-1.64)	1.15 (0.73-1.79)
	p-trend	0.39	0.55
Average lifetime exposure: 0 year lag (µg/L)	0-38	1.00 (Ref)	1.00 (Ref)
	39-129	1.02 (0.70-1.48)	1.03 (0.65-1.62)
	≥130	1.43 (0.98-2.07)	1.44 (0.89-2.32)
	p-trend	0.04	0.11
Average exposure: 40 year lag (µg/L)	0-22	1.00 (Ref)	1.00 (Ref)
	23-222	0.99 (0.68-1.44)	0.97 (0.61-1.53)
	≥223	1.36 (0.93-1.97)	1.32 (0.82-2.13)
	p-trend	0.07	0.20

Abbreviations: CI, confidence interval; OR, odds ratio; Ref, reference group

*Adjusted for age (<60, 60-70, >70 years old), sex, cancer status (in all subjects analysis only), BMI (<25, 25-30, ≥30 kg/m^2), smoking (never-smokers, >0 to <10, ≥10 cigarettes/day)

Table S3. Diabetes odds ratios for categories of cumulative arsenic water concentrations lagged 40 years stratified by healthy (<25 kg/m^2), overweight (≤25 to <30 kg/m^2), and obese (≥30 kg/m^2) BMI among all subjects and in only non-cancer controls

BMI level (kg/m^2)	Arsenic level (µg/L)	All subjects	Non-cancer controls only
		OR (95% CI)*	OR (95% CI)*
Healthy (<25)	0-609	1.00 (Ref)	1.00 (Ref)
	610-5279	0.75 (0.36-1.56)	0.78 (0.32-1.88)
	≥5280	1.45 (0.74-2.84)	1.41 (0.58-3.38)
	p-trend	0.09	0.36
Overweight (≤25 to <30)	0-609	1.00 (Ref)	1.00 (Ref)
	610-5279	1.12 (0.62-2.00)	1.75 (0.85-3.61)
	≥5280	1.34 (0.76-2.35)	1.55 (0.74-3.25)
	p-trend	0.31	0.33
Obese (≥30)	0-609	1.00 (Ref)	1.00 (Ref)
	610-5279	1.04 (0.49-2.20)	0.55 (0.21-1.46)
	≥5280	2.64 (1.14-6.11)	2.23 (0.74-6.70)
	p-trend	0.02	0.15

Abbreviations: BMI, body mass index; CI, confidence interval; OR, odds ratio; Ref, reference group
*Adjusted for age (<60, 60-70, >70 years old), sex, cancer status (in all subjects analysis only), and smoking (never-smokers, >0 to <10, ≥10 cigarettes/day)

Table S4. Diabetes odds ratios and Rothman synergy indices by categories of low and high BMI and arsenic among all subjects and in only non-cancer controls

BMI*	Arsenic*	All subjects	Non-cancer controls only
		OR (95% CI)#	OR (95% CI)#
Low	Low	1.00 (Ref)	1.00 (Ref)
High	Low	1.99 (1.30-3.05)	2.29 (1.36-3.87)
Low	High	1.41 (0.99-2.00)	1.43 (0.90-2.28)
High	High	4.48 (2.25-8.92)	6.39 (2.63-15.55)
Rothman synergy index		2.49 (0.87-7.09)	3.12 (0.91-10.70)

Abbreviations: BMI, body mass index; CI, confidence interval; OR, odds ratio; Ref, reference group

*Low and high BMI defined as < and ≥30 kg/m^2. Low and high arsenic defined as <5280 and ≥5280 µg/L-year cumulative arsenic water concentration lagged 40 years

#Adjusted for age (<60, 60-70, >70 years old), sex, cancer status (in all subjects analysis only), smoking (never-smokers, >0 to <10, ≥10 cigarettes/day)

Chapter 3. Chronic Low-Dose Arsenic Exposure Impairs Adaptive Thermogenesis *In Vivo*

Felicia Castriota[1], Peter-James H. Zushin[2], Sylvia S. Sanchez[1], Rachael V. Phillips[1], Alan Hubbard[1], Andreas Stahl[2], Martyn T. Smith[1], Jen-Chywan Wang[1,2], Michele A. La Merrill[3]

[1] Superfund Research Program, University of California, Berkeley, CA, USA
[2] Department of Nutritional Sciences & Toxicology, University of California, Berkeley, CA, USA
[3] Department of Environmental Toxicology, University of California, Davis, CA USA

*A version of this manuscript is in preparation for submission: Castriota F, Zushin PJH, Sanchez SS, Phillips RV, Hubbard A, Stahl A, Smith MT, Wang JC, La Merrill MA. Chronic Low-Dose Arsenic Exposure Impairs Adaptive Thermogenesis *In Vivo*.
This chapter is printed with the explicit consent of all co-authors.

Abstract

The global prevalence of type 2 diabetes (T2D) has doubled since 1980. Human studies worldwide support arsenic exposure as an emerging risk factor for T2D. We propose that low-dose chronic arsenic ingestion impairs another emerging T2D risk factor called adaptive thermogenesis, e.g. heat production in cold environments. Male C57BL/6J mice exposed to arsenic-contaminated drinking water (300 parts per billion (ppb) for 9 weeks) experienced significantly decreased metabolic heat production when acclimated to chronic cold tolerance testing, as evidenced by indirect calorimetry, despite no change in physical activity. Arsenic increased total fat mass, and increased unilocular lipid droplet size in both subcutaneous inguinal white-adipose tissue (iWAT) and brown adipose tissue (BAT). This hypertrophy appeared to be specific to BAT and WAT, given the lack of observed liver lipidosis. RNA sequencing analysis of iWAT indicated that arsenic dysregulated mitochondrial processes, including fatty acid metabolism. Western blotting of adipose confirmed that arsenic significantly decreased TOMM20 in both BAT and WAT, a correlate of mitochondrial abundance, while in iWAT alone arsenic decreased PPARG2, a glucose-sensitizing master regulator of adipogenesis; PGC1A, a master regulator of mitochondrial biogenesis; and, CPT1B, the rate limiting step of fatty acid oxidation. Our findings reveal the impact of chronic low-level arsenic exposure on thermogenic tissues involved in energy expenditure and glucose regulation, thereby providing novel mechanistic evidence for arsenic's role in T2D development.

Introduction

Type 2 diabetes (T2D) is a chronic disease, affecting 8.3% of adults worldwide (Peng et al. 2015). This metabolic disorder is characterized by hyperglycemia, insulin resistance, and abnormal insulin secretion. Arsenic has been classified as a metabolic disrupting chemical due to its potential to interfere in metabolic pathways (Heindel et al. 2017). Epidemiological studies of people residing in South America, Asia, and North America indicate that exposure to arsenic-contaminated drinking water is associated with an increased risk of T2D (Huang et al, 2014; Islam, 2012; Lai et al, 1994; Navas-Acien et al 2008; Pan et al, 2013; Rahman 1998; Rahman 1999; Rahman 1996; Steinmaus et al, 2009; Wang 2014; Tseng 2000; Tseng 2000b; Tseng et al. 2004). Further, individuals with excess body mass index (BMI) have increased susceptibility to arsenic-induced T2D, raising the possibility that WAT is a potential target tissue of arsenic toxicity (Castriota et al. 2018).

The mechanism by which arsenic leads to T2D has been evaluated in experimental systems, yet their relevance to the human condition is unclear given that these studies have often been conducted at doses outside the range relevant to humans. For example, a recent study demonstrated that mice with chronic exposure to high doses of arsenic had a lower defense of body temperature maintenance in response to acute cold exposure, couple with impaired expression of RNA and proteins critical to adipogenesis, thermogenesis, and mitochondrial activity in BAT (Zuo et al. 2019). However, BAT may not be the only or primary target tissue of this impaired thermogenesis as this acute cold exposure would elicit shivering thermogenesis from skeletal muscle (Cannon and Nedergaard 2010), and could extend to other thermogenic tissues, such as beige adipose tissue and liver, none of which were examined (Seale et al. 2008; Young et al. 1984). Despite the limited scope of identifying the target tissue, whether the molecular and physiological impairments in thermogenesis observed in mice exposed to high levels of arsenic (Zuo et al. 2019) would occur after exposure to doses of arsenic relevant to humans is a logical follow-up question given the association of BAT and metabolic pathologies

in rodent transplant- and human studies (Liu et al. 2015; Gunawardana and Piston 2012; Gunawardana and Piston 2015; Soler-Vásquez et al. 2018).

An expert panel assembled by the National Toxicology Program (NTP) workshop urged researchers to elucidate the influence of white and brown adipose tissue on arsenic-induced T2D (Maull et al. 2012; Thayer et al. 2012). The research presented here aims to address this knowledge gap, and clarify the role of different adipose tissues in arsenic pathogenesis consistent with risk of developing T2D. We hypothesize that impaired adaptive thermogenesis is a key mechanism involved in arsenic-induced metabolic disruption, with both BAT and recruitable beige adipocytes in iWAT as targets of arsenic toxicity. We utilized a mouse model of low dose arsenic exposure relevant to public health to evaluate its effects on adaptive thermogenesis using a step-wise gradient of cold exposure during indirect calorimetry assessment combined with a survey of thermogenic tissue pathology and its molecular validation.

Materials and Methods

Animals and Treatment

Wildtype C57BL/6J male mice (*Mus musculus*) were purchased at five weeks of age from Jackson Laboratory (Bar Harbor, ME, USA). This mouse strain is a well-accepted model for arsenic toxicity (Ellacott et al. 2010), as well as diet-induced obesity and insulin resistance (Tschöp et al. 2012), and the strain used by the Genome Reference Consortium for the mouse reference genome assembly (GRC 2019). Mice were group-housed in sterile ventilated cages with Sani-Chip wood bedding (Lab Supply, Fort Worth, TX, USA) on a 12-hr light/dark cycle at 23°C, after acclimation for seven days. This study included an initial cohort of 10 mice (n=5/treatment), and a subsequent cohort of 16 mice (n=8/treatment), in order to ensure reproducibility. Therefore, this manuscript includes a total of 26 mice (n=13/treatment). After one-week of acclimation, male mice (n=13/treatment) were administered 300 ppb inorganic arsenic in the form of sodium (meta)arsenite ($NaAsO_2$, Sigma-Aldrich) for nine weeks. $NaAsO_2$ was dissolved at a final concentration of 300 ppb using autoclaved water. Both arsenic-treated and control water were freshly prepared and replaced thrice weekly, in order to minimize oxidation from trivalent to pentavalent arsenical species. The mice were fed *ad libitum* purified casein-based AIN-76A chow (Teklad Adjusted Vitamins Diet; Harlan Laboratories, Inc). Published trace metal analyses have shown the AIN-76A diet to have the lowest inorganic arsenic concentrations (<20 ppb), as compared to non-purified diets, which can yield changes in gene and protein expression consistent with arsenic contamination (Kozul et al. 2008). Water intake was measured thrice weekly to coincide with water changes. All mice were euthanized by cervical dislocation following isoflurane overdose. These methods are consistent with the American Veterinary Medical Association Guidelines for the Euthanasia of Animals and approved by both the UC Berkeley and UC Davis Animal Care and Use Committees (ACUC), protocols #2015-06-2681 and #20429, respectively. All personnel working with mice were specially trained and followed specific standard operating procedures (SOPs) as required by both ACUC and the National Institute of Health (NIH).

Respirometry via Indirect Calorimetry

Respirometry was performed using ventilated, open-circuit indirect calorimetry (CLAMS, Columbus Instruments, Columbus, OH). Indirect calorimetry is the gold standard for assessing *in vivo* energy expenditure (Cannon and Nedergaard 2010; Meyer et al. 2015). For the

energy balance studies, we housed a maximum of 16 mice (8 mice/treatment) individually in metabolic chambers with a constant light and dark cycle of 12h. We repeated the experiment, with a total of 13 mice/treatment. Pulverized diet (AIN-76A) and water were provided *ad libitum*. Oxygen consumption, carbon dioxide production, food intake, and three plane locomotion were monitored in sequential intervals (≤35s). A minimum 24h acclimation period allowed the mice to adjust to their new housing conditions (Tschöp et al. 2012). A cold tolerance acclimation test was performed, comprising of a slow, step-wise decrease in temperature. The metabolic cages were set to the following temperatures: 30°C, 23°C, 12°C, and 4°C, each for a 24h interval. Acute cold exposure without prior acclimation was avoided in order to prevent prolonged muscle shivering (Cannon and Nedergaard 2004; 2010; 2011). Energy expenditure and respiratory exchange ratio (RER), a quotient of vCO_2/vO_2, was calculated for each treatment, ambient temperature, and photoperiod. Once indirect calorimetry was completed, all mice were re-acclimated to the ambient temperature (22°C) of their long-term vivarium where they were housed in standard caging for one week prior to any additional experiments.

Body Composition

We measured body composition by either EchoMRI™ (Echo Medical Systems, Houston, TX) or Dual-energy X-ray absorptiometry (DEXA) (PixiMus densitometer, GE Medical Systems, LUNAR) of each mouse at week six of exposure, prior to indirect calorimetry. Body weights and food intake were measured weekly. Tissue weights were weighed and collected *post-mortem* for additional analysis.

Histopathology

Upon dissection, liver, BAT, and iWAT were submerged in 10% neutral buffered formalin for at least 24 hr at room temperature. Formalin-fixed samples were routinely processed for histology, embedded in paraffin, cut into 5uM sections and stained with Hematoxylin and Eosin (H&E). Liver sections were evaluated blindly by a board-certified veterinary pathologist. Hepatic lipidosis was scored based on percentage of hepatocytes that contain lipid: 0 = no lipid; 1 = < 10% of area within a 200x field contains lipid; 2 = 11 - 33%; 3 = 34 - 66%; 4 = > 66%. Object area fraction was calculated at 200x magnification using a binary threshold of 185 to 238 on red, green and blue channels. Fat content was calculated as percent region of interest in epididymal, brown and inguinal fat. Light microscopy was performed using a BX43 Olympus microscope fitted with an Olympus DP74 camera. Digital measurements were done using Cell Sens Dimensions 2.1 with Count and Measure. All histological sectioning and evaluation were conducted at the UC Davis Comparative Pathology Laboratory and performed by a trained veterinary pathologist.

RNA Isolation and Sequencing

Total RNA was isolated and extracted from iWAT (~30 mg) using a lipid-specific RNeasy kit (Qiagen, Hilden, Germany), according to the manufacturer's protocol. The quantity of total RNA was calculated using Qubit™ Fluorometer (Invitrogen, Burlington, ON, Canada). Library preparation and RNA sequencing performed at the Beijing Genome Institute (BGI, Hong Kong) using the BGISEQ-500 instrumentation. The sequence was aligned with the Genome Reference Consortium Mouse Build 38 (GRCm38, mm10), generating 20 M mapped reads per sample.

Protein Quantification and Western Blotting

Inguinal white (~250 mg) and brown adipose tissues (~100 mg) were homogenized in RIPA buffer containing a protease and phosphatase inhibitor cocktail (Halt™, ThermoFisher Scientific) for tissue disruption (TissueLyser II, Qiagen). A bicinchoninic acid assay (BCA) was performed to quantify protein lysate concentrations (Pierce™ BCA Protein Assay Kit, ThermoFisher Scientific). Western Blotting was conducted on 4-15% Mini-PROTEAN TGX Precast 15-well protein gels (BioRad), according to the manufacturer's protocol, with ~50 µg total protein per well. Western blot analysis was performed with primary antibodies UCP1 (14670; Cell Signaling), ELOVL6 (ab69857; Abcam), PGC1A (ab54481; Abcam), PPARG*2* (sc7273 E-8; Santa Cruz Biotechnology), CPT1B (ab134988; Abcam), ATGL (ab109251; Abcam), TOMM20 (ab186735; Abcam), ACTB (A2228; Sigma), and TUBB (T8328; Sigma). The secondary antibodies were goat anti-mouse 680 (925-68020) and goat anti-rabbit 800 (925-32211) (Li-Cor). Proteins were detected by chemiluminescence (Western Lighting Plus-ECL; Perkin Elmer), with signal intensity identified with Li-Cor Odyssey Software. Image Studio Lite software (Li-Cor) was used to quantify band intensity, dividing the signal intensity of the protein of interest by the intensity of housekeeping gene ACTB or TUBB.

Statistical Analysis

We performed statistical analyses for treatment differences in body weight, consumption of water and calories, body composition, and tissue weights in R (v. 3.5.2) using linear mixed models based on previously published methods (La Merrill et al. 2014). We accounted for cohort as a random effect in order to capture differences between experimental blocks. To identify the effects of temperature and circadian rhythm on differences in energy expenditure during indirect calorimetry, longitudinal modeling was performed with treatment and percent body fat as fixed-effects and both cohort and mouse identifiers (ID) as random effects while stratifying by photoperiod and ambient temperature (La Merrill et al. 2014). Since percent body fat differed significantly between arsenic and controls, this was included as a covariate in the indirect calorimetry analyses (La Merrill et al. 2014). Downregulated genes that exhibited a log2-fold change < -1 (i.e., 50% decrease in expression) were considered in Gene Set Enrichment Analysis (GSEA). GSEA was performed in R (v. 3.5.2) using the *clusterProfiler* package, and included the following enrichment analyses: Gene Ontology (GO) for biological processes, Kyoto Encyclopedia Of Genes And Genomes (KEGG), and WikiPathways. GSEA findings were deemed significant based on Benjamini-Hochberg adjusted p-values. The signal intensity of the proteins examined were divided by the intensity of the housekeeping protein for normalization. Fold changes were calculated by dividing the normalized signal of the arsenic exposed mice by the average of the controls.

Results

Chronic arsenic exposure increases percent body fat, but not body weight or food consumption

To determine whether chronic arsenic exposure increased body weight and measures of food and water consumption, adult mice were monitored weekly for the status of these parameters (Figure 1A). No significant differences were observed in body weight throughout the duration of the study (Figure 1B). While caloric intake was not significantly different across treatments throughout the majority of the study duration, significant differences between treatment groups were observed during weeks one and eight, in which arsenic-exposed mice had

increased caloric intake, and week nine, during which controls had increased caloric intake (Figure 1D). Water intake was consistently increased among controls, with significant differences noted in weeks two, three, four, and eight (Figure 1C). Arsenic exposed mice had a significantly higher body fat percentage when compared to controls, despite no treatment differences in lean-, fat-, or total body- mass (Figure 2).

Chronic arsenic exposure decreases energy expenditure during cold-tolerance acclimation

To examine the effect of chronic arsenic exposure on non-shivering thermogenesis, arsenic and control adult mice were subjected to a cold tolerance acclimation test at 6 weeks of exposure (Cannon and Nedergaard 2010). Arsenic-treated mice exhibited significantly decreased energy expenditure when challenged with progressively colder ambient temperatures (Figure 3A). Upon reaching 4°C, arsenic exposed mice had a 7% reduction in energy expenditure, as compared to controls during both light and dark photoperiods (Figure 3A). Oxygen consumption reduction by arsenic treatment followed a similar pattern (Figure 3B). Further the reduction of oxygen consumption decreased by 8% at 4°C, suggestive of impaired thermogenesis (Cannon and Nedergaard 2011). Despite the reduced energy expenditure and oxygen consumption by arsenic treatment, no significant treatment differences were observed in movement, indicating that decreased energy expenditure was independent of physical activity of mice (Figure 3C). Indeed we observed a qualitatively increased activity of arsenic exposed mice during the dark photoperiod. No significant differences were observed in RER (data not shown), suggesting that the effect of arsenic exposure on energy expenditure and oxygen consumption is not mediated by an interference with substrate utilization.

Chronic arsenic exposure induces whitening of thermogenic adipose tissues

To determine the tissue site responsible for reduced energy expenditure by arsenic during indirect calorimetry, histopathological analysis of liver, iWAT, and BAT were conducted at study week nine. H&E staining of iWAT and BAT sections revealed increased unilocular lipid droplet accumulation in arsenic exposed mice compared to controls (Figure 4A-D), consistent with adipose whitening (Kotzbeck et al. 2018). Tissue weight was also determined at dissection in order to assess changes in relative and absolute organ mass as an indicator of tissue dysfunction. Absolute and relative weight of iWAT was significantly increased among arsenic exposed mice compared to controls (Figure 4E, D). However we did not observe an increase in the absolute or relative weight of other thermogenic tissue, e.g. BAT, skeletal muscle, heart, or liver (Figure 4E, D). Furthermore, no evidence of hepatic lipid accumulation or other lesions were observed (Figure SF1), consistent with increased lipid droplet formation that is specific to thermogenic adipose tissues.

Chronic arsenic exposure downregulates the expression of genes involved thermogenesis and fatty acid oxidation in inguinal WAT

Given the increased iWAT mass (Virtue and Vidual-Puig 2013) and increasing biomedical evidence for a role of recruitable beige adipocytes in energy balance (Kajimura et al. 2015), we sought to establish whether arsenic exposure interferes with the beiging of iWAT by performing RNA sequencing analysis of iWAT from arsenic exposed and control mice. Arsenic significantly decreased the expression of genes in involved in adaptive thermogenesis, adipogenesis, lipolysis, inflammation, and metabolism (Figure 5, Table 1, Figure SF2). Arsenic exposure decreased the expression of *Ucp1* in iWAT, the primary gene responsible for energy

dissipation and non-shivering thermogenesis (Table 1, Figure SF2). Several additional genes critical to beiging and energy generation were also significantly reduced with arsenic exposure, including *Dio2*, *Cidea*, and both *Acss1* and *Acss2* (Table 1).

Genes that were expressed differentially with respect to arsenic among the significantly enriched KEGG pathways (Table 1) were validated via protein quantification in both iWAT and BAT given both tissues exhibited increased whitening (Figure 4). Arsenic induced changes in protein expression were more pronounced in iWAT than those observed in BAT (Figure 6). For example, although mitochondrial membrane protein TOMM20 was significantly downregulated in BAT, no significant differences were observed in BAT proteins associated with adaptive thermogenesis (Figure 6). In contrast, arsenic exposure significantly decreased the expression of not only TOMM20, but also PGC1A, PPARG2, and CPT1B in iWAT (Figure 6). This 39.3% decrease in CPT1B protein levels in iWAT from arsenic exposed mice validated the 46.3% decrease in *Cpt1b* expression revealed by RNA sequencing (Table 1). Further, the trend of 57.8% decreased UCP1 expression in iWAT (p-value: 0.08) corroborated with the RNA sequencing results, where *Ucp1* was decreased 42.3% due to arsenic exposure (Table 1).

Discussion

We tested our hypothesis that low-dose chronic arsenic exposure impairs adaptive thermogenesis in adult male C57BL/6J mice. Low dose chronic arsenic exposure reduced adaptive thermogenesis and induced thermogenic adipose tissue whitening. Histopathologic analyses revealed that brown fat and especially subcutaneous fat, but not liver, were target tissues of this thermogenic impairment by arsenic. Our research indicates that arsenic does this, at least in part, by remodeling adipose tissue.

Arsenic increased the presence of unilocular lipid droplets in both subcutaneous and brown adipose tissue. This may explain the significantly increased body fat percentage and subcutaneous adipose tissue mass in arsenic exposed mice compared to controls. Consistent with our observations, previous studies have reported arsenic exposure to decrease the expression of the master regulator of adipogenesis, PPARG (Hou et al. 2013; Wauson et al. 2002). Arsenic has also been shown to inhibit the interaction between C/EBPA and PPARG, a critical step in adipogenic differentiation (Yadav et al. 2012). Based on our findings, we confirm Maull et al's speculation regarding arsenic's effects on both brown and white adiposity in the context of T2D (Maull et al. 2012).

A strength of this study lies in the administered exposure concentration, which was designed to be highly relevant to the route and dose of exposure experienced by communities worldwide (Maull et al. 2012). An allometric scaling approach was used to convert treatment concentrations administered to animals to human equivalence doses (FDA 2005). The dose of 300 ppb in mice approximates 58.5 ppb in humans, which corresponds to the current standard of inorganic arsenic exposure in drinking water established in several nations, including Bahrain, Bangladesh, Bolivia, China, Egypt, India, Indonesia, Oman, Philippines, Saudi Arabia, Sri Lanka, Vietnam, and Zimbabwe (Yamamura et al. 2001). This study also relies on low-dose chronic arsenic ingestion via oral exposure, unconfounded by the ingestion of arsenic-rich dietary sources. Our study adds to the experimental animal literature by relying on a study design that is not only applicable to human exposures but also informed with established methodologies in the field of metabolic biology.

Our molecular studies also suggest that arsenic targeted mitochondria in its impairment of adipose thermogenesis, either the numbers or functions of mitochondria, or both. With respect to

mitochondria abundance, chronic cold exposure should have remodeled adipose to increase mitochondria, and consequently, thermogenic capacity (Choe et al. 2016; Altshuler and Kajimura 2017). Instead, arsenic exposure appeared to diminish mitochondrial abundance in both white and brown adipose tissue following cold exposure, as evidenced by the significantly decreased expression of TOMM20. This is consistent with the decreased mitochondrial abundance observed with the 'anti-thermogenic' phenomenon of increased whitening, also known as beige-to-white adipocyte conversion (Altshuler-Keylin et al. 2016).

We present molecular evidence suggesting that arsenic impairs numerous mitochondria functions. Previous research has shown high arsenic exposure is associated with mitochondrial dysfunction (Pan et al. 2014; Tseng et al. 2004), with arsenic decreasing expression of electron transport related genes (COX IV, COX7a1, COX8B) in BAT (Zuo et al. 2019). Because thermogenic adipose tissue prefers using fatty acids as a substrate for thermogenesis (Bartelt and Heeren 2014), the reduction of the rate limiting step of mitochondrial fatty acid oxidation (CPT1B) in the subcutaneous white adipose of arsenic -exposed mice after a cold challenge supports the role of chronic low-dose arsenic exposure in maladaptive thermogenesis and impaired beiging observed here (Inagaki et al. 2016). Indeed, the decreased expression of CPT1B and UCP1 which we observed across protein and RNA after arsenic exposure further underscore the biological plausibility of arsenic decreasing mitochondrial lipid oxidation and uncoupled respiration, respectively (Greenland et al. 2016). It remains to be determined whether arsenic interferes with adaptive thermogenesis and fatty acid metabolism in adipose tissue through impaired adipogenesis, reduced mitochondria abundance or by targeting mitochondrial function independent of these pathologies. Future studies should be conducted to examine the effects of arsenic exposure on mitochondrial degradation in thermogenic adipose tissue, and its association with metabolic pathologies (Altshuler-Keylin and Kajimura 2017).

Conclusions

This is the first study to investigate the effects of inorganic arsenic exposure on adaptive thermogenesis. While chronic arsenic exposure is associated with increased susceptibility to T2D in communities worldwide, the exact mechanism by which arsenic exerts its diabetogenic effects remains unclear. Our findings provide additional evidence of potential pathways by which chronic low-dose arsenic exposure impairs thermogenesis, fatty acid oxidation, and mitochondrial abundance, increasing the risk of metabolic diseases such as T2D. shift in adipose tissue architecture to more lipid droplets with molecular analysis suggesting they have less mitochondria and thermogenic capacity. There is increasing interest in the role of environmental toxicants on thermogenic adipose tissues, linking environmental health to the growing prevalence of metabolic diseases worldwide.

Glossary

Acly ATP citrate lyase
Adcy3 Adenylate cyclase 3
Acot1 Acyl-CoA thioesterase 1
Acot11 Acyl-CoA thioesterase 11
Acsl5 Acyl-CoA synthetase long-chain family member 5
Acss1 Acyl-CoA synthetase short-chain family member 1
Acss2 Acyl-CoA synthetase short-chain family member 2
ACUC Animal Care And Use Committee
Amd1 S-adenosylmethionine decarboxylase 1
ATB Beta actin
BAT Brown adipose tissue
BMI Body mass index
C/EBPA CCAAT-enhancer binding protein alpha
Ccl8 Chemokine **(**C-C Motif) ligand 8
Ccl19 Chemokine (C-C Motif) ligand 19
Ccl21a Chemokine (C-C Motif) ligand 21a (serine)
Cidea Cell death-inducing DNA fragmentation factor, alpha subunit-like effector a
Cox8b Cytochrome c oxidase subunit 8b
Cpt1b Carnitine palmitoyltransferase 1b
Cyp2b10 Cytochrome P450, family 2, subfamily b, polypeptide 10
Cyp51 Cytochrome P450, family 51
Cxcr6 Chemokine **(**C-X-C motif) receptor 6
Dhrs9 Dehydrogenase/reductase (SDR Family) member 9
Dio2 Deiodinase, iodothyronine, type II
Dnmt3l DNA (cytosine-5-)-methyltransferase 3-like
ELOVL6 ELOVL family member 6, elongation of long chain fatty acids
EPA Environmental Protection Agency
Fabp3 Fatty acid binding protein 3
Fbp2 Fructose bisphosphatase 2
Gyk Glycerol kinase
Idi1 Isopentenyl-diphosphate delta isomerase
Impa2 Inositol (myo)-1(or 4)-monophosphatase 2
iWAT Subcutaneous inguinal white adipose tissue
KEGG Kyoto Encyclopedia Of Genes And Genomes
Lipg Lipase, endothelial
MDC Metabolic disrupting chemical
Me1 Malic enzyme 1, NADP(+)-dependent, cytosolic
NIH National Institute of Health
NTP National Toxicology Program
Odc1 Ornithine decarboxylase, structural 1
Pank1 Pantothenate kinase 1
PGC1A Peroxisome proliferator activated receptor, gamma, coactivator 1 alpha
Phosopho1 Phosphatase, orphan 1

Plcb2 Phospholipase c, beta 2
Plcd4 Phospholipase c, delta 4
PPARG2 Peroxisome proliferator activated receptor gamma 2
Ppb Parts per billion
RER Respiratory exchange ratio
Slc27a2 Solute carrier family 27 (fatty acid transporter), member 2
Scd2 Stearoyl-Coenzyme A desaturase 2
SOP Standard Operating Procedure
St3gal5 ST3 beta-galactoside alpha-2,3-sialyltransferase 5
T2D Type 2 diabetes
TOMM20 Translocase of outer mitochondrial membrane 20
TUBB Beta tubulin
Ucp1 Uncoupling protein 1 (mitochondrial, proton carrier)
Uqcr10 Ubiquinol-cytochrome c reductase, complex III subunit X
USGS United States Geological Survey

References

Adebayo AO, Zandbergen F, Kozul-Horvath CD, Gruppuso PA, and Hamilton JW. (2015). Chronic Exposure to Low-Dose Arsenic Modulates Lipogenic Gene Expression in Mice: Arsenic Effect on Lipid-Regulating Genes. *J Biochem Mol Toxicol* 29:1–9; doi:10.1002/jbt.21600.

Altshuler-Keylin S, Shinoda K, Hasegawa Y, Ikeda K, Hong H, Kang Q, et al. (2016). Beige Adipocyte Maintenance Is Regulated by Autophagy-Induced Mitochondrial Clearance. *Cell Metab* 24(3):402-419; doi: 10.1016/j.cmet.2016.08.002.

Altshuler-Keylin S, and Kajimura S. (2017). Mitochondrial homeostasis in adipose tissue remodeling. *Sci Signal* 10(468). pii:eaai9248; doi: 10.1126/scisignal.aai9248.

Bartelt A, and Heeren J. (2014). Adipose tissue browning and metabolic health. *Nat. Rev. Endocrinol.* 10(1):24-36; doi: 10.1038/nrendo.2013.204.

Cannon B, and Nedergaard J. (2004). Brown adipose tissue: function and physiological significance. *Physiol Rev* 84(1):277-359; doi: 10.1152/physrev.00015.2003.

Cannon B, and Nedergaard J. (2010). Metabolic consequences of the presence or absence of the thermogenic capacity of brown adipose tissue in mice (and probably in humans). *Int J Obes (Lond)* 34 Suppl 1:S7-16; doi: 10.1038/ijo.2010.177.

Cannon B, and Nedergaard J. (2011). Nonshivering thermogenesis and its adequate measurement in metabolic studies. *Journal of Experimental Biol* 214:242-253; doi:10.1242/jeb.050989.

Castriota F, Acevedo J, Ferreccio C, Smith AH, Liaw J, Smith MT, et al. (2018). Obesity and increased susceptibility to arsenic-related type 2 diabetes in Northern Chile. *Environ Res* 167:248–254; doi:10.1016/j.envres.2018.07.022.

Choe SS, Huh JY, Hwang IJ, Kim JI, and Kim JB. (2016). Adipose Tissue Remodeling: Its Role in Energy Metabolism and Metabolic Disorders. *Front Endocrinol (Lausanne)* 7:30; doi: 10.3389/fendo.2016.00030.

Ditzel EJ, Nguyen T, Parker P, and Camenisch TD. (2016). Effects of Arsenite Exposure during Fetal Development on Energy Metabolism and Susceptibility to Diet-Induced Fatty Liver Disease in Male Mice. *Environ Health Perspect* 124; doi:10.1289/ehp.1409501.

Ellacott KL, Morton GJ, Woods SC, Tso P, and Schwartz MW. (2010). Assessment of feeding behavior in laboratory mice. *Cell Metab* 12(1):10-17; doi: 10.1016/j.cmet.2010.06.001.

Fernandez-Marcos PJ, Auwerx J. 2011. Regulation of PGC-1a, a nodal regulator of mitochondrial biogenesis. *Am J Clin Nutr* 93(4):884S-90; doi: 10.3945/ajcn.110.001917.

Fisher FM, Kleiner S, Douris N, Fox EC, Mepani RJ, Verguer F, et al. (2012). FGF21 regulates PGC-1a and browning of white adipose tissues in adaptive thermogenesis. *Genes Dev* 26(3):271-281; doi: 10.1101/gad.177857.111.

Garciafigueroa DY, Klei LR, Ambrosio F, and Barchowsky A. (2013). Arsenic-Stimulated Lipolysis and Adipose Remodeling Is Mediated by G-Protein-Coupled Receptors. *Toxicol Sci* 134:335–344; doi:10.1093/toxsci/kft108.

Gill JA, La Merrill MA. (2017). An emerging role for epigenetic regulation of Pgc-1 expression in environmentally stimulated brown adipose thermogenesis. *Environ Epigenet* 3(2):dvx009; doi: 10.1093/eep/dvxo009.

[GRC] Genome Reference Consortium (GRC). (2019). Mouse Genome Overview. Available at: <https://www.ncbi.nlm.nih.gov/grc/mouse>

Greenland S, Senn SJ, Rothman KJ, Carlin JB, Poole C, Goodman SN, et al. (2016). Statistical tests, P values, confidence intervals, and power: a guide to misinterpretations. *Eur J Epidemiol* 31:337–350; doi:10.1007/s10654-016-0149-3.

Gunawardana SC, and Piston DW. (2012). Reversal of type 1 diabetes in mice by brown adipose tissue transplant. *Diabetes* 61(3):674-682; doi: 10.2337/db11-0510.

Gunawardana SC, and Piston DW. (2015). Insulin-independent reversal of type 1 diabetes in non-obese diabetic mice with brown adipose tissue transplant. *Am J Physiol Endocrine Metab* 308(12):E1043-1055; doi: 10.1152/ajpendo.00570.2014.

Heindel JJ, Blumberg B, Cave M, Machtinger R, Mantovani A, Mendez MA, et al. (2017). Metabolism disrupting chemicals and metabolic disorders. *Reprod Toxicol* 68:3–33; doi:10.1016/j.reprotox.2016.10.001.

Hou Y, Xue P, Woods CG, Wang X, Fu J, Yarborough K, et al. (2013). Association between Arsenic Suppression of Adipogenesis and Induction of CHOP10 via the Endoplasmic Reticulum Stress Response. *Environ Health Perspect* 121:237–243; doi:10.1289/ehp.1205731.

Huang JW, Cheng YY, Sung TC, Guo HR, and Sthiannopkao S. (2014). Association between arrsenic exposure and diabetes mellitus in Cambodia. *Biomed Res Int*: 683124; doi: 10.1155/2014/683124.

Huang MC, Douillet C, Dover EN, Zhang C, Beck R, Tejan-Sie A, et al. (2018). Metabolic Phenotype of Wild-Type and *As3mt* -Knockout C57BL/6J Mice Exposed to Inorganic Arsenic: The Role of Dietary Fat and Folate Intake. *Environ Health Perspect* 126:127003; doi:10.1289/EHP3951.

Inagaki T, Sakai J, and Kajimura S. (2017). Transcriptional and epigenetic control of brown and beige adipose cell fate and function. *Nat Rev Mol Cell Biol* 17(8):480-495; doi: 10.1038/nrm.2016.62.

Islam MR, Khan I, Hassan SMN, McEvoy M, D'Este C, et al. (2012). Association between type 2 diabetes and chronic arsenic exposure in drinking water: A cross sectional study in Bangladesh. *Environ Health* 11(38); doi: 10.1186/1476-069X-11-38.

Kotzbeck P, Giordano A, Mondini E, Murano I, Severi I, Venema W, et al. (2018). Brown adipose tissue whitening leads to brown adipocyte death and adipose tissue inflammation. *J Lipid Res* 59(5):784-794; doi: 10.1194/jlr.M079665.

Kozul CD, Nomikos AP, Hampton TH, Warnke LA, Gosse JA, et al. (2008). Laboratory diet profoundly alters gene expression and confounds genomic analysis in mouse liver and lung. *Chem Biol Interact* 173(2):129-40; doi: 10.1016/j.cbi.2008.02.008.

La Merrill M, Karey E, Moshier E, Lindtner C, La Frano MR, Newman JW, et al. (2014). Perinatal Exposure of Mice to the Pesticide DDT Impairs Energy Expenditure and Metabolism in Adult Female Offspring. B.T. Alexander, ed *PLoS ONE* 9:e103337; doi:10.1371/journal.pone.0103337.

Lai MS, Hsueh YM, Chen CJ, Shyu MP, Chen SY, et al. (1994). Ingested Inorganic Arsenic and Prevalence of Diabetes Mellitus. *Am J Epidemiol* 139(5):484-492.

Liu X, Wang S, You U, Meng M, Zheng Z, Dong M, et al. (2015). Brown Adipose Tissue Transplantation Reverses Obesity in Ob/Ob Mice. *Endocrinology* 156(7):2461-2469; doi: 10.1210/en.2014-1598.

Maull EA, Ahsan H, Edwards J, Longnecker MP, Navas-Acien A, Pi J, et al. (2012). Evaluation of the association between arsenic and diabetes: a National Toxicology Program workshop review. *Environ Health Perspect* 120: 1658; doi: 10.1289/ehp.1104579.

Meyer CW, Reitmeir P, and Tschöp MH. (2015). Exploration of Energy Metabolism in the Mouse Using Indirect Calorimetry: Measurement of Daily Energy Expenditure (DEE) and Basal Metabolic Rate (BMR). *Curr Protoc Mouse Biol* 5(3):205-222; doi: 10.1002/9780470942390.mo140216.

Navas-Acien A, Silbergeld EK, Pastor-Barriuso R, and Guallar E. (2008). Arsenic exposure and prevalence of type 2 diabetes in US adults. *JAMA* 300(7):814-822; doi: 10.1001/jama.300.7.814.Pan et al, 2013.pdf.

Pan X, Jiang L, Zhong L, Geng C, Jia L, Liu S, et al. (2016). Arsenic induces apoptosis by the lysosomal-mitochondrial pathway in INS-1 cells. *Environ Toxicol* 31(2):133-141; doi: 10.1002/tox.22027.

Peng XR, Gennemark P, O'Mahony G, and Bartesaghi S. (2015). Unlock the Thermogenic Potential of Adipose Tissue: Pharmacological Modulation and Implications for Treatment of Diabetes and Obesity. *Front Endocrinol* 6:174; doi: 10.3389/fendo.2015.00174.

Rahman M, Wingren G, and Axelson O. (1996). Diabetes among Swedish art glass workers--an effect of arsenic exposure? *Scand J Work Environ Health* 22(2):146-149.

Rahman M, Tondel M, Ahmad SA, and Axelson O. (1998). Diabetes Mellitus Associated with Arsenic Exposure in Bangladesh. *Am J Epidemiol* 148(2):198-203.

Rahman M, Martin T, Chowdhury IA, and Axelson O. (1999). Relations between exposure to arsenic, skin lesions, and glucosuria. *Occup Environ Med* 56(4):277-281.

Schmidt CW. (2014). Low-Dose Arsenic: In Search of a Risk Threshold. *Environ Health Perspect* 122:A130–A134; doi:10.1289/ehp.122-A130.

Seale P, Bjork B, Yang W, Kajimura S, Chin S, Kuang S, et al. (2008). PRDM16 controls a brown fat/skeletal muscle switch. *Nature* 454:961–967; doi:10.1038/nature07182.

Soler-Vásquez MC, Mera P, Zagmutt S, Serra D, and Herrero L. (2018). New approaches targeting brown adipose tissue transplantation as a therapy in obesity. *Biochem Pharmacol* 155:346-355; doi: 10.1016/j.bcp.2018.07.022.

Steinmaus C, Yuan Y, Liaw J, and Smith AH. (2009). Low-level population exposure to inorganic arsenic in the United States and diabetes mellitus: a reanalysis. *Epidemiology* 20(6):807-815; doi: 10.1097/EDE.0b013e3181b0fd29.

Thayer KA, Heindel JJ, Bucher JR, and Gallo MA. (2012). Role of environmental chemicals in diabetes and obesity: a National Toxicology Program workshop review. *Environ Health Perspect* 120: 779.

Trouba KJ, Wauson EM, and Vorce RL. (2000). Sodium Arsenite Inhibits Terminal Differentiation of Murine C3H 10T1/2 Preadipocytes. *Toxicol Appl Pharmacol* 168:25–35; doi:10.1006/taap.2000.9012.

Tschöp MH, Speakman JR, Arch JRS, Auwerx J, Brüning JC, et al. (2012). A guide to analysis of mouse energy metabolism. *Nat Methods* 9(1):57-63; doi: 10.1038/nmeth.1806.

Tseng CH, Chong CK, Heng LT, Tseng CP, and Tai TY. (2000). The incidence of type 2 diabetes mellitus in Taiwan. *Diabetes Res Clin Pract* 50 Suppl 2:S61-64.

Tseng CH, Tai TY, Chong CK, Tseng CP, Lai MS, et al. (2000b). Long-term arsenic exposure and incidence of non-insulin-dependent diabetes mellitus: a cohort study in arseniasis-hyperendemic villages in Taiwan. *Environ Health Perspect* 108(9):847-851; doi: 10.1289/ehp.00108847.

Tseng CH. (2004). The potential biological mechanisms of arsenic-induced diabetes mellitus. *Toxicol Appl Pharmacol* 197(2):67-83; doi: 10.1016/j.taap.2004.02.009.

US Food and Drug Administration (FDA). 2005. Guidance for Industry: Estimating the Maximum Safe Starting Dose in Adult Healthy Volunteer. Rockville, MD: Available at: <https://www.fda.gov/downloads/Drugs/Guidances/UCM078932.pdf%23search=%27guidekines+for+industry+sfe+starting%27 >

Virtue S, and Vidal-Puig A. (2013). Assessment of brown adipose tissue function. *Front Physiol* 4(4):128; doi: 10.3389/fphys.2013.00128.

Wang W, Xie Z, Lin Y, and Zhang D. (2014). Association of inorganic arsenic exposure with type 2 diabetes mellitus: a meta-analysis. *J Epidemiol Community Health* 68(2):176-184; doi: 10.1136/jech-2013-203114.

Wauson EM, Langan AS, and Vorce RL. (2002). Sodium arsenite inhibits and reverses expression of adipogenic and fat cell-specific genes during in vitro adipogenesis. *Toxicol Sci* 65: 211–219.

Yadav S, Anbalagan M, Shi Y, Wang F, and Wang H. (2013). Arsenic inhibits the adipogenic differentiation of mesenchymal stem cells by down-regulating peroxisome proliferator-activated receptor gamma and CCAAT enhancer-binding proteins. *Toxicol In Vitro* 27:211–219; doi:10.1016/j.tiv.2012.10.012.

Yamamura S, Bartram, Csanady M, Gorchev HG, and Redekopp A. (2001). Chapter 5: Drinking Water Guidelines and Standards. Geneva, Switzerland: World Health Organization (WHO). Available: < https://www.who.int/water_sanitation_health/dwq/arsenicun5.pdf>

Young P, Arch JR, and Ashwell M. (1984). Brown adipose tissue in the parametrial fat pad of the mouse. *FEBS Lett* 167(1):10-4.

Zuo Z, Liu Z, Gao T, Yin Y, Wang Z, Hou Y, et al. (2019). Prolonged inorganic arsenic exposure via drinking water impairs brown adipose tissue function in mice. *Sci Total Environ* 668:310–317; doi:10.1016/j.scitotenv.2019.03.008.

Figure 1. Chronic arsenic exposure does not significantly alter body weight. (A) Study design of male C57BL.6J mice exposed to arsenic (300 ppb) in drinking water for 9 weeks (B) Body weight, (C) Body weight adjusted water intake, (D) Weekly caloric intake; (n=26; 13 arsenic vs 13 controls). Data represented as LS means ± SEM arsenic vs controls, with statistical significance determined by linear mixed models; ***p<0.001; **p<0.01; *p<0.05; arsenic vs controls. Data from week 7 omitted, as mice were in the metabolic chambers.

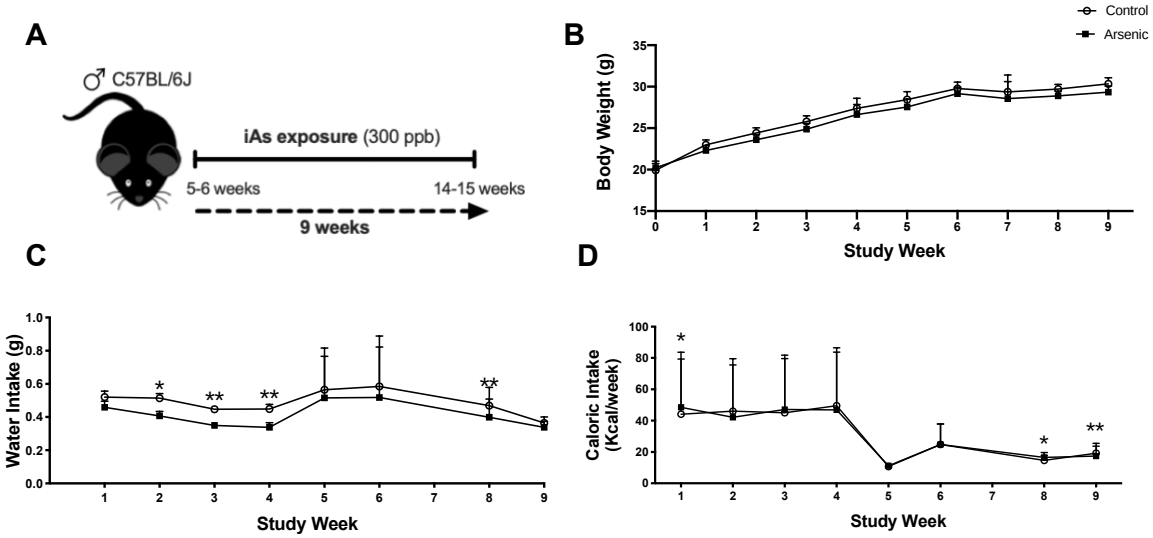

Figure 2. Chronic arsenic exposure significantly increases percent body fat, but not lean or fat body mass. (A) Fat and lean body mass, (B) Percent body fat, and (C) Percent lean mass, determined via DEXA and EchoMRI at week 6. No significant differences observed comparing arsenic (n=26; 13 arsenic vs 13 controls). Data represented in least squares (LS) means, with statistical significance determined by linear mixed models accounting for cohort as a random effect; ***p<0.001; **p<0.01; *p<0.05.

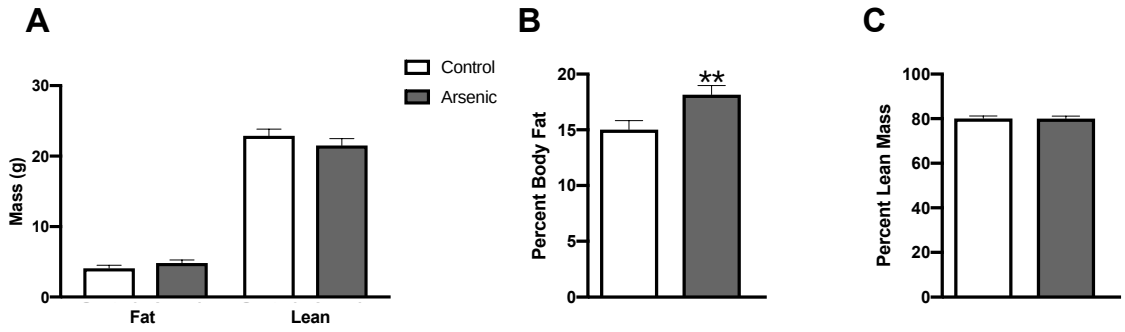

Figure 3. Chronic arsenic exposure decreases adaptive thermogenesis during chronic cold tolerance testing. (A) Energy expenditure, (B) Oxygen consumption, (C) Movement; (n=26; 13 arsenic vs 13 controls). Black bars indicate the dark photoperiod. Data represented as LS means ± SEM arsenic vs controls, with statistical significance determined by linear mixed models accounting for both cohort and mouse ID as random effects; ***p<0.001; **p<0.01; *p<0.05; †p<0.1 arsenic vs controls.

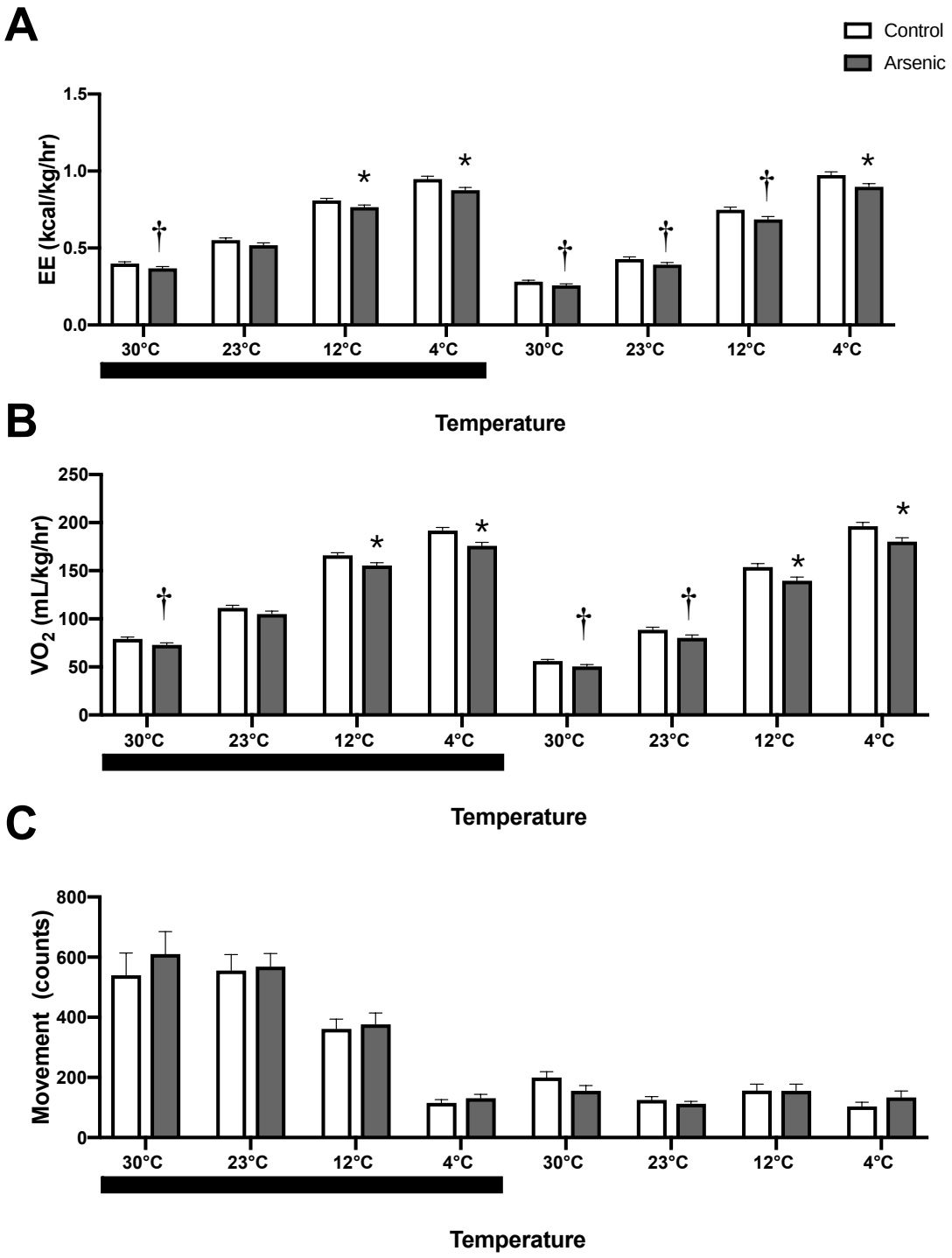

Figure 4. Chronic arsenic exposure induces whitening of iWAT and BAT, and increases iWAT relative and absolute tissue weight. Representative Hematoxylin and eosin (H&E) staining (10x) depicting (A) Control iWAT (B) Arsenic-treated iWAT (C) Control BAT (D) Arsenic-treated BAT; (n=10; 5 arsenic vs 5 controls). (E) Absolute tissue weight and (F) Relative tissue weight; (n = 13 arsenic vs n = 13 controls). Data represented as LS means + SEM, with statistical significance determined by linear mixed models accounting for cohort as a random effect; ***p<0.001; **p<0.01; *p<0.05; †p=0.05 arsenic vs controls. Abbreviations: iWAT, inguinal WAT; eWAT, epididymal WAT; BAT, brown adipose tissue; TA, tibilias anterior; GM, gastrocnemius muscle. No statistical differences in pancreas absolute or relative weight tissue observed (data not shown).

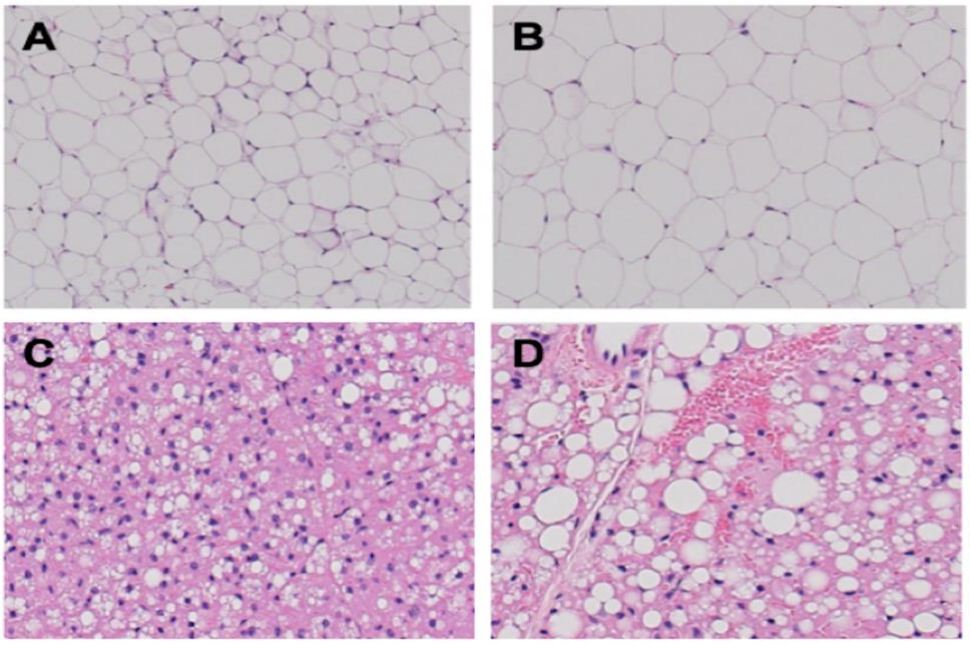

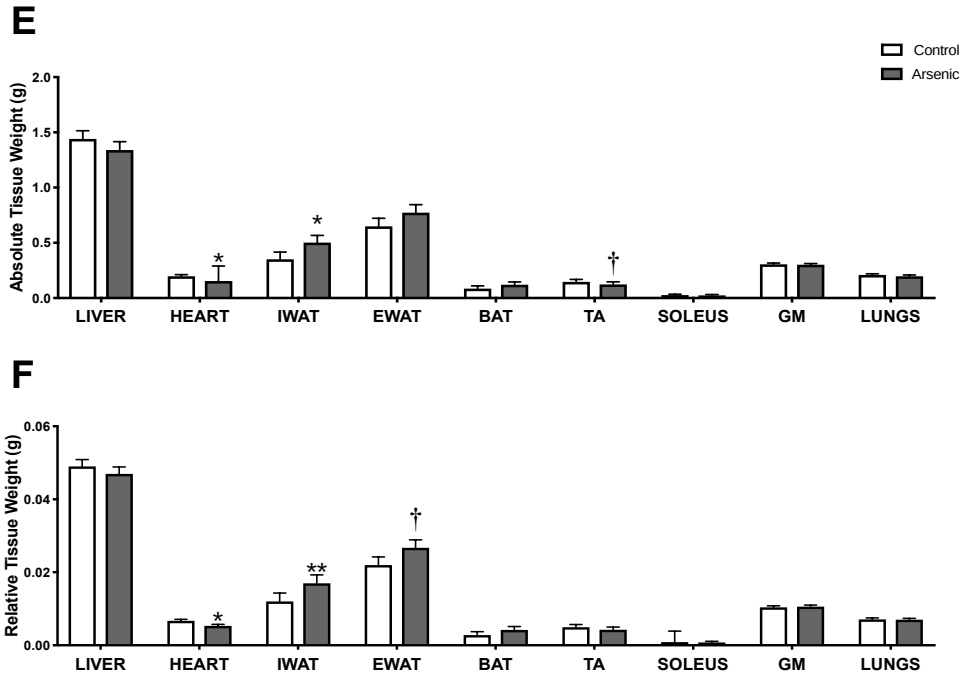

Figure 5. GO Biological Process Enrichment Analysis of arsenic downregulated genes in iWAT. Downregulated biological processes (doubling) shown with Benjamini-Hochberg adjusted p-values; (n=6; 3 arsenic vs 3 controls). Analysis conducted in R using the *clusterProfiler* package.

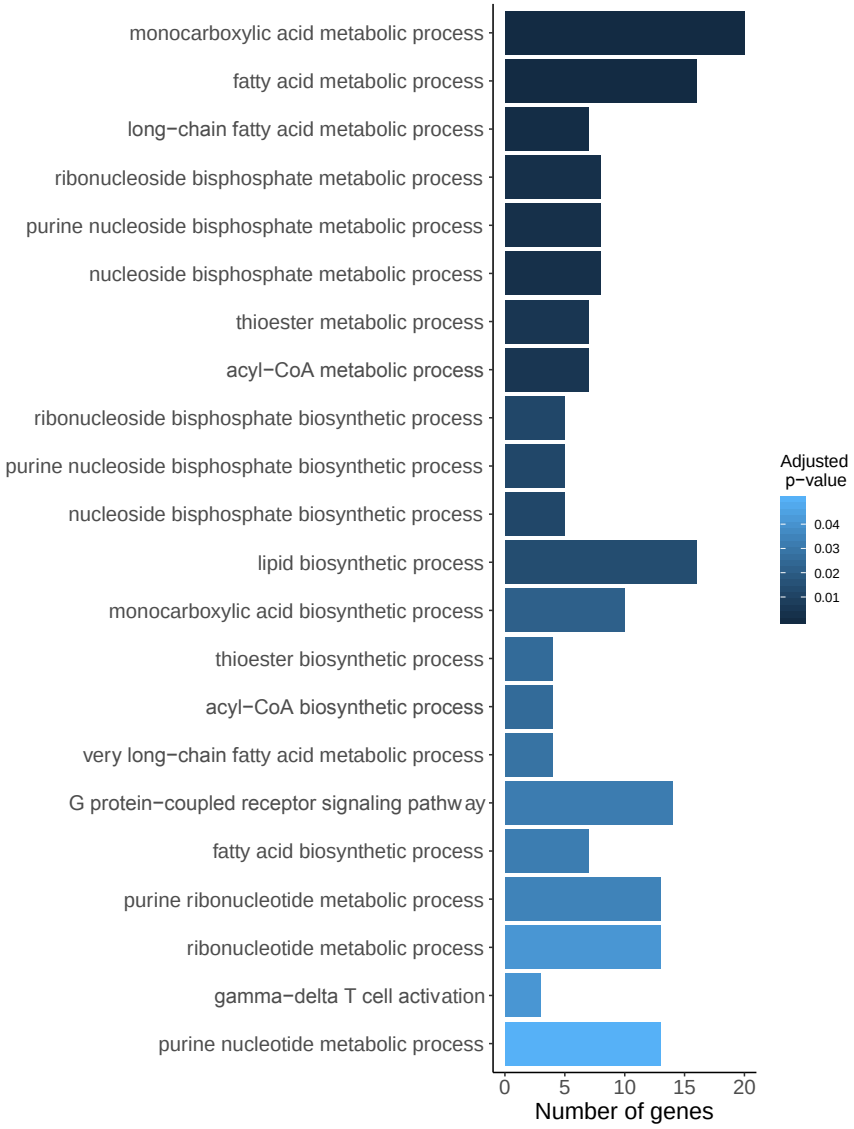

Table 1. KEGG Pathway Analysis of arsenic downregulated genes in iWAT. Pathway-specific Benjamini-Hochberg adjusted p-values, with gene-specific log2 fold changes and percent decrease in expression; (n=6; 3 arsenic vs 3 controls). Pathway-specific analysis conducted in R using the *clusterProfiler* package.

Pathway-Specific Genes	***Adjusted p-value***	***Log2 fold change (Arsenic/Control)***	***Decrease in gene expression (%)***
PPAR signaling (8 genes)	6.47×10^{-6}		
Slc27a2		-1.67	31.4
Fabp3		-1.45	36.6
Ucp1		-1.24	42.3
Acsl5		-1.13	45.7
Scd2		-1.12	46.0
Cpt1β		-1.11	46.3
Gyk		-1.04	48.6
Me1		-1.00	50.0
Metabolism (23 genes)	1.85×10^{-4}		
Dhrs9		-1.41	37.6
Lipg		-1.39	38.2
Phospho1		-1.39	38.2
Cyp2b10		-1.33	40.0
Acly		-1.32	40.0
Impa2		-1.30	40.1
Pank1		-1.22	42.9
St3gal5		-1.21	43.2
Amd1		-1.18	44.1
Cyp51		-1.17	44.4
Cox8b		-1.14	45.4
Acsl5		-1.13	45.7
Plcd4		-1.13	45.7
Fbp2		-1.11	46.3
Idi1		-1.11	46.3
Dnmt3l		-1.05	48.3
Uqcr10		-1.05	48.3
Gyk		-1.04	48.6
Acss2		-1.04	48.6
Odc1		-1.03	49.0
Plcb2		-1.03	49.0
Acss1		-1.01	50.0
Me1		-1.00	50.0
Chemokine signaling (6 genes)	3.82×10^{-2}		
Ccl21a		-7.12	0.72
Ccl19		-1.51	35.1
Cxcr6		-1.34	39.5
Adcy3		-1.21	43.2
Ccl8		-1.09	47.0
Plcb2		-1.03	49.0

Figure 6. Chronic arsenic exposure downregulates fatty acid oxidation, adipogenesis and thermogenesis targets in iWAT. (A) Immunoblots and densitometry analyses of (B) BAT and (C) iWAT; (n=14; 7 arsenic vs 7 controls). Data represented as relative protein levels (fold of control samples), normalized by either ACTB, or TUBB. Statistical significance determined by an unpaired one-tailed Student t-test analysis using Prism (GraphPad). ***p<0.001; **p<0.01; *p<0.05, †p<0.09 (UCP1 p-value: 0.08) arsenic vs controls.

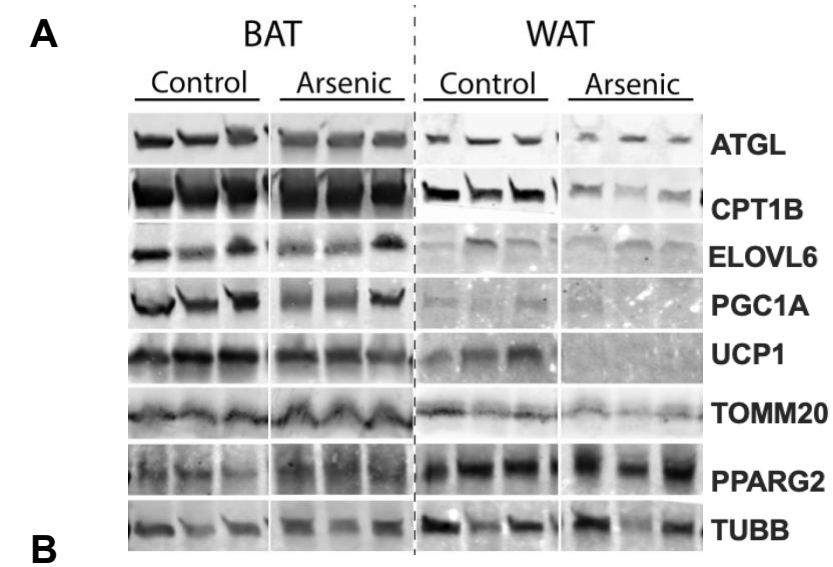

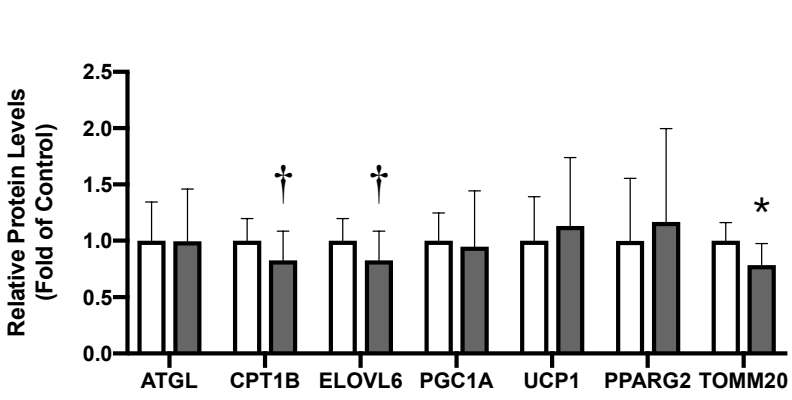

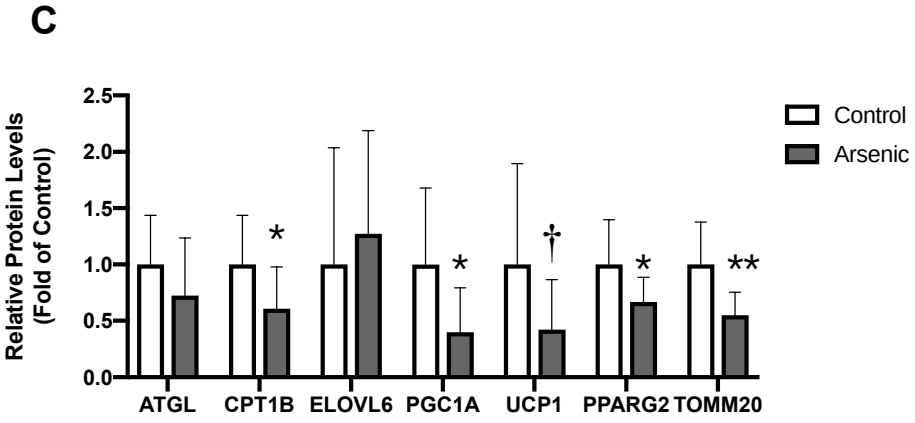

Supplementary Material

Supplementary Figure 1 (SF1). Arsenic exposure does not cause histomorphological changes or liver lesions (lipidosis)

Supplementary Figure 2 (SF2). Significant WikiPathway PPAR Signaling (*Mus musculus*) downregulated genes

Figure SF1. Arsenic exposure does not cause histomorphological changes or liver lesions (lipidosis). Representative Hematoxylin and eosin (H&E) staining (10x) depicting liver sections in (A) Controls and (B) Arsenic-exposed mice. (C) Liver lipidosis scores based on scoring from a certified pathologist. (n=10; 5 arsenic vs 5 controls). Data are represented as means ± SEM. Statistical significance determined by unpaired two-tailed Student t-test analysis using Prism (GraphPad). ***p<0.001; *p<0.001; *p<0.05 arsenic vs controls.

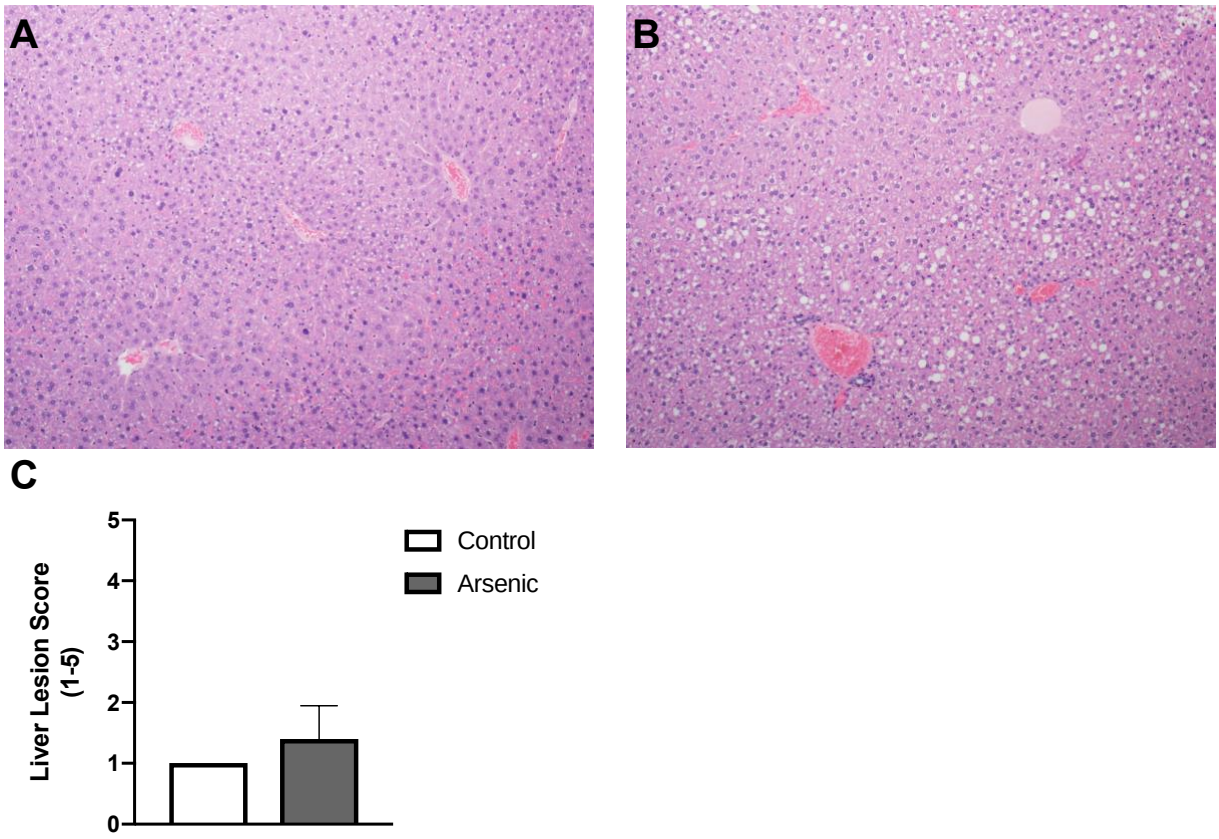

Figure SF2. Significant WikiPathway PPAR Signaling (Mus musculus) downregulated genes. Highlighted genes (in blue) were downregulated due to arsenic exposure, and found in adaptive thermogenesis, fatty acid transport, fatty acid oxidation, and gluconeogenesis. (n=6; 3 arsenic vs 3 controls).

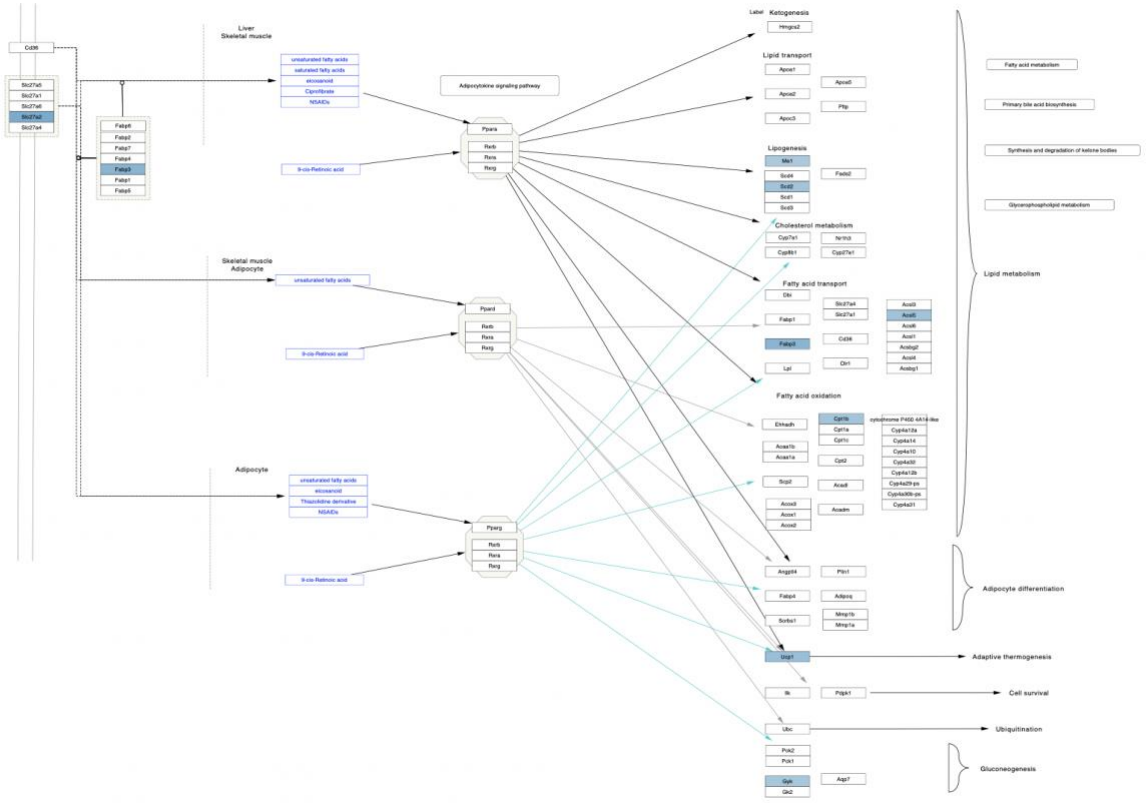

Chapter 4. Leveraging Longitudinal Approaches and Randomization-based Inference in Indirect Calorimetry Studies

Felicia Castriota[*1] and Rachael V. Phillips[*1], Alan E. Hubbard[1], Michele A. La Merrill[2]

[1] Superfund Research Program, University of California, Berkeley, CA, USA
[2] Department of Environmental Toxicology, University of California, Davis, CA USA

Abstract

Indirect calorimetry is considered the gold standard for energy expenditure analysis, with vast applications in diverse research settings. Biologists studying pharmaceutical, toxicological, dietary, or genetic interventions use indirect calorimetry to quantify energy expenditure. These studies are longitudinal, measuring outcomes such as energy expenditure and substrate metabolism repeatedly, across many time intervals for each animal. This longitudinal data structure can provide researchers with an understanding of changes in metabolic outcomes between intervention groups over time. These experiments induce within-animal dependency, as the outcome of an animal measured from one time point to the next is correlated. Another feature of indirect calorimetry studies is that they often randomize animals to intervention groups. With randomized experiments, researchers can identify and estimate causal effects. Further, randomization-based statistical inference can be used to test null hypotheses. Randomization inference does not depend on distributional assumptions or asymptotic theory (large sample approximations) to obtain *p*-values and confidence intervals. Unfortunately, the current practice of indirect calorimetry analysis does not leverage randomization for statistical inference. It instead, relies on large sample theory that is unlikely to hold, since these studies typically consist of small sample sizes. Here, we point out the limitations of the current statistical approaches and present alternatives that do not rely on asymptotic theory to obtain *p*-values. We provide an intuitive comparison of the methods and include R code to facilitate implementation.

Introduction

Indirect calorimetry is the gold standard of energy metabolism research, and relevant to the study of the effects of genetic manipulations, as well as dietary and pharmaceutical interventions on metabolic outcomes, such as respiratory exchange ratio (RER), oxygen consumption (VO_2), carbon dioxide production (VCO_2), and energy expenditure (EE) (Rozman et al. 2014). Indirect calorimetry is performed in gas-tight metabolic chambers, each hosting a single animal with access to both food and water. Repeated measures are obtained for each animal over a determined period of time, and studies are commonly conducted during both light and dark photoperiods in order to account for differences in circadian rhythm and activity levels (Meyer et al. 2015). Since animal studies are costly, and indirect calorimetry studies are typically limited by the number of chambers available, researchers often employ studies with small sample sizes to test hypotheses. In settings of small sample experiments, researchers commonly randomize animals to intervention groups. This randomization of treatment allocation allows them to use randomization-based inference instead of asymptotic-based inference. Asymptotic-based inference is based on the Central Limit Theorem (CLT), a statement that holds as sample size grows to infinity. Randomization-based inference does not depend on distributional assumptions (i.e., it is model-free) or on the CLT to obtain *p*-values and confidence intervals. By eliminating procedures that are based on approximations, randomization-based inference produces more accurate results which are valid for any sample size, also known as exact statistics. Further, researchers eliminate confounding by body mass and composition with randomization, since the intervention assignment does not depend on any covariates (i.e., the act of randomization itself removes confounding). Covariates in a randomized design may still be correlated, so randomized block designs (such as matched pairs) or regression adjustment may be a reasonable addition to randomization. For these reasons, we highly recommend metabolic biologists to utilize randomization in their experimental design in order to unlock the statistical power of randomization-based inference in their analysis.

Experiments with repeated observations over time are known as *longitudinal*. Longitudinal studies differ from *cross-sectional* studies, in which data is captured as a single snapshot in time. Longitudinal data, such as those derived from indirect calorimetry experiments, includes both time-independent (such as sex and age) and time-dependent variables (such as RER, VO_2, VCO_2, and EE). Since longitudinal studies include data from both time-independent and time-dependent variables, they can be used to (1) assess an animal's change in an outcome over time (longitudinal differences), and (2) compare an outcome between animals under varying interventions (cross-sectional differences). Cross-sectional methods have become the standard for the analysis of indirect calorimetry studies. These cross-sectional approaches require reducing the repeated observations to a single summary measure for each animal (e.g., average EE across time, slope of EE, change in EE between two time points). Longitudinal approaches enhance the sensitivity of indirect calorimetry analyses because they (1) do not require the user to compress the data to a summary measure per animal and condition (such as the mean per intervention and photoperiod combination), and (2) are capable of modeling non-independent data as is typically encountered with the repeated measures of indirect calorimetry.

In this perspective, we shed light on the flaws associated with popularized methods for indirect calorimetry analysis. We also present randomization-based approaches that (1) are commonly used, just not yet standardized in metabolic biology analyses; (2) take advantage of repeated measures in estimating potential longitudinal effects of interest; and (3) produce honest statistical inference that does not rely on large samples. We compare the methods we consider and include relevant R code to assist users in implementing these more robust methods.

Randomization-based inference for indirect calorimetry

In indirect calorimetry studies, the null hypothesis (the hypothesis that researchers aim to refute) routinely claims no difference in the outcome between animals in the intervention versus control groups. Evidence in support of or against the null hypothesis is determined by specifying an appropriate test statistic, such as the difference in means between intervention versus control groups. The choice of both the test statistic and null hypothesis should be guided by the research question of interest. Once these are decided upon, the distribution of the test statistic under the null (i.e., the *p*-value) is calculated, and defined as the probability that the test statistic is at least as extreme as its observed value, given the null hypothesis is true. Under the null distribution of no intervention effect, the intervention assignment does not matter, as it would not change the observed distribution of the outcome (Kempthorne 1995). Randomization-based inference utilizes this fact to obtain statistical inference. Specifically, the intervention assignments are reshuffled among the animals while the outcomes remain fixed, and the test statistic is calculated for each reshuffle, thus generating a distribution of test statistics that exhibit a null intervention effect (Kempthorne 1995). If a true difference in the outcome is present between intervention groups, then the *p*-value ascertained from the experiment will be sufficiently small (i.e., *p*-value < 0.05) (Kempthorne 1996). The randomization based hypothesis test is valid in that for a test rejection threshold of 5% ($\alpha = 0.05$), this randomization based hypothesis test will falsely reject the null less than 5% of the time. Moreover, randomized intervention assignment tends to balance any additional covariates in the data (i.e., body mass), since randomization is independent of covariate values (Kempthorne 1996). Randomization is especially practical in low powered studies, where the sample size is small (Kempthorne 1996). Randomization-based inference approaches can easily be applied to both the longitudinal and cross-sectional approaches outlined in Figure 1, and discussed in detail in the following sections.

Cross-sectional analysis of indirect calorimetry data

The field of indirect calorimetry analysis has attempted to implement statistical approaches that account for body mass and composition as potential confounders of energy metabolism (Poehlman and Toth 2018; Arch et al. 2006; Kaiyala and Schwartz 2011). The practice of ratio normalization, which involves dividing the outcome of interest by lean body mass (LBM), was widely practiced until studies revealed spurious findings due to an overestimation of the effect of LBM on EE (Tschöp et al. 2012). Later, the Mouse Metabolic Phenotyping Centers (MMPC) of the National Institute of Diabetes and Digestive and Kidney Diseases (NIDDK) adopted the analysis of covariance (ANCOVA) as the standardized model for indirect calorimetry research (Kaiyala et al. 2017; 2017b; 2017c; 2017d). ANCOVA adjusts the outcome estimates for a confounder such as LBM or fat mass (FM). This assumes that the size of the effect of LBM or FM on the outcome is the same (i.e., equal regression slopes) across all intervention groups (Laughlin et al. 2012). Depending on the research question (and the experimental design, this assumption (often termed homogeneity of regression slopes) is likely to be violated (Kaiyala et al. 2017; 2017b; 2017c; 2017d). Examples of research questions and study designs that may violate this assumption include those with obese versus wildtype mice, or adaptive thermogenesis (Kaiyala et al. 2017; 2017b; 2017c; 2017d; Cannon and Nedergaard 2011). As a cautionary note, the MMPC website does not notify users that repeated measures indirect calorimetry data must be condensed into a single value for each animal *before* uploading it to the website. It is severely problematic to apply the repeated measures data structure to cross-sectional approaches. That is, a single summary measure from all repeated measures on a single mouse must be calculated before implementing a cross-sectional approach (Figure 2). Otherwise, all observations are assumed to be uncorrelated, and independently sampled. This naive implementation leads to severely underestimated variances and incorrectly small *p*-values.

Researchers at Harvard University recently developed a web-based analytical tool called CalR, which allows users to input their raw repeated measures data and perform cross-sectional approaches (Mina et al. 2018). CalR and MMPC are functionally different; CalR derives the summary measure for each animal as a preliminary step before implementing the cross-sectional statistical approach, whereas MMPC assumes the repeated measures data has already been summarized to a single measurement for each animal. CalR also boasts an adaptive methodology that provides users with an alternative model that relaxes the assumptions implicit in MMPC, in the case that the regression slopes between intervention groups are not homogeneous (Mina et al. 2018). The R statistical software syntax for the cross-sectional approaches implemented by CalR and MMPC are provided in red in Figure 1. Condensing the data into a single value for each animal is statistically sound, and can be equivalent in validity to longitudinal methods that maintain the repeated measures structure. These cross-sectional approaches however, limit our understanding of within-animal patterns that vary over time.

Longitudinal analysis of indirect calorimetry data

An intrinsic property of indirect calorimetry data is the repeated measures. Simply taking an average of these repeated measures significantly diminishes statistical power by condensing the data into a single summary value per subject (often as a mean). This single summary value neglects to capture within-subject variability. For example, if relative to the control, the intervention produces greater minute to minute variability in gas exchange or has greater gas exchange values at opposite ends of the photoperiod, a mean of that overall gas exchange would fail to capture these differences.

Indirect calorimetry data analyses that utilize longitudinal approaches can assess (1) how characteristics such as LBM, FM, and treatment, affect an animal's change in an outcome across time, known as longitudinal differences, and (2) how an outcome differs at one point in time between groups of animals under varying interventions, known as cross-sectional differences (Morrell et al. 2009). Linear mixed effect models (LME) are a common longitudinal approach, and have greatly advanced our understanding of longitudinal events (Morrell et al. 2009). LME captures patterns at both the individual level, or "random" effects, and group averages level, or "fixed" effects (Morrell et al. 2009). In LME, the random effects capture the within-animal variance. In indirect calorimetry, random effects capture the fluctuations of gas exchange measured within a single animal during an experimental condition (such as during an administered treatment, a given photoperiod, or temperature setting). In LME, similar to typical ANCOVA, the fixed effects model the between-animal variance (Figure 2) such that error bars can be included, representing the variance in the outcome observed in multiple animals within an experimental condition. LME accounts for both within- and between- animal sources of variation, and therefore allows researchers to utilize their raw indirect calorimetry repeated measures data directly. In contrast, ANCOVA only accounts for the variance between animals, and ignores the variance within an animal over time. LME models the dependency in the outcome nested within an individual through the correlation structure between repeated measurements within each animal. LME also supports higher-order nesting/hierarchical data structures (such as a cohort). For example, in the case for which an indirect calorimetry system holds a maximum of ten animals but the investigator wants to evaluate 20 animals, there will be two cohorts. These two cohorts would often differ from each other beyond intervention and photoperiod status in a random manner that generates experimental noise. This noise may mask the intervention effect. Examples of random cohort to cohort variability often include unexpected changes in the facility environment between cohorts. Also, mixed effect models extend ANCOVA by allowing varying intercepts and slopes across animals.

Other popular longitudinal modeling approaches include the use of repeated measures ANOVA and generalized estimating equations (GEE). Repeated measures ANOVA cannot handle missing data and requires the same number of repeated observations for all animals. Indirect calorimetry data can be missing due to equipment malfunctions but also can occur due to non-symmetrical data collection, where one animal is measured for more intervals in a given photoperiod compared to another. LME and GEE are more flexible longitudinal approaches. LME and GEE are both sound modeling choices. Both LME and GEE model the within-animal correlation, but their difference lies in how they model this structure. GEE and LME are also different in the interpretation of the model coefficients. Of note, GEE is robust to misspecification of the structure of the within-animal correlation; however, GEE assesses the population average effect of a treatment and cannot assess animal-specific effects. For an in-depth review of LME, GEE, and repeated measures ANOVA, we refer to the literature (Zeger and Liang 1992; Burton et al. 1998). The R statistical software implementation for LME and GEE is provided in Figure 1.

Conclusion

Indirect calorimetry studies that explore the effects of genetic, dietary, or compound administration on energy dissipation have considerable therapeutic potential for chronic diseases such as obesity and type 2 diabetes. The metabolic biology community must adopt statistical approaches that limit the potential for false discoveries and unreliable conclusions. In this

perspective, we aim to advance the literature on the use of longitudinal approaches and randomization-based statistical inference for indirect calorimetry research.

Glossary

NIDDK National Institute of Diabetes and Digestive and Kidney Diseases
MMPC Mouse Metabolic Phenotyping Center
Cross-sectional Study design that examines an association based on a snapshot in time
Longitudinal Study design that examines an association based on repeated measures over time
ANOVA Analysis of Variance
Statistical model that analyzes differences among group means
ANCOVA Analysis of Covariance
General linear model that analyzes differences among group means, while controlling for a continuous covariate
GEE Generalized Estimating Equations
General linear model that analyzes differences among group means, and not only controls for covariates but also includes subject-specific random effects.
LME Linear Mixed Effect models
General linear model that allows for both fixed and random effects
Random effects Capture subject-level variation
Fixed effects Capture group-level variation
EE Energy Expenditure (heat)
VO_2 Oxygen consumption (mL/kg/hr)
VCO_2 Carbon dioxide production (mL/kg/hr)
RER Respiratory exchange ratio (VCO_2/VO_2)
A value between 0.7 and 1.0 that indicates the predominant fuel source utilized
LBM Lean body mass (grams)
FM Fat mass (grams)
BW Body weight (grams)
ID Mouse identification number
Unique individual mouse identifiers, commonly determined by ear notches via ear punching, but may also be determined via ear tags, tattoos, or microchip implants
TX Treatment
Treatment may refer to a genetic or dietary intervention, or compound administration
CLT Central limit theorem
Given repeated samples of size *n* from a population, the distribution of the sample means will approach a Normal distribution as the sample size *n* increases.
p-value Probability value
The probability that the statistical summary (i.e., such as the difference in sample means) is greater than or equal to the actual observed value, given the null hypothesis (H_0) is true.
Randomization A mechanism that allocates intervention assignment according to a known distribution. A coin toss for example, can be used to allocate individuals to the intervention with probability of 0.5 for a fair coin.
Null hypothesis (H_0) A general statement that there is no relationship or difference of statistical significance among groups.
Test statistic A statistical summary which measures the degree of agreement between the observed data and the null hypothesis.

References

Arch, J. R. S., Hislop, D., Wang, S. J. Y., and Speakman, J. R. (2006). Some mathematical and technical issues in the measurement and interpretation of open-circuit indirect calorimetry in small animals. *Int. J. Obes.* **30**, 1322–1331.

Burton P., Gurirn L., and Sly P. (1998). Tutorial in Biostatistics: Extending the simple linear regression model to account for correlated responses: an introduction to generalized estimating equations and multi-level mixed modelling. *Statist. Med*. **17,** 1261-1291.

Cannon, B., and Nedergaard, J. (2011). Nonshivering thermogenesis and its adequate measurement in metabolic studies. *J. Exp. Biol.* **214**, 242–253.

Kaiyala, K. J., and Schwartz, M. W. (2011). Toward a More Complete (and Less Controversial) Understanding of Energy Expenditure and Its Role in Obesity Pathogenesis. *Diabetes* **60**, 17–23.

Kaiyala, K.K., Spiekerman C.F., Podolsky R.H., and McGuinness O.P. (2017a). NIDDK Mouse Metabolic Phenotyping Centers Energy Expenditure Analysis. Module 1: Why is it Invalid to Normalize Energy Expenditure by Dividing by Total or Lean Body Mass? Available at: <https://www.mmpc.org/shared/regression.aspx>

Kaiyala, K.K., Spiekerman C.F., Podolsky R.H., and McGuinness O.P. (2017b). NIDDK Mouse Metabolic Phenotyping Centers Energy Expenditure Analysis. Module 2: Introduction to Analysis of Covariance to Adjust Energy Expenditure for Body Size. Available at: <https://www.mmpc.org/shared/regression.aspx>

Kaiyala, K.K., Spiekerman C.F., Podolsky R.H., and McGuinness O.P. (2017c). NIDDK Mouse Metabolic Phenotyping Centers Energy Expenditure Analysis. Module 3: Using the MMPC Web Tool to Revisit a "Hypometabolic" Phenotype in Myostatin Knockout Mice. Available at: <https://www.mmpc.org/shared/regression.aspx>

Kaiyala, K.K., Spiekerman C.F., Podolsky R.H., and McGuinness O.P. (2017d). NIDDK Mouse Metabolic Phenotyping Centers Energy Expenditure Analysis. Module 4: Analyzing Data That Involve a Significant Group by Body Mass Interaction. Available at: <https://www.mmpc.org/shared/regression.aspx>

Kempthorne O. (1995). The Randomization Theory of Experimental Inference. *J Am Stat Assoc.* **50**, 946-967.

Laughlin, M. R., Lloyd, K. C. K., Cline, G. W., and Wasserman, D. H. (2012). NIH Mouse Metabolic Phenotyping Centers: the power of centralized phenotyping. *Mamm. Genome* **23**, 623–631.

Meyer, C. W., Reitmeir, P., and Tschöp, M. H. (2015). Exploration of Energy Metabolism in the Mouse Using Indirect Calorimetry: Measurement of Daily Energy Expenditure (DEE) and Basal Metabolic Rate (BMR). *Curr. Protoc. Mouse Biol*. **5**, 205-222.

Mina, A. I. LeClair R.A., LeClair K.B., Cohen D.E., Lantier L., and Banks A.S. (2018). CalR: A Web-Based Analysis Tool for Indirect Calorimetry Experiments. *Cell Metab.* **28**, 656-666.

Morrell, C.H., Brant, L.J., and Ferrucci, L. (2009). Model Choice Can Obscure Results in Longitudinal Studies. *J Gerontol A Biol Sci Med Sci*. **64,** 215-222.

Poehlman, E. T., and Toth, M. J. (2018). Mathematical ratios lead to spurious conclusions regarding age- and sex-related differences in resting metabolic. *Am. J Clin Nutr*. **61**, 482-485.

Rozman, J., Klingenspor, M., and Hrabě de Angelis, M. (2014). A review of standardized metabolic phenotyping of animal models. *Mamm. Genome* **25**, 497–507.

Tschöp, M. H. Speakman J.R., Arch J.R., Auwerx J., Brüning J.C., Chan L., *et al.* (2012). A guide to analysis of mouse energy metabolism. *Nat. Methods* **9**, 57–63.

Zeger, S.L., and Liang K-Y. (1992). An overview of methods for the analysis of longitudinal data. *Statist. Med*. **11,** 1825-1839.

Figure 1. Flow chart of the relevant R syntax based on experimental characteristics.

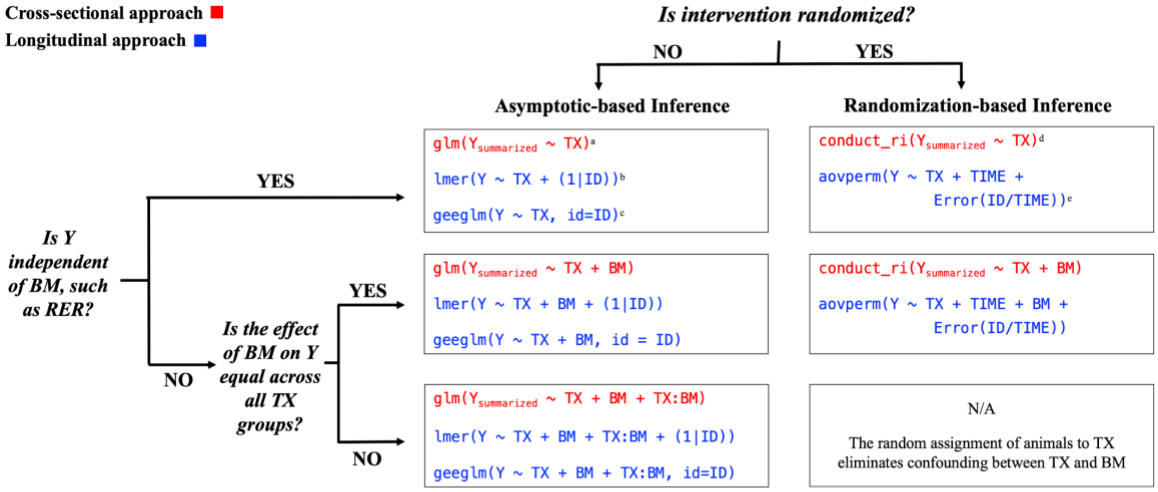

Abbreviations: Y (metabolic outcome of interest); BM (body mass, or other covariate); TX (treatment).

[a] $Y_{summarized}$ represented a summarized outcome for each animal, such as the average outcome for each animal represented in Figure 2.
[b] `lmer()` runs a linear mixed effects model (LME) and requires the `lmerTest` R package.
[c] `geeglm()` runs a generalized estimating equation (GEE) requires the `geepack` R package.
[d] `conduct_ri()` runs a linear model then obtains randomization-based inference and requires the `ri2` R package.
[e] `aovperm()` runs a repeated measures ANOVA then obtains randomization-based inference and requires the `permuco` R package.

Note: The provided R code is an illustrative guide. Consult software documentation before implementation.

Figure 2. Experimental design demonstrating group-level versus subject-level variation, and data structures demonstrating repeated measures (represented as subscripts 1-3) versus summarized EE data.

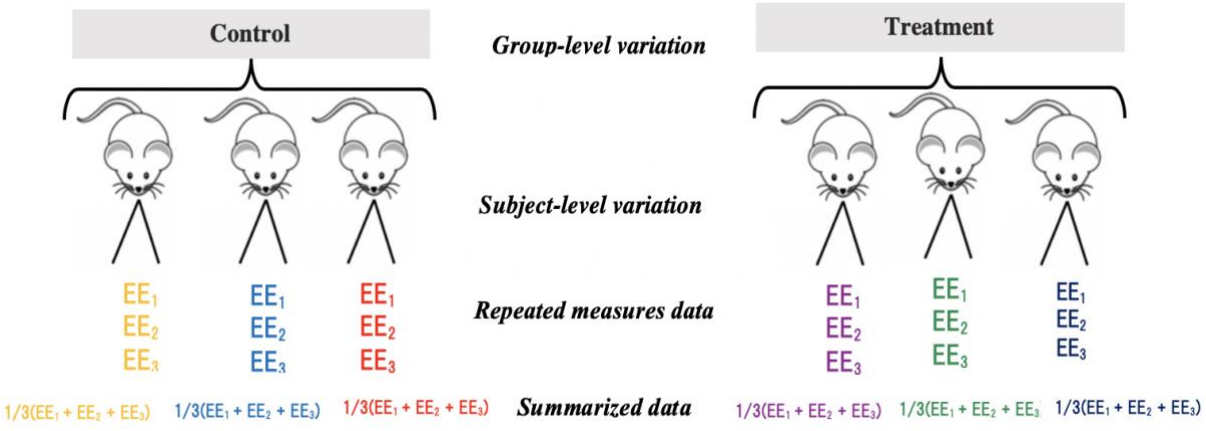

Chapter 5. Conclusions

The objective of this dissertation is to examine the effects of arsenic on T2D development using a multi-disciplinary approach that relies on both human epidemiologic data and mammalian experimental models. Arsenic has been classified as an endocrine disruptor due to its inhibitory effects on hormone receptors, glucose-stimulated insulin secretion, glucose homeostasis, and adipogenesis (Gore et al. 2015; Hou et al; 2012). Both epidemiologic and experimental research studies have reported an increased risk of T2D with chronic exposure to inorganic arsenic, with increasing interest in the interaction of arsenic and obesity on T2D susceptibility (Huang et al. 2018; Castriota et al. 2018).

Chapter 1 is a comprehensive state-of-the-science review of experimental research conducted specifically on arsenite exposure and its effects on glucose homeostasis. Findings from both *in vitro* and *in vivo* studies highlight arsenic's widespread toxicity in multiple metabolic pathways, including insulin-stimulated glucose uptake, glucose-stimulated insulin secretion, hepatic glucose metabolism, and both adipose and pancreatic β-cell dysfunction. Chapter 1 however, also highlights the discrepancies in the dose, duration, and route of administration in the published literature, which can yield varying results. Our ability to fully capture these differences and understand their effects on physiology and susceptibility to T2D, has the potential to inform future medical treatment and current public health interventions for susceptible individuals.

The cross-sectional analysis in Chapter 2 is the first human epidemiologic investigation of a synergistic relationship between arsenic and obesity for the development of T2D. Given the current obesity epidemic and the widespread occurrence of arsenic exposure worldwide, this synergistic relationship could have significant public health implications. A unique aspect of the epidemiology study in northern Chile is the ability to assess the effects of past arsenic exposure on T2D risk, relying on comprehensive exposure estimates and detailed demographic information. Because these analyses are novel, future research in arsenic exposed areas similar to northern Chile, with a wide range of arsenic exposure and adequate information on potential confounding variables, should seek to replicate these findings. The interdisciplinary nature of my research builds upon epidemiologic findings with the use of *in vivo* models. Markers of tissue alterations and gene expression profiles in target organs of arsenic toxicity are viewed as necessary in linking findings from human studies, which report exposure-disease associations. This is crucial to identifying the causal pathways of arsenic-induced diseases, which rely on cell-specific responses (States et al. 2011).

The state-of-the-science review of experimental research in Chapter 1 and epidemiologic analyses in Chapter 2 are complemented by explorations in mammalian models in Chapter 3. Chapter 3 relies on *in vivo* experiments, as no alternative model incorporates all elements of mammalian metabolism. One of the principal advantages of the mouse is the ability to assess arsenic's systemic effects on whole body composition and thermogenesis. Chapter 3 relies on the extensive use of animal monitoring equipment and next-generation sequencing technology. The use of metabolic chambers, rectal thermometry, DEXA and EchoMRI, are all gold standards in the assessment of energy expenditure and whole body composition. Moreover, the use of both RNA sequencing and western blot provide a greater understanding of the role that arsenic has on gene regulation in pathways involved in adipogenesis, thermogenesis, and fatty acid oxidation. This is the first study to examine the effect of inorganic arsenic on adaptive thermogenesis and recruitable beige adipocytes. Future studies should confirm our findings in different mouse

strains and both murine- and human-derived cell lines.

The scientific advances of the past decades in the field of metabolic biology have clearly demonstrated the importance of thermogenic adipose tissues, and their role in energy expenditure, glucose homeostasis, and insulin resistance (Kajimura 2017; Kiefer 2017). As a consequence, energy expenditure instrumentation is now widely utilized across academic, government, and industry research settings. Our understanding of how environmental exposures drive energy expenditure can have significant implications for public health interventions for highly prevalent metabolic diseases. Energy expenditure data is however, limited by the current use of statistical approaches that ignore the correlated structure of dependent observations, which can lead to biased inference. Chapter 4 educates biologists in longitudinal data statistical techniques that take advantage of the repeated measures study designs implicit in indirect calorimetry. Since animal studies are limited by their small sample sizes, the implementation of longitudinal mixed models and randomization-based approaches should be applied to yield more valid inference.

This dissertation integrates advanced knowledge in the fields of toxicology, epidemiology, and metabolic biology. The advancement of environmental health research requires interdisciplinary training in both experimental study design and statistical approaches that allow for the quantification of bias. Since randomized control trials are inherently unethical in our field, novel findings must integrate these methods in order to pinpoint the exact mechanisms of action of ubiquitous environmental pollutants. In 2012, an expert panel assembled by the National Toxicology Program (NTP) reviewed the association between arsenic and T2D based on available epidemiologic and experimental studies (Maull et al. 2012). The committee encouraged researchers to address current gaps in the literature by assessing the effect of adiposity on arsenic and T2D risk, particularly within brown and beige adipocytes (Maull et al. 2012). My dissertation aims to address this knowledge gap via the use of both human data and experimental research. These findings lend mechanistic support to epidemiologic studies that consistently report the role of arsenic in the etiology of T2D in communities worldwide.

References

Castriota F, Acevedo J, Ferreccio C, Smith AH, Liaw J, Smith MT, et al. (2018). Obesity and increased susceptibility to arsenic-related type 2 diabetes in Northern Chile. *Environ. Res.* 167:248–254; doi:10.1016/j.envres.2018.07.022.

Gore AC, Chappell VA, Fenton SE, Flaws JA, Nadal A, Prins G. et al. (2015). EDC-2: The Endocrine Society's Second Scientific Statement on Endocrine-Disrupting Chemicals. *Endocr. Rev.* **36**: E1–E150; doi: 10.1210/er.2015-1010.

Hou Y, Xue P, Woods CG, Wang X, Fu J, Yarborough K, et al. (2013). Association between Arsenic Suppression of Adipogenesis and Induction of CHOP10 via the Endoplasmic Reticulum Stress Response. *Environ. Health Perspect.* 121:237–243; doi:10.1289/ehp.1205731.

Huang MC, Douillet C, Dover EN, Zhang C, Beck R, Tejan-Sie A, et al. (2018). Metabolic Phenotype of Wild-Type and *As3mt* -Knockout C57BL/6J Mice Exposed to Inorganic Arsenic: The Role of Dietary Fat and Folate Intake. *Environ. Health Perspect.* 126:127003; doi:10.1289/EHP3951.

Kajimura, S. (2017). Adipose tissue in 2016: Advances in the understanding of adipose tissue biology: Adipose tissue. *Nat. Rev. Endocrinol.* 13: 69–70; doi: 10.1038/nrendo.2016.211.

Kiefer, F. W. (2017). The significance of beige and brown fat in humans. *Endocr. Connect.* 6: R70–R79; doi: 10.1530/EC-17-0037.

Maull EA, Ahsan H, Edwards J, Longnecker MP, Navas-Acien A, Pi J, et al. (2012). Evaluation of the association between arsenic and diabetes: a National Toxicology Program workshop review. *Environ. Health Perspect.* 120: 1658; doi: 10.1289/ehp.1104579.

States JC, Barchowsky A, Cartwright IL, Reichard JF, Futscher BW, Lantz RC. (2011). Arsenic Toxicology: Translating between Experimental Models and Human Pathology. *Environ. Health Perspect.* 119:1356–1363; doi:10.1289/ehp.1103441.